

May 2017

Fundamental Studies of Metal Ion Extraction into Ionic Liquids By Macrocyclic Polyethers

James Lee Wankowski
University of Wisconsin-Milwaukee

Follow this and additional works at: <https://dc.uwm.edu/etd>

 Part of the [Analytical Chemistry Commons](#)

Recommended Citation

Wankowski, James Lee, "Fundamental Studies of Metal Ion Extraction into Ionic Liquids By Macrocyclic Polyethers" (2017). *Theses and Dissertations*. 1550.
<https://dc.uwm.edu/etd/1550>

This Dissertation is brought to you for free and open access by UWM Digital Commons. It has been accepted for inclusion in Theses and Dissertations by an authorized administrator of UWM Digital Commons. For more information, please contact open-access@uwm.edu.

FUNDAMENTAL STUDIES OF METAL ION EXTRACTION INTO IONIC LIQUIDS

BY MACROCYCLIC POLYETHERS

by

James L. Wankowski

A Dissertation Submitted in

Partial Fulfillment of the

Requirements for the Degree of

Doctor of Philosophy

in Chemistry

at

The University of Wisconsin-Milwaukee

May 2017

ABSTRACT

FUNDAMENTAL STUDIES OF METAL ION EXTRACTION INTO IONIC LIQUIDS BY MACROCYCLIC POLYETHERS

by

James L. Wankowski

The University of Wisconsin-Milwaukee, 2017
Under the Supervision of Professor Mark Dietz, Ph.D.

The liquid-liquid extraction (LLX) of metal ions from aqueous media into ionic liquids (ILs) by macrocyclic polyethers has proven to be an efficient and selective, but complex approach to their separation. Partitioning in these systems has previously been described using a so-called ‘three-path’ model comprising three distinct extraction pathways: neutral complex / ion pair extraction, exchange of the IL cation for a metal-extractant complex, and exchange of the metal ion for a hydronium ion bound to the extractant. The balance of these three paths has been reported to be affected by several characteristics of the LLX system, including the structure of the IL, the stereochemistry of the extractant, and the Lewis acidity of the metal ion, among others. Qualitative trends for many of these factors have been reported, but despite the tremendous number of anion-cation combinations yielding an ionic liquid (*i.e.*, $> 10^8$), only a single family (*i.e.*, 1, 3-dialkylimidazolium) has been systematically studied. Evaluating the benefit (*i.e.*, improved efficiency or selectivity), if any of employing other families of ILs as extraction solvents requires extensive partitioning studies. Consequently, the performance of most IL families remains largely unknown. Furthermore, a quantitative description of metal ion extraction from acidic media into ionic liquids is necessary before they can be considered useful

extraction solvents. In general terms then, the objective of this work is to investigate several families of ionic liquids to determine whether qualitative trends reported previously represent a ‘generic’ description of metal ion extraction in IL-based systems and if these trends can be confirmed quantitatively.

To this end, extraction studies employing quaternary ammonium- and *N*-alkylpyridinium-based ILs and alkali and alkaline earth cations have been conducted to determine if the ‘three-path’ model provides a satisfactory description of metal ion partitioning in these LLX systems. The results of these studies are consistent with those reported previously for systems employing 1, 3-dialkylimidazolium-based ILs, but they have also unexpectedly revealed a significant effect of the self-aggregation of the IL cation on extraction behavior. In an attempt to reduce the number of experimental measurements required to describe metal ion extraction into an ionic liquid, several parameters that define the hydrophobicity of an IL (*e.g.*, hydrophilicity index, water solubility, and D_{ow}) have been investigated and found to accurately predict extraction behavior. Lastly, a process by which to quantitatively describe the balance of pathways in an IL-based extraction system that can be used as a basis for future evaluation of ILs as extraction solvents has been developed.

© Copyright by James L. Wankowski, 2017
All Rights Reserved

For
my wife
and my
son

TABLE OF CONTENTS

LIST OF FIGURES	ix
LIST OF TABLES	xii
ACKNOWLEDGEMENTS	xiii

CHAPTER 1: INTRODUCTION	1
1.1 Overview and Scope	1
1.2 Ionic liquids	5
1.3 Characteristics of ionic liquids as solvents	7
1.4 Extraction of metal ions into traditional organic solvents and ionic liquids	8
1.5 IL-based extractions involving ionizable ligands	11
1.6 Factors affecting metal ion extraction into ionic liquids	12
1.7 Overview of chapters	13
1.8 References	15

CHAPTER 2: EXTRACTION OF ALKALI AND ALKALINE EARTH METALS BY DICYCLOHEXANO-18-CROWN-6 (DCH18C6) INTO QUATERNARY AMMONIUM-BASED IONIC LIQUIDS (ILs)	20
2.1 Introduction	20
2.2 Experimental	21
2.2.1 Materials	21
2.2.2 Instruments	22
2.2.3 Methods	23
2.3 Results and Discussion	25
2.3.1 Physical properties	25
2.3.2 Three-path model of metal ion extraction	27
2.3.3 Extraction from water	30
2.3.4 Effect of IL cation hydrophobicity on extraction from acidic nitrate media	32
2.3.5 Effect of IL anion hydrophobicity on extraction from acidic nitrate media	36
2.3.6 Effect of IL cation hydrophobicity on extraction from acidic chloride media	38
2.3.7 Effect of IL anion hydrophobicity on extraction from acidic chloride media	40
2.3.8 Extraction selectivity of $N_{n,111}^+Tf_2N^-$ and $N_{n,111}^+BETf^-$ ILs	43
2.4 Conclusions	47
2.5 References	49

CHAPTER 3: MECHANISTIC IMPLICATIONS OF MICELLIZATION IN THE EXTRACTION OF METAL IONS INTO <i>N</i> -ALKYLPYRIDINIUM-BASED ILs BY DCH18C6	52
3.1 Introduction	52
3.2 Experimental	53

3.2.1	Materials	53
3.2.2	Instruments	54
3.2.3	Methods	55
3.3	Results and Discussion	60
3.3.1	Physical properties	60
3.3.2	Extraction from water	60
3.3.3	Extraction of Sr ²⁺ from nitric acid media into C _n pyr ⁺ Tf ₂ N ⁻ ILs	63
3.3.4	Micelle formation by C _n pyr ⁺ ILs	67
3.3.5	Mechanistic implications of micelle formation	73
3.3.6	Effect of IL cation hydrophobicity on extraction from acidic nitrate media	75
3.3.7	Effect of IL anion hydrophobicity on extraction from acidic nitrate media	75
3.3.8	Effect of IL cation hydrophobicity on extraction from acidic chloride media	80
3.3.9	Effect of IL anion hydrophobicity on extraction from acidic chloride media	80
3.3.10	Extraction selectivity	83
3.3.11	Effect of IL cation structure on the formation of micelles	86
3.4	Conclusions	95
3.5	References	96

CHAPTER 4: OCTANOL-WATER DISTRIBUTION COEFFICIENTS AND THEIR POTENTIAL USE IN PREDICTING EXTRACTION BEHAVIOR		100
4.1	Introduction	100
4.2	Experimental	103
4.2.1	Materials	103
4.2.2	Instruments	104
4.2.3	Methods	104
4.3	Results and Discussion	107
4.3.1	Relationship of the IL hydrophilicity index to extraction behavior	107
4.3.2	Relationship of the IL water solubility to extraction behavior	108
4.3.3	Measured octanol-water distribution coefficients	111
4.3.4	Relationship of D _{ow} values to extraction behavior	114
4.3.5	Theoretical prediction of D _{ow}	114
4.4	Conclusions	119
4.5	References	120

CHAPTER 5: QUANTIFICATION OF INDIVIDUAL MODES OF Sr ²⁺ PARTITIONING INTO 1-METHYL-3-PENTYLIMIDAZOLIUM BIS[(TRIFLUOROMETHYL)SULFONYL]IMIDE (C ₅ mim ⁺ Tf ₂ N ⁻)		125
5.1	Introduction	125
5.2	Experimental	128
5.2.1	Materials	128
5.2.2	Instruments	129

5.2.3	Methods	130
5.2.4	Extraction studies – Details and Rationale	132
5.3	Results and Discussion	141
5.4	Conclusions	146
5.5	References	148

CHAPTER 6: CONCLUSIONS AND RECOMMENDATIONS

6.1	Conclusions	150
6.2	Recommendations	152
6.3	References	157

APPENDIX	158
-----------------------	------------

CURRICULUM VITAE	182
-------------------------------	------------

LIST OF FIGURES

Figure 1.1: The nuclear fuel cycle	2
Figure 1.2: Various IL cations, anions and alkyl chain lengths	6
Figure 2.1: Three pathway model of metal ion extraction for a system comprising a neutral extractant (DCH18C6) dissolved in a $C_n\text{mim}^+$ -based IL in contact with nitric acid	29
Figure 2.2: Effect of HNO_3 concentration on the extraction of Sr^{2+} by 0.1 M DCH18C6 into 1-octanol (open, black squares), $\text{N}_{7,7,7}^+\text{Tf}_2\text{N}^-$ (solid, blue circles), $\text{N}_{8,8,8}^+\text{Tf}_2\text{N}^-$ (solid, red squares) and $\text{N}_{10,10,10}^+\text{Tf}_2\text{N}^-$ (solid, purple triangles)	33
Figure 2.3: Effect of HNO_3 concentration on the extraction of Na^+ (left), Sr^{2+} (middle) and Ba^{2+} (right) by 0.1 M DCH18C6 into $\text{N}_{8,111}^+\text{Tf}_2\text{N}^-$ (solid, blue circles), $\text{N}_{10,111}^+\text{Tf}_2\text{N}^-$ (solid, red squares), $\text{N}_{12,111}^+\text{Tf}_2\text{N}^-$ (solid, green diamonds)	35
Figure 2.4: Effect of HNO_3 concentration on the extraction of Na^+ (left), Sr^{2+} (middle) and Ba^{2+} (right) by 0.1 M DCH18C6 into $\text{N}_{8,111}^+\text{BETI}^-$ (open, blue circles), $\text{N}_{10,111}^+\text{BETI}^-$ (open, red squares), $\text{N}_{12,111}^+\text{BETI}^-$ (open, green diamonds)	37
Figure 2.5: Effect of HCl concentration on the extraction of Na^+ (left), Sr^{2+} (middle) and Ba^{2+} (right) by 0.1 M DCH18C6 into $\text{N}_{8,111}^+\text{Tf}_2\text{N}^-$ (solid, blue circles), $\text{N}_{10,111}^+\text{Tf}_2\text{N}^-$ (solid, red squares), $\text{N}_{12,111}^+\text{Tf}_2\text{N}^-$ (solid, green diamonds)	39
Figure 2.6: Effect of HCl concentration on the extraction of Na^+ (left), Sr^{2+} (middle) and Ba^{2+} (right) by 0.1 M DCH18C6 into $\text{N}_{8,111}^+\text{BETI}^-$ (solid, blue circles), $\text{N}_{10,111}^+\text{BETI}^-$ (solid, red squares), $\text{N}_{12,111}^+\text{BETI}^-$ (open, green diamonds)	41
Figure 2.7: Comparison of the effect of HNO_3 concentration on the extraction of Sr^{2+} by 0.1 M DCH18C6 into $\text{N}_{10,111}^+\text{Tf}_2\text{N}^-$ (solid, red squares), $\text{N}_{10,111}^+\text{BETI}^-$ (open, red squares)	42
Figure 3.1: Effect of temperature on the extraction of Sr^{2+} by 0.1 M DCH18C6 into $\text{C}_4\text{pyr}^+\text{Tf}_2\text{N}^-$ (room temperature – solid, black circles and 50 °C – open, black circles), $\text{C}_7\text{pyr}^+\text{Tf}_2\text{N}^-$ (room temperature – solid, purple triangles and 50 °C – open, purple triangles) and $\text{C}_{10}\text{pyr}^+\text{Tf}_2\text{N}^-$ (room temperature – solid, red squares and 50 °C – open, red squares)	59
Figure 3.2: Effect of HNO_3 concentration on the extraction of Sr^{2+} by 0.1 M DCH18C6 into several $C_n\text{pyr}^+\text{Tf}_2\text{N}^-$ ILs. Left panel: $\text{C}_4\text{pyr}^+\text{Tf}_2\text{N}^-$ (black exes), $\text{C}_6\text{pyr}^+\text{Tf}_2\text{N}^-$ (open, green plus sign), $\text{C}_7\text{pyr}^+\text{Tf}_2\text{N}^-$ (solid, purple diamonds), $\text{C}_8\text{pyr}^+\text{Tf}_2\text{N}^-$ (solid, blue circles) and $\text{C}_{10}\text{pyr}^+\text{Tf}_2\text{N}^-$ (solid, red squares); Right panel: $\text{C}_{10}\text{pyr}^+\text{Tf}_2\text{N}^-$ (solid, red squares), $\text{C}_{12}\text{pyr}^+\text{Tf}_2\text{N}^-$ (solid, green diamonds), and $\text{C}_{14}\text{pyr}^+\text{Tf}_2\text{N}^-$ (black crosses)	65
Figure 3.3: Effect of HNO_3 concentration on the extraction of Sr^{2+} by 0.1 M DCH18C6 into several ILs. Left panel: $\text{N}_{8,111}^+\text{Tf}_2\text{N}^-$ (solid, blue circles), $\text{N}_{10,111}^+\text{Tf}_2\text{N}^-$ (solid, red squares), $\text{N}_{12,111}^+\text{Tf}_2\text{N}^-$ (solid, green diamonds), and $\text{N}_{14,111}^+\text{Tf}_2\text{N}^-$ (black crosses); Right panel: $\text{C}_{10}\text{mim}^+\text{Tf}_2\text{N}^-$ (solid, red squares), $\text{C}_{12}\text{mim}^+\text{Tf}_2\text{N}^-$ (solid, green diamonds), and $\text{C}_{14}\text{mim}^+\text{Tf}_2\text{N}^-$ (black crosses)	66
Figure 3.4: Structures of several representative ionic liquids and surfactants	68

Figure 3.5: Aqueous phase surface tension at various concentrations of IL. Panel A: C₁₀mim⁺Tf₂N⁻ (solid, red squares), C₁₂mim⁺Tf₂N⁻ (solid, green diamonds), and C₁₄mim⁺Tf₂N⁻ (solid, black circles); Panel B: N_{10,111}⁺Tf₂N⁻ (solid, red squares), N_{12,111}⁺Tf₂N⁻ (solid, green diamonds) and N_{14,111}⁺Tf₂N⁻ (solid, black circles); Panel C: C₁₀pyr⁺Tf₂N⁻ (solid, red squares), C₁₂pyr⁺Tf₂N⁻ (solid, green diamonds), and C₁₄pyr⁺Tf₂N⁻ (solid, black circles); Panel D: C₁₂pyr⁺Tf₂N⁻ (solid, green diamonds), and C₁₄pyr⁺Tf₂N⁻ (solid, black circles) 70

Figure 3.6: Three-path model of metal ion extraction for a system comprising a neutral extractant (e.g., DCH18C6) dissolved in a micelle-forming IL (e.g., C₁₄pyr⁺Tf₂N⁻) in contact with a nitric acid solution 74

Figure 3.7: Effect of HNO₃ concentration on the extraction of Na⁺ (left) and Ba²⁺ (right) by 0.1 M DCH18C6 into C₄pyr⁺Tf₂N⁻ (black exes), C₇pyr⁺Tf₂N⁻ (solid, purple triangles), C₁₀pyr⁺Tf₂N⁻ (solid, red squares) and C₁₄pyr⁺Tf₂N⁻ (black crosses) 76

Figure 3.8: Effect of HNO₃ concentration on the extraction of Na⁺ (left), Sr²⁺ (middle) and Ba²⁺ (right) by 0.1 M DCH18C6 into C₄pyr⁺BETI⁻ (black exes), C₇pyr⁺BETI⁻ (open, purple triangles), C₁₀pyr⁺BETI⁻ (open, red squares) and C₁₄pyr⁺BETI⁻ (black crosses) 78

Figure 3.9: Aqueous phase surface tension at various concentrations of C₁₀pyr⁺BETI⁻ (open, red squares) and C₁₄pyr⁺BETI⁻ (open, black circles) 79

Figure 3.10: Effect of HCl concentration on the extraction of Na⁺ (left), Sr²⁺ (middle) and Ba²⁺ (right) by 0.1 M DCH18C6 into C₄pyr⁺Tf₂N⁻ (black exes), C₇pyr⁺Tf₂N⁻ (solid, purple triangles), C₁₀pyr⁺Tf₂N⁻ (solid, red squares) and C₁₄pyr⁺Tf₂N⁻ (black crosses) 81

Figure 3.11: Effect of HCl concentration on the extraction of Na⁺ (left), Sr²⁺ (middle) and Ba²⁺ (right) by 0.1 M DCH18C6 into C₄pyr⁺BETI⁻ (black exes), C₇pyr⁺BETI⁻ (open, purple triangles), C₁₀pyr⁺BETI⁻ (open, red squares) and C₁₄pyr⁺BETI⁻ (black crosses) 82

Figure 3.12: Structures of *N*-alkylpyridinium (C_{*n*}pyr⁺), *N*-alkyl-4-ethylpyridinium (C_{*n*}etpyr⁺) and *N*-alkyl-4-(dimethyl)aminopyridinium (C_{*n*}dmapyr⁺) IL cations 87

Figure 3.13: Left panel: Effect of HNO₃ concentration on the extraction of Sr²⁺ by 0.1 M DCH18C6 into C₆etpyr⁺Tf₂N⁻ (open, green crosses), C₈etpyr⁺Tf₂N⁻ (solid, blue circles), C₁₀etpyr⁺Tf₂N⁻ (solid, red squares) and C₁₂etpyr⁺Tf₂N⁻ (solid, green diamonds). Right panel: Aqueous phase surface tension at various concentrations of C₈etpyr⁺Tf₂N⁻ (solid, blue circles), C₁₀etpyr⁺Tf₂N⁻ (solid, red squares) and C₁₂etpyr⁺Tf₂N⁻ (solid, green diamonds) 88

Figure 3.14: Effect of HNO₃ concentration on the extraction of Sr²⁺ by 0.1 M DCH18C6. Panel A: C₈pyr⁺Tf₂N⁻ (solid, blue circles) and C₆etpyr⁺Tf₂N⁻ (open, blue circles). Panel B: C₁₀pyr⁺Tf₂N⁻ (solid, red squares) and C₈etpyr⁺Tf₂N⁻ (open, red squares). Panel C: C₁₂pyr⁺Tf₂N⁻ (solid, green diamonds) and C₁₀etpyr⁺Tf₂N⁻ (open, green diamonds). Panel D: C₁₄pyr⁺Tf₂N⁻ (solid, black triangles) and C₁₂etpyr⁺Tf₂N⁻ (open, black triangles) 90

Figure 3.15: Left panel: Effect of HNO₃ concentration on the extraction of Sr²⁺ by 0.1 M DCH18C6 into C₈dmapyr⁺Tf₂N⁻ (solid, blue circles) and C₁₂dmapyr⁺Tf₂N⁻ (solid, green diamonds). Right panel: Aqueous phase surface tension at various concentrations of C₈dmapyr⁺Tf₂N⁻ (solid, blue circles) and C₁₂dmapyr⁺Tf₂N⁻ (solid, green diamonds) 93

Figure 3.16: Effect of HNO₃ concentration on the extraction of Sr²⁺ by 0.1 M DCH18C6. Left panel: C₁₀pyr⁺Tf₂N⁻ (solid, red squares) and C₈dmapyr⁺Tf₂N⁻ (open, red squares). Right panel: C₁₄pyr⁺Tf₂N⁻ (black plus signs) and C₁₂dmapyr⁺Tf₂N⁻ (black exes) 94

Figure 4.1: Slow stir device used for determination of D_{ow} values 106

Figure 4.2: Relationship between R and the hydrophilicity index for C_nmim⁺ (solid circles), C_npyr⁺ (solid triangles), and N_{n,111}⁺ (solid diamonds) ILs 109

Figure 4.3: Relationship between R and the water solubility of C_nmim⁺ (solid circles), C_npyr⁺ (solid triangles), and N_{n,111}⁺ (solid diamonds) ILs 110

Figure 4.4: Relationship between log D_{ow} and the alkyl chain length, n, of C_nmim⁺ (solid circles), C_npyr⁺ (solid triangles), and N_{n,111}⁺ (solid diamonds) ILs. Curves are lines of best fit 113

Figure 4.5: Relationship between R and measured D_{ow} values for strontium (solid symbols) and barium (open symbols) into C_nmim⁺ (circles), C_npyr⁺ (triangles), and N_{n,111}⁺ (diamonds) ILs 115

Figure 4.6: Correlation between predicted and measured values using several theoretical models. Left panel: PDH combined with COSMO-SAC (segmented activity coefficients); middle panel: QSPR; right panel: LFER 117

Figure 4.7: Correlation between predicted and measured (this work) values of log D_{ow} for C_nmim⁺ (solid circles), C_npyr⁺ (solid triangles), and N_{n,111}⁺ (solid diamonds) ILs 118

Figure 5.1: Various extraction systems considered to correct for the mutual solubility of the IL and aqueous phases. System I represents the simplest system and System IV is currently under investigation 134

Figure 5.2: The effect of HNO₃ concentration on the extraction percentage of Sr²⁺ (solid, black circles), NC/IPE (solid, blue triangles), IX-1 (solid, red diamonds), and IX-2 (solid, green squares) 143

Figure 5.3: The effect of HNO₃ concentration on %E_{Sr} (solid, black circles) and on the contributions from NC/IPE (solid, blue triangles) and IX (IX-1 + IX-2; solid, orange diamonds) 145

Figure 6.1: Effect of HNO₃ concentration on the extraction of Na⁺ (solid, red squares) and Sr²⁺ (open, red squares) by 0.1 M DCH18C6 into C₁₀mim⁺Tf₂N⁻ 155

LIST OF TABLES

Table 2.1: Physical properties of ILs studied	26
Table 2.2: Effect of IL structure on metal ion and nitrate extraction from water by DCH18C6 (0.2 M) into various $N_{n,111}^+$ ILs	31
Table 2.3: Effect of HNO_3 concentration on $\alpha_{Sr/Ba}$ ($= D_{Sr} / D_{Ba}$) and $\alpha_{Sr/Na}$ ($= D_{Sr} / D_{Na}$) values for various traditional organic solvents, $N_{n,111}Tf_2N$ ILs, $N_{n,111}BETI$ ILs, and $C_{10}mimTf_2N$ from extraction data for 0.1 M DCH18C6 in the specified organic or IL phase	44
Table 2.4: Effect of HCl concentration on $\alpha_{Sr/Ba}$ ($= D_{Sr} / D_{Ba}$) and $\alpha_{Sr/Na}$ ($= D_{Sr} / D_{Na}$) values for $N_{n,111}Tf_2N$ ILs, $N_{n,111}BETI$ ILs, $C_{10}mimTf_2N$, and 1-octanol from extraction data for 0.1 M DCH18C6 in the organic or IL phase	45
Table 3.1: Physical properties of ILs studied	61
Table 3.2: Effect of IL structure on metal ion and nitrate extraction from water by DCH18C6 (0.2 M) into various C_npyr^+ ILs	62
Table 3.3: Results of carbon, hydrogen, and nitrogen elemental analysis of $C_{12}pyr^+Tf_2N^-$ and $C_{14}pyr^+Tf_2N^-$	72
Table 3.4: Results of carbon, hydrogen, and nitrogen elemental analysis of $C_{14}pyr^+BETI^-$	77
Table 3.5: Effect of HNO_3 concentration on $\alpha_{Sr/Ba}$ ($= D_{Sr} / D_{Ba}$) and $\alpha_{Sr/Na}$ ($= D_{Sr} / D_{Na}$) values for $C_npyr^+Tf_2N^-$ ILs, $C_npyr^+BETI^-$ ILs, $C_{10}mim^+Tf_2N^-$, $N_{12,111}^+Tf_2N^-$ and 1-octanol from extraction data for 0.1 M DCH18C6 in the specified organic or IL phase	84
Table 3.6: Effect of HCl concentration on $\alpha_{Sr/Ba}$ ($= D_{Sr} / D_{Ba}$) and $\alpha_{Sr/Na}$ ($= D_{Sr} / D_{Na}$) values for $C_npyr^+Tf_2N^-$ ILs, $C_npyr^+BETI^-$ ILs, $C_{10}mim^+Tf_2N^-$, $N_{12,111}^+Tf_2N^-$ and 1-octanol from extraction data for 0.1 M DCH18C6 in the organic or IL phase	85
Table 3.7: Comparison of IL water solubilities	91
Table 4.1: LC-MS instrument parameters for IL cation quantification	105
Table 4.2: Experimentally measured values of $\log D_{ow}$ from the present study ^a and found in literature	112
Table 5.1: LC-MS instrument parameters for IL cation and anion quantification	131
Table 5.2: Quantification of Sr^{2+} extraction by NC/IPE and IX-1 from water into $C_5mim^+Tf_2N^-$	138
Table 5.3: Possible contributions from anion exchange processes at 4 and 6 M HNO_3	140
Table 5.4: Contributions from each mode of Sr^{2+} partitioning by DCH18C6 into $C_5mim^+Tf_2N^-$ at various nitric acid concentrations	142

ACKNOWLEDGEMENTS

First and foremost, I would like to extend my deepest thanks to my advisor, Mark Dietz, who has spent the last six years guiding me on my journey through the doctoral program. His willingness to spend countless hours discussing my project and matching excitement for every result, expected or unexpected, kept me focused and inspired me to continue pushing forward. My wife, Sarah, has provided a loving foundation throughout my schooling. Her patience and support has kept me motivated through my successes and failures. Past and current members of the Dietz research group have celebrated and struggled with me through the years. Alan Pawlak was integral in developing my abilities as an analytical chemist. Always willing to lend a hand or an ear, he was a role model and a true friend. Cory Hawkins and Sarah Garvey laid the foundation for my research. They trained me on the techniques necessary to begin my research and provided a wealth of information. Md. Abdul Momen was an endless source of conversation and knowledge. His constant attention and curiosity strengthened every conclusion arising from my research. Michael Kaul will continue my work and will no doubt easily 'fill the shoes' left by myself and those before me. He has been a tremendous pleasure to work with and has been a constant and much needed relief from the stresses of research. Charlie Smith and Kevin Wolters have proven to be excellent students of the knowledge I can offer them; may it serve them well in their future research. My committee members, Joseph Aldstadt, Andrew Pacheco, Alan Schwabacher, and Jorg Woehl, have followed me through my research program and provided invaluable guidance over the years. I thank them especially for the time they have spent in my milestone meetings and reviewing my work. Lastly, I must thank my fellow classmates and the faculty and staff in the Chemistry & Biochemistry Department. Their support and friendship has been much appreciated. I would not have succeeded without them.

Chapter 1:

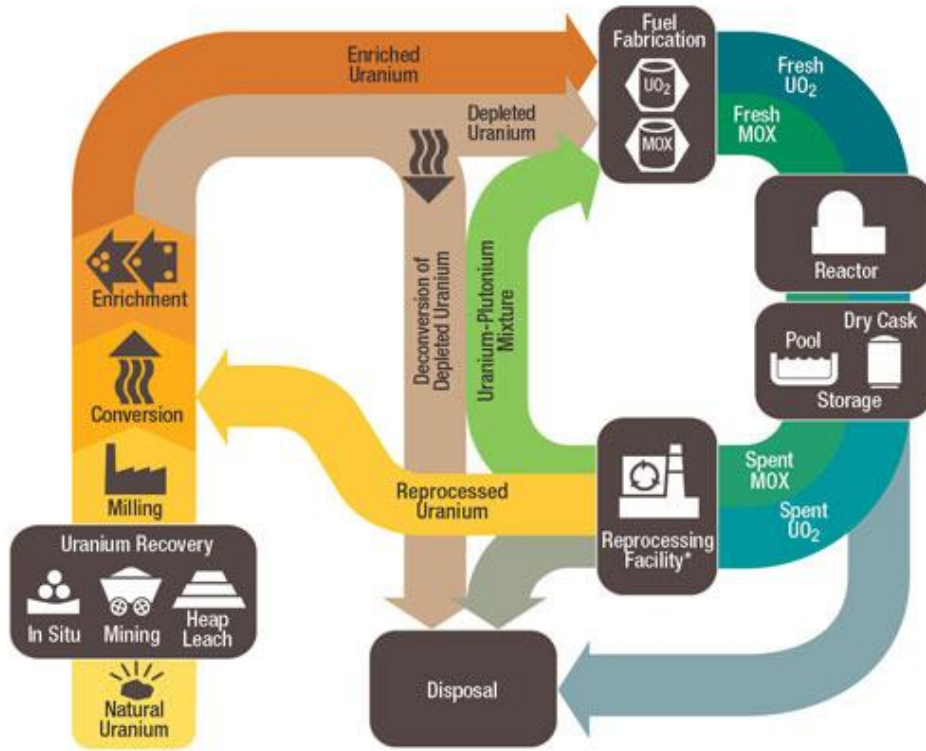
Introduction

1.1 Overview and Scope

Nuclear power in the United States has accounted for ~20% of the nation's total production of electricity for more than 20 years [1.1]. In 2015, 99 operational reactors in the US, the most in any country and 22% of the world-wide total, produced nearly 800 terawatt hours of electricity [1.1]. It is estimated that by the end of 2015, the amount of spent nuclear fuel (SNF) generated by reactors in the US had reached nearly 76,000 metric tons [1.2], with an increase of approximately 2,000 metric tons expected each year. The majority (two thirds) of this waste is currently stored in spent fuel pools, but the United States Department of Energy (DOE) has targeted 2048 as the year in which a geological repository for dry storage of SNF will be operational [1.3].

Figure 1.1 [1.4] depicts the nuclear fuel cycle, which begins with fabrication of fuel rods (generated from the mining of natural uranium or from reprocessed SNF) and proceeds to their use in a nuclear reactor. The 'front end' of the nuclear cycle involves the mining, milling, conversion, enrichment and fuel fabrication. Mining of the uranium ore is done by traditional excavation techniques or by *in situ* leach (ISL) by dissolving uranium oxide with oxygenated groundwater in an orebody and bringing the solution back to the surface. The uranium is then extracted from the ore or leachate, converted to uranium dioxide or uranium hexafluoride prior to enrichment of U-235, and then converted back to uranium dioxide following enrichment. Fuel rods are prepared by filling metal alloy tubes with sintered uranium dioxide pellets. Up to several hundred fuel rods are loaded into reactor cores to produce electricity. The 'back end' of the cycle involves

The Nuclear Fuel Cycle



* Reprocessing of spent nuclear fuel including MOX is not practiced in the U.S.
Note: The NRC has no regulatory role in mining uranium.

Figure 1.1. The nuclear fuel cycle

disposal of fuel after it has been depleted. SNF can be transferred directly into storage or sent for reprocessing.

Despite ongoing research efforts to close the nuclear fuel cycle and reduce the cost of the current 'once-through' fuel cycle, the US has not practiced reprocessing of SNF since 1977 [1.5], but it is routinely performed in Europe, Russia and Japan. The focus of research on SNF reprocessing, or recycling, has been greatly influenced by political agendas and the fear of nuclear proliferation. Deep geological repositories (*e.g.*, Yucca Mountain) have been proposed as long-term storage facilities for SNF in the US including waste that is presently stored in nuclear reservations (*e.g.*, Savannah River Site, Hanford Site, etc.), but these storage facilities have received much opposition.

Spent nuclear fuel comprises about 93% uranium, 5% fission products (predominantly strontium-90 and cesium-137), 1% plutonium and < 1% other transuranic elements (*e.g.*, neptunium, americium, and curium) [1.2]. Successful reprocessing of SNF is achieved by separating each of these components for reentry into the front end of the fuel cycle (*i.e.*, uranium and plutonium) or other purposes such as research or industrial applications (*i.e.*, transuranic elements, fission products). As mentioned before, current practice in the US utilizes a once-through fuel cycle in which all SNF is removed from the reactor and stored. Closing the fuel cycle by reprocessing SNF will allow for used uranium and plutonium to be made into new fuel rods and greatly reduce the burden of SNF disposal by reducing the overall amount in inventory. The most immediate concern when it comes to SNF handling and storage is dealing with the radioactivity and thermal output resulting from the relatively short-lived fission products, namely strontium-90 and cesium-137. With half-lives around 30 years, the removal of these isotopes is a priority in order to simplify the SNF storage process.

Various techniques have been studied for the removal of fission products from SNF (*e.g.*, ion exchange [1.6] and precipitation [1.7]), but the most commonly used method is solvent extraction (or liquid-liquid extraction) [1.8]. Several solvent extraction processes have been developed and are currently in use outside the US, including PUREX (Plutonium URanium EXtraction) [1.10], SREX (StRontium EXtraction) [1.11], TRUEX (TRansUranic EXtraction) [1.12] and other variations (*e.g.*, DIAMEX [1.13], SANEX [1.14] and UNEX [1.15]) [1.8]. The effectiveness of the separation depends on the ability of these processes to remove the radioisotope(s) of interest from the complex mixture of elements present in SNF. Two or more of these processes would typically be run in succession in order to expedite the treatment process.

Work in this laboratory has focused on a variation of the SREX process in which ionic liquids are used in place of the conventional organic solvents typically employed. Considerations for the use of the SREX process center around the complex matrix from which the strontium is extracted. The first step of SNF reprocessing involves the dissolution of the fuel rod pellets in acid (typically nitric acid) [1.16]. Therefore, strontium extraction must function for an acidic aqueous phase. This extraction would probably occur downstream of other extraction processes (*e.g.*, PUREX or TRUEX) that would remove some of the contaminant species in the waste stream. Despite this, the presence of alkali and alkaline earth metals and a multitude of other fission products must be considered. Thus, selective extraction of strontium from a complex and highly acidic aqueous solution is necessary.

The objective of studies described in the following chapters is to investigate the extraction of strontium from acidic media into several ionic liquids (ILs) by a neutral extractant (*i.e.*, a crown ether). The focus of these studies begins with the utilization of various IL families to confirm the generality of trends seen previously for extraction into 1, 3-dialkylimidazolium-based ILs.

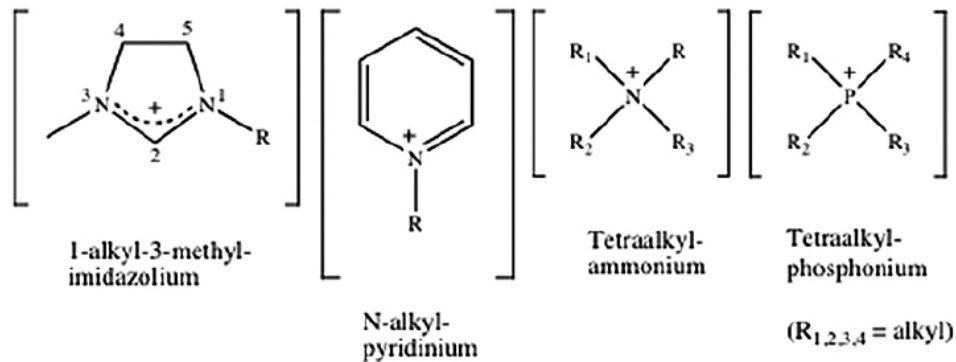
Specifically, the effects of IL structure and aqueous phase anion on the mechanism(s) of metal ion extraction are systematically explored for two additional IL families (*i.e.*, quaternary ammonium- and *N*-alkylpyridinium-based ILs). In an attempt to simplify the selection of ILs for use as extraction solvents and to facilitate the rational design of ILs for specific applications, our emphasis then shifts to the search for a single parameter for use in predicting the balance of extraction pathways in various IL-based systems. Finally, we describe the development of a much-needed method to quantify the individual contributions of the various extraction pathways to the overall extraction mechanism observed in a 1-alkyl-3-methylimidazolium ($C_n\text{mim}^+$) IL-based solvent extraction system.

1.2 Ionic liquids

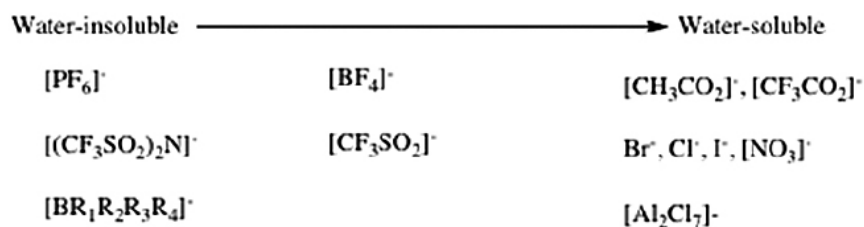
Early reports of ionic liquids [1.17], then known as molten salts, date back to the 1800s, but Walden reported the synthesis of ethylammonium nitrate, the first truly ‘room temperature’ ionic liquid (melting point = 13-14 °C) in 1914 [1.18]. Despite their unique ionic character, their susceptibility to reduction, moisture sensitivity and the limited number of ion combinations yielding a liquid at room temperature resulted in little attention to them until 1992, when Wilkes and Zwartko successfully developed and popularized air- and water-stable room-temperature ILs [1.19]. Their report resulted in an immense increase in attention for these novel liquids across a breadth of applications [1.20-1.22].

The most widely accepted description of an ionic liquid is a salt whose melting point falls below 100 °C. Typically they consist of a bulky, asymmetric organic cation in combination with any of a wide range of anions (Figure 1.2), both organic and inorganic. Low lattice energies caused by the IL cation structure frustrates crystal formation, which drives down the melting point. The IL anion dictates the hydrophobicity of the liquid, and careful selection can yield a hydrophobic

Most commonly used cations:



Some possible anions:



Most commonly used alkyl chains:

ethyl	octyl
butyl	decyl
hexyl	dodecyl

Figure 1.2. Various IL cations, anions and alkyl chain lengths

IL that will create a biphasic mixture when in contact with water. Many physical and chemical properties of ILs are superior to those of conventional organic solvents [1.18, 1.22, 1.23] and are exploited for various uses. Some of these characteristics include a wide liquid range, high thermal stability, low melting points, a near absence of vapor pressure, and tunability. Of particular interest is the ease with which the structure of the cation and anion can be modified, earning ILs the distinction of being ‘designer solvents’. Because of the enormous number of possible IL combinations ($> 10^8$) [1.21], a trial by error approach to identifying the most useful IL for a desired application is clearly illogical, making the identification of structure-property relationships for these compounds essential.

1.3 Characteristics of ionic liquids as solvents

Unlike traditional organic solvents (*i.e.*, molecular) or water, ionic liquids are made up entirely of ions, but they can nonetheless be hydrophobic media [1.20, 1.24]. Many conventional ideas about organic solvents do not apply to ILs because of this characteristic, but it affords them unique properties not observed for molecular organic solvents (*e.g.*, the ability to solvate species with a net charge). Numerous simulation studies have attempted to understand ILs as solvents by describing the general nature of the IL as well as various solvent-solute interactions [1.25-1.40]. Previous reports indicate that the positively charged head groups of the IL cation and the IL anion form a region with highly ionic character, while the aliphatic IL cation tails comprise a second, low-polarity region [1.25, 1.26]. The presence of this inhomogeneity, even for ILs containing high molar fractions of water [1.27, 1.28], has been confirmed experimentally [1.27-1.32] and results in the ability of ILs to solubilize a variety of species (*i.e.*, polar, nonpolar, aromatic, and charged). Polar molecules are solvated by the association of IL cations to the net-negative portion of the molecular dipole of the solute, while the IL anions associate to the net-positive portion [1.33, 1.34].

Nonpolar molecules partition into the aliphatic regions of the ionic liquid due to its overall hydrophobic nature [1.35]. The solubility of aromatic solutes in molecular solvents has been shown to be a result of π - π stacking [1.36-1.38]. ILs have also been shown to effectively solubilize aromatic solutes by the same interactions [1.39, 1.40]. Finally, the ability of ionic liquids to solubilize charged species such as metal complexes due to their ionic character [1.35] makes them complex, but remarkable extraction solvent alternatives.

1.4 Extraction of metal ions into traditional organic solvents and ionic liquids

Conventional liquid-liquid extraction (LLX) of metal ions involves the partitioning of one or more metal-containing species from an aqueous phase into an organic phase. This system can be modified to favor extraction by changing the organic phase, adjusting the aqueous phase pH or ionic strength, or by adding a metal ion-specific extractant to the organic phase. All of these aim to increase the distribution ratio, D_M (Eqn. 1.1), which, when equal volumes of each phase are used, is defined as the concentration of the metal ion in the organic phase divided by the concentration of metal ion in the aqueous phase at equilibrium.

$$D_M = \frac{[M^{n+}]_{org}}{[M^{n+}]_{aq}} \quad (1.1)$$

Extraction is considered to be satisfactory when D_M is greater than 10 (which corresponds to greater than 90.9% extraction). Careful selection of conditions can result in D_M values up to and greater than 10,000 (corresponding to greater than 99.99% extraction). Conversely, ‘poor’ extraction is evident when D_M values fall below 1, which indicates that the metal ion does not favor the organic phase over the aqueous phase under the experimental conditions. (Accordingly, < 50% of the metal ion is found in the organic phase at equilibrium.) In the presence of other species, the metal ion of interest can be selectively extracted using LLX systems by exploiting

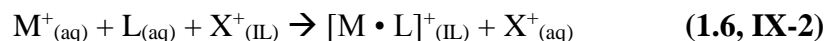
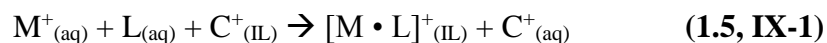
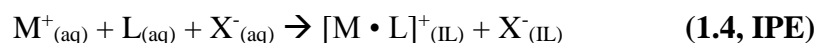
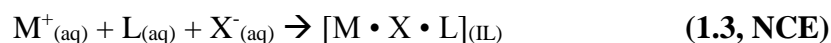
differences in the distribution ratios of the species involved. Equation 1.2 defines α , the separation factor, which is used to describe the selectivity of extraction between two species. Large separation factors indicate that species 1 is extracted selectively, whereas small separation factors (< 1) indicate that the extraction of species 2 is favored.

$$\alpha_{1/2} = \frac{M_1}{M_2} \quad (1.2)$$

Liquid-liquid extraction employing traditional organic solvents represents the major technique used in the various stages of SNF reprocessing (*e.g.*, PUREX, UREX, TRUEX, etc.). The prevalence of LLX is a result of the ability of the technique to be customized to increase the efficiency and selectivity of extraction. Unfortunately, LLX typically employs volatile and / or toxic organic solvents. Huddleston *et al.* [1.41] and Dai *et al.* [1.42] first proposed the use of ILs as alternatives to traditional extraction solvents in the late 1990's. Dai noted that significant improvements in strontium extraction efficiency from acidic solution could be achieved if ILs were employed in place of organic solvents. This study represents the first of many in which organic solvent-based systems were outperformed by IL-based systems.

The higher extraction efficiency sometimes observed for ILs is the result of the presence of several extraction mechanisms that are not possible in systems employing conventional organic solvents. A recent review on metal ion extraction into ILs by Janssen *et al.* [1.35] describes four general modes by which metal ions can partition into ILs in the presence of a neutral extractant while still maintaining electroneutrality. Neutral extraction (or neutral complex extraction, NCE) is defined by Equation 1-3 and involves the formation of a neutral metal-ligand-counterion complex. A similar mechanism is neutral co-extraction (or ion pair extraction, IPE) in which a positive metal-ligand forms an ion pair with the counterion that partitions into the IL phase

(Equation 1-4). (In the case of metal ion extraction from acidic media into an IL by a neutral extractant, the counterion is the aqueous phase anion.) These two modes represent the only means by which metal ions are extracted in systems employing conventional organic solvents and the desired mechanisms when ILs are used as replacements. These modes can be differentiated by assessment of the metal coordination sphere by EXAFS analysis [1.35], but because of their similarity the two will be referred to as a single mechanism, neutral complex / ion pair extraction (NC/IPE).



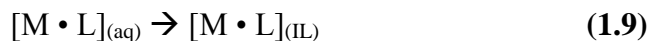
Two additional mechanisms are described for IL-based systems that are forbidden for systems employing conventional organic solvents. Both involve the exchange of a positively charged metal-ligand complex for a positively charged species present in the IL phase, either the IL cation itself (Equation 1-5) or a more hydrophilic counter-cation (Equation 1-6) sometimes added to the system to avoid loss of the IL cation. The process in which the IL cation is exchanged into the aqueous phase is referred to as ‘native’ ion exchange (hereafter abbreviated as IX-1). This process results in depletion of the IL phase and contamination of the aqueous phase. A more hydrophilic (compared to the IL cation) counterion either present in or added to the system will act as a ‘sacrificial’ ion exchanger to compete with the exchange of the IL cation for the metal-ligand complex (hereafter abbreviated as IX-2) [1.43]. (In the case of metal ion extraction from acidic media into an IL by a neutral extractant, the sacrificial ion exchanger is the hydronium ion.)

The improved extraction efficiency first observed by Dai *et al.* [1.42] in IL-based systems originates from the ability of cationic metal species to be extracted *via* ion exchange [1.44], which is not possible in organic solvent-based systems employing a neutral extractant.

1.5 IL-based extractions involving ionizable ligands

The general description of metal ion extraction into ILs in the previous section is confined to the use of a neutral extractant, but numerous studies have explored the use of ionizable extractants in IL-based systems [1.45-1.50]. Examples of the use of ionizable ligands include the extraction of lanthanides into 1-butyl-3-methylimidazolium *bis*[(trifluoromethyl)sulfonyl]imide ($C_4mim^+Tf_2N^-$) by 2-thenoyltrifluoroacetone (HTTA) [1.46], rare earth metals into 1-octyl-3-methylimidazolium *bis*[(trifluoromethyl)sulfonyl]imide ($C_8mim^+Tf_2N^-$) with *N,N*-dioctyldiflycol amic acid (DODGAA) [1.48], copper into 3-butylpyridinium $^+Tf_2N^-$ (in this case, the protic IL cation acts as the ionizable ligand) [1.49], and divalent uranium dioxide into 1-decyl-3-methylimidazolium *bis*[(trifluoromethyl)sulfonyl]imide ($C_{10}mim^+Tf_2N^-$) by dialkylphosphoric or dialkylphosphinic acids [1.50]. Equations 1.3-1.6 do not completely define the mechanism of metal ion extraction when an ionizable ligand is employed. Janssen *et al.* offers two additional descriptions of such systems employing a weakly acidic ligand:

Path A:



Path B:



Path A closely resembles neutral extraction in that a neutral metal-ligand complex partitions into the IL phase, but this requires the formation of the neutral metal-ligand complex which is preceded by the dissociation of the ligand in the aqueous phase. Comparatively, Path B involves the dissociation of the ligand in the IL phase followed by the exchange of the metal ion for an appropriate number of protons to maintain electroneutrality and formation of the neutral metal-ligand complex in the IL phase. It is clear from Equations 1.7-1.11 that several factors influencing the extraction of metal ions by an ionizable extractant include the acidic strength of the ligand, the pH of the aqueous phase, and the hydrophobicity of the metal-ligand complex. The use of ionizable ligands results in multiple additional pathways of ion transfer (*i.e.*, exchange of an anionic complex, exchange of a cationic complex, and partitioning of a neutral complex) each with its own factors affecting metal extraction that further complicate these systems.

1.6 Factors affecting metal ion extraction into ionic liquids

The mechanisms by which metal ion extraction proceeds in IL-based systems is determined by the components making up the extraction system. Numerous studies have investigated the fundamental factors that regulate metal ion extraction into ionic liquids by neutral extractants [1.51-1.59]. Perhaps the most studied factor is the structure of the IL [1.54-1.58]. Generally, when the IL cation hydrophobicity is increased, its exchange into the aqueous phase, and therefore, extraction by IX-1, becomes more difficult [1.54, 1.56, 1.57] due to energetic requirements for the exchange process. Conversely, an increase in the IL anion hydrophobicity favors ion exchange

processes due to mass action considerations [1.55, 1.58]. Metal ion extraction by NC/IPE requires the presence of a counterion, such as the aqueous phase anion when an acidic aqueous phase is employed. Therefore, a higher concentration of aqueous phase anion tends to favor NC/IPE, but may also facilitate extraction by IX-2 due to the presence of a large amount of ‘sacrificial’ ion (Equation 1.6). A very hydrophilic counterion or ‘sacrificial’ ion will be less likely to partition into the IL phase as part of a neutral complex and therefore favor extraction by ion exchange. Another means of suppressing ion exchange in these systems is by the addition of a salt containing one of the ions comprising the IL used to the aqueous phase, thereby exploiting the common ion effect [1.53, 1.54].

It should be obvious at this point that IL-based extraction systems represent complex, but remarkable systems. Despite the recent popularity of ILs, the majority of studies investigating fundamental factors of metal ion extraction employ $C_n\text{mim}^+$ -based ILs, which are still not fully understood. Thorough studies in our laboratory focused on identifying general trends that can be used for the rational design of ILs as extraction solvents have revealed the effects of IL cation structure [1.56, 1.57], IL anion structure [1.58], and aqueous phase anion [1.59] on metal ion extraction by crown ethers. The applicability of these trends to other IL families is currently not known, and is one of several motivations behind the work described in the following chapters.

1.7 Overview of chapters

Chapter 2 extends previous studies conducted in our laboratory focused on investigating the effect of IL cation and anion structure and aqueous phase anion on the extraction of alkali and alkaline earth metal ions into ionic liquids. Quaternary ammonium-based ILs were employed in order to determine if the trends observed previously for 1, 3-dialkylimidazolium-based ILs are general and therefore useful in the rational design of ionic liquids for separation applications.

Chapter 3 describes the extraction behavior of alkali and alkaline earth metal ions into *N*-alkylpyridinium-based ILs. The results of this study confirm the generality of extraction trends observed for both 1, 3-dialkylimidazolium and quaternary ammonium-based ILs. In addition, a previously inadequately appreciated characteristic of hydrophobic ILs, namely the resemblance of the structure of certain IL cations to that of various conventional surfactants, proved powerful in explaining the observed extraction behavior.

Chapter 4 explores the possibility that the octanol-water distribution coefficient of an IL represents the most important single parameter governing the extraction behavior of metal ions in IL-based systems. Comparison of octanol-water distribution coefficients with metal ion extraction data and theoretical models presented in literature suggests that the predominant extraction mechanism could be predicted based solely on the structure of the IL.

Chapter 5 summarizes work that represents the first description of a means to quantify the contributions from each individual mode of metal ion partitioning from acidic media into ionic liquids by a neutral extractant. The quantitative results of this study agree with qualitative trends observed previously for the IL studied 1-pentyl-3-methylimidazolium *bis*[(trifluoromethyl)sulfonyl]imide ($C_5mim^+Tf_2N^-$) [1.56-1.59], and the method developed can be used to confirm many other qualitative trends, such as the effect of IL cation structure, IL anion structure, aqueous phase anion and the Lewis acidity of the metal ion on extraction behavior.

1.8 References

- [1.1] International Atomic Energy Agency, Power Reactor Information System (PRIS), <https://www.iaea.org/PRIS/home.aspx>, accessed 10 February 2017.
- [1.2] U.S. Nuclear Waste Technical Review Board, Commercial Spent Nuclear Fuel, **2016**.
- [1.3] Department of Energy, Strategy for the Management and Disposal of Used Nuclear Fuel and High-Level Radioactive Waste, **2013**.
- [1.4] U.S. Nuclear Regulatory Commission, Stages of the Nuclear Fuel Cycle, <https://www.nrc.gov/materials/fuel-cycle-fac/stages-fuel-cycle.html>, accessed 10 February 2017.
- [1.5] Werner, J.D., U.S. Spent Nuclear Fuel Storage. <https://fas.org/sgp/crs/misc/R42513.pdf>, accessed 10 February 2017.
- [1.6] Wei, Y. Development of an Advanced Ion Exchange Process for Reprocessing Spent Nuclear Fuels. *Journal of Ion Exchange*, **2005**, 16, 102-113.
- [1.7] Mullins, D.; Jarvinen, G.; Mayne, M.; Ford, D.; Long, K.; Reichert, H.; Palmer, P.; Tait, C.D.; Keogh, D.W.; and Gordon, P., Chapter 12 - Crystallization of Uranium Complexes for Partitioning of Spent Nuclear Fuel in Separations for the Nuclear Fuel Cycle in the 21st Century, ACS Symposium Series, American Chemical Society, Washington D.C., **2006**, 183-197.
- [1.8] Sun, X.; Luo, H.; Dai, S., Ionic Liquids-Based Extraction: A Promising Strategy for the Advanced Nuclear Fuel Cycle. *Chemical Reviews*, **2011**, 112, 2100-2128.
- [1.9] Choppin, G.R., Solvent Extraction Processes in the Nuclear Fuel Cycle. *Solvent Extraction Research and Development, Japan* **2005**, 12, 1-10.
- [1.10] Anderson, H.H.; and Asprey, L.B., Solvent Extraction Process for Plutonium, US patent 2924506, 9 February 1960.
- [1.11] Horwitz, E.P.; Dietz, M.L.; Fisher, D.E., SREX. A New Process for the Extraction and Recovery of Strontium from Acidic Nuclear Waste Streams. *Analytical Chemistry*, **1991**, 63, 522-525.
- [1.12] Horwitz, E.P.; Kalina, D.G.; Diamond, H.; Vandegrift, G.F., The TRUEX Process – A Process for the Extraction of the Transuranic Elements from Nitric Acid Wastes Utilizing Modified PUREX Solvent. *Solvent Extraction and Ion Exchange*, **1985**, 3, 75-109.
- [1.13] Musikas, C., Results and Prospects for Some Actinide Extractants Usable in Actinide Partitioning. CEA-CONF—10069, France, **1989**.
- [1.14] Kolarik, Z.; Müllich, U.; Gassner, F., Selective Extraction of Am(III) over Eu(III) by 2,6-ditriazolyl- and 2,6-ditriazinylpyridines. *Solvent Extraction and Ion Exchange*, **1999**, 17, 23-32.

- [1.15] Romanovskiy, V.N.; Smirnov, I.V.; Babain, V.A.; Todd, T.A.; Herbst, R.S; Law, J.D.; Brewer, K.N., The Universal Solvent Extraction (UNEX) Process. I. Development of the UNEX Process Solvent for the Separation of Cesium, Strontium, and the Actinides from Acidic Radioactive Waste. *Solvent Extraction and Ion Exchange*, **2001**, 19, 1-21.
- [1.16] Desigan, N.; Bhatt, N.P.; Pandey, N.K.; Mudali, U.K.; Natarajan, R.; Joshi, J.B., Mechanism of Dissolution of Nuclear Fuel in Nitric Acid Relevant to Nuclear Fuel Reprocessing. *Journal of Radioanalytical and Nuclear Chemistry*, **2017**, 312, 141-149.
- [1.17] Davy, H, *Researches, Chemical and Philosophical: Chiefly Concerning Nitrous Oxide or Dephlogisticated Nitrous Air and Its Respiration*. Biggs and Cottle, Bristol: London, **1800**.
- [1.18] Brennecke, J.F.; Maginn, E.J., Ionic Liquids: Innovative Fluids for Chemical Processing. *AIChE Journal*, **2001**, 47, 2384-2389.
- [1.19] Wilkes, J.S.; Zaworotko, M.J., Air and Water Stable 1-ethyl-3-methylimidazolium Based Ionic Liquids. *Journal of the Chemical Society, Chemical Communications*, **1992**, 965-967.
- [1.20] Hallett, J.P.; Welton, T., Room-Temperature Ionic Liquids: Solvents for Synthesis and Catalysis. *Chemical Reviews*, **2011**, 111, 3508-3576.
- [1.21] Plechkova, N.V; Seddon, K.R. Applications of Ionic Liquids in the Chemical Industry. *Chemical Society Reviews*, **2008**, 37, 123-150.
- [1.22] Dietz, M.L, Ionic Liquids as Extraction Solvents: Where do We Stand? *Separation Science and Technology*, **2006**, 41, 2047-2063.
- [1.23] Seddon, K.R., Room-Temperature Ionic Liquids: Neoteric Solvents for Clean Catalysis. *Kinetic Catalysis*, **1996**, 37, 693-697.
- [1.24] Chiappe, C.; Malvadi, M.; Pomelli, C.S., Influence of Chloride, Water, and Organic Solvents on the Physical Properties of Ionic Liquids. *Pure and Applied Chemistry*, **2000**, 72, 2275-2287.
- [1.25] Shimizu, K.; Bernardes, C.E.S.; Lopes, J.N.C., The Complex Structure of Ionic Liquids at an Atomistic Level: From “Red-and-Greens” to Charge Templates. *Pure and Applied Chemistry*, **2014**, 86, 119-133.
- [1.26] Wang, Y.; Voth, G.A., Unique Spatial Heterogeneity in Ionic Liquids. *Journal of the American Chemical Society*, **2005**, 127, 12192-12193.
- [1.27] Hanke, C.G.; Lynden-Bell, R.M., A Simulation Study of Water—Dialkylimidazolium Ionic Liquid Mixtures. *Journal of Physical Chemistry B*, **2003**, 107, 10873-10878.
- [1.28] Rollet, A.-L.; Porion, P.; Vaultier, M.; Billard, I.; Deschamps, M.; Bessada C.; Jouvensal, L., Anomalous Diffusion of Water in [BMIM][TFSI] Room-Temperature Ionic Liquid. *Journal of Physical Chemistry B*, **2007**, 111, 11888-11891.

- [1.29] Triolo, A.; Russina, O.; Bleif, H.-J.; Di Cola, E., Nanoscale Segregation in Room Temperature Ionic Liquids. *Journal of Physical Chemistry B*, **2007**, 111, 4641-4644.
- [1.30] Russina, O.; Triolo, A., New Experimental Evidence Supporting the Mesoscopic Segregation Model in Room Temperature Ionic Liquids. *Faraday Discussions*, **2012**, 154, 97-109.
- [1.31] Xiao, D.; Rajian, J.R.; Cady, A.; Li, S.; Bartsch, R.A.; Quitevis, E.L., Nanostructural Organization and Anion Effects on the Temperature Dependence of the Optical Kerr Effect Spectra of Ionic Liquids. *Journal of Physical Chemistry B*, **2007**, 111, 4669-4677.
- [1.32] Ghoshdastidar, D.; Senapati, S., Nanostructural Reorganization Manifests in *Sui-Generis* Density Trend in Imidazolium Acetate/Water Binary Mixtures. *Journal of Physical Chemistry B*, **2015**, 119, 10911-10920.
- [1.33] Kobrak, M.N., Electrostatic Interactions of a Neutral Dipolar Solute with a Fused Salt: A New Model for the Solvation in Ionic Liquids. *Journal of Physical Chemistry B*, **2007**, 111, 4755-4762.
- [1.34] Kobrak, M.N., The Relationship Between Solvent Polarity and Molar Volume in Room-Temperature Ionic Liquids. *Green Chemistry*, **2008**, 10, 80-86.
- [1.35] Janssen, C.H.C.; Macías-Ruvalcaba, N.A.; Aguilar-Martinez, M.; Kobrak, M.N., Metal Extraction to Ionic Liquids: The Relationship between Structure, Mechanism and Application. *International Reviews in Physical Chemistry*, **2015**, 34, 591-622.
- [1.36] Cabarcos, O.M.; Weinheimer, C.J.; Lisy, J.M., Quantum-Chemistry-Based Force Field for 1,2-Dimethoxyethane and Poly(ethylene oxide) in Aqueous Solution. *Journal of Physical Chemistry B*, **1998**, 102, 996-1001.
- [1.37] Dougherty, D.A., The Cation- π Interaction. *Accounts of Chemical Research*, **2013**, 46, 885-893.
- [1.38] Mecozzi, S.; West, A.P.; Dougherty, D.A., Cation- π Interactions in Aromatics of Biological and Medicinal Interest: Electrostatic Potential Surfaces as a Useful Qualitative Guide. *Proceedings of the National Academy of Sciences USA*, **1996**, 93, 10566-10571.
- [1.39] Hanke, C.G.; Johansson, A.; Harper, J.B.; Lynden-Bell, R.M., Why are Aromatic Compounds More Soluble than Aliphatic Compounds in Dimethylimidazolium Ionic Liquids? A Simulation Study. *Chemical Physics Letters*, **2003**, 374, 85-90.
- [1.40] Cao, Z.; Li, S.; Yan, T., Cation- π Interactions between a Free-Base Porphyrin and an Ionic Liquid: A Computational Study. *ChemPhysChem*, **2012**, 13, 1743-1747.
- [1.41] Huddleston, J.G.; Visser, A.E.; Reichert, W.M.; Willauer, H.D.; Broker, G.A.; Rogers, R.D., Characterization and Comparison of Hydrophilic and Hydrophobic Room Temperature Ionic Liquids Incorporating the Imidazolium Cation. *Green Chemistry*, **2001**, 3, 156-162.

- [1.42] Dai, S.; Ju, Y.H.; Barnes, C.E., Solvent Extraction of Strontium Nitrate by a Crown Ether Using Room-Temperature Ionic Liquids. *Journal of the Chemical Society, Dalton Transactions*, **1999**, 1201-1202.
- [1.43] Katsuta, S.; Yoshimoto, Y.; Okai, M.; Takeda, Y.; Bessho, K., Selective Extraction of Palladium and Platinum from Hydrochloric Acid Solutions by Trioctylammonium-Based Mixed Ionic Liquids. *Industrial and Engineering Chemistry Research*, **2011**, 50, 12735-12740.
- [1.44] Dietz, M.L.; Dzielawa, J.A., Ion-Exchange as a Mode of Cation Transfer into Room-Temperature Ionic Liquids Containing Crown Ethers: Implications for the “Greenness” of Ionic Liquids as Diluents in Liquid-Liquid Extraction. *Chemical Communications*, **2001**, 2124-2125.
- [1.45] Jensen, M.P.; Borkowski, M.; Laszak, I.; Beitz, J.V.; Rickert, P.G.; Dietz, M.L., Anion Effects in the Extraction of Lanthanide 2-Thenoyltrifluoroacetone Complexes into an Ionic Liquid. *Separation Science and Technology*, **2012**, 47, 233-243.
- [1.46] Jensen, M.P.; Neufeind, J.; Beitz, J.V.; Skanthakumar, S.; Soderholm, L., Mechanisms of Metal Ion Transfer into Room-Temperature Ionic Liquids: The Role of Anion Exchange. *Journal of the American Chemical Society*, **2003**, 125, 15466-15473.
- [1.47] Ouadi, A.; Gadenne, B.; Hesemann, P.; Moreau, J.J.E.; Billard, I.; Gaillard, C.; Mekki, S.; Moutiers, G., Task-Specific Ionic Liquids Bearing 2-Hydroxybenzylamine Units: Synthesis and Americium-Extraction Studies. *Chemistry – A European Journal*, **2006**, 12, 3074-3081.
- [1.48] Yang, F.; Baba, Y.; Kubota, F.; Kamiya, N.; Goto, M., Extraction and Separation of Rare Earth Metal Ions with DODGAA in Ionic Liquids. *Solvent Extraction Research and Development, Japan*, **2012**, 19, 69-76.
- [1.49] Reyna-González, J.M.; Galicia-Pérez, R.; Reyes-López, J.C.; Aguilar-Martínez, M., Extraction of Copper (II) from Aqueous Solutions with the Ionic Liquid 3-Butylpyridinium Bis(trifluoromethanesulfonyl)imide. *Separation and Purification Technology*, **2012**, 89, 320-328.
- [1.50] Cocalia, V.A.; Jensen, M.P.; Holbrey, J.D.; Spear, S.K.; Stepinski, D.C.; Rogers, R.D., Identical Extraction Behavior and Coordination of Trivalent or Hexavalent f-element Cations Using Ionic Liquid and Molecular Solvents. *Dalton Transactions*, **2005**, 11, 1966-1971.
- [1.51] Domńska, U.; Rekawek, A., Extraction of Metal Ions from Aqueous Solutions Using Imidazolium Based Ionic Liquids. *Journal of Solution Chemistry*, **2009**, 38, 739-751.
- [1.52] Heitzman, H.; Young, B.A.; Rausch, D.J.; Rickert, P.; Stepinski, D.C.; Dietz, M.L., Fluorous Ionic Liquids as Solvents for the Liquid-Liquid Extraction of Metal Ions by Macrocyclic Polyethers. *Talanta*, **2006**, 69, 527-531.

- [1.53] Janssen, C.H.C.; Sánchez, A.; Kobrak, M.N., Selective Extraction of Metal Ions from Aqueous Phase to Ionic Liquids: A Novel Thermodynamic Approach to Separations. *ChemPhysChem*, **2014**, 15, 3536-3543.
- [1.54] Janssen, C.H.C.; Sánchez, A.; Witkamp, G.J.; Kobrak, M.N., A Novel Mechanism for the Extraction of Metals from Water to Ionic Liquids. *ChemPhysChem*, **2013**, 14, 3806-3813.
- [1.55] Luo, H.; Dai, S.; Bonnesen, P.V.; Haverlock, T.J.; Moyer, B.A.; Buchanan III, A.C., A Striking Effect of Ionic-Liquid Anions in the Extraction of Sr^{2+} and Cs^+ by Dicyclohexano-18-Crown-6. *Solvent Extraction and Ion Exchange*, **2006**, 24, 19-31.
- [1.56] Dietz, M.L.; Dzielawa, J.A., Laszak, I.; Young, B.A., Jensen, M.P., Influence of Solvent Structural Variations on the Mechanism of Facilitated Ion Transfer into Room-Temperature Ionic Liquids. *Green Chemistry*, **2003**, 5, 682-685.
- [1.57] Hawkins, C.A.; Garvey, S.L.; Dietz, M.L., Structural Variations in Room-Temperature Ionic Liquids: Influences on Metal Ion Partitioning Modes and Extraction Selectivity. *Separation and Purification Technology*, **2012**, 89, 31-38.
- [1.58] Garvey, S.L.; Dietz, M.L., Ionic Liquid Anion Effects in the Extraction of Metal Ions by Macrocyclic Polyethers. *Separation and Purification Technology*, **2014**, 123, 145-152.
- [1.59] Garvey, S.L.; Hawkins, C.A.; Dietz, M.L., Effect of Aqueous Phase Anion on the Mode of Facilitated Ion Transfer into Room-Temperature Ionic Liquids. *Talanta*, **2012**, 95, 25-30.

Chapter 2:

Extraction of alkali and alkaline earth metals by dicyclohexano-18-crown-6 (DCH18C6) into quaternary ammonium-based ionic liquids (ILs)

2.1 Introduction

Although numerous ILs have been evaluated for their use in LLX extraction, studies of the factors underlying the observed extraction behavior have been largely confined to 1, 3-dialkylimidazolium ILs (hereafter abbreviated as $C_n\text{mim}^+\text{X}^-$ where X^- = hexafluorophosphate (PF_6^-), *bis*[(trifluoromethyl)sulfonyl]imide (Tf_2N^-) or *bis*[(perfluoroethyl)sulfonyl]imide (BETI^-)) [2.1-2.10]. These studies have demonstrated that the process of metal ion extraction into ILs in the presence of a neutral extractant is significantly more complex than is the corresponding process in a conventional organic solvent, with the overall partitioning incorporating contributions from neutral complex / ion-pair extraction (NC/IPE) and one or more forms of ion exchange (IX-1 and/or IX-2). These studies have also clarified the effect of a variety of IL and solution characteristics on the balance among these possible extraction pathways, including the IL cation [2.7, 2.3] and anion [2.4] hydrophobicity and the aqueous phase anion hydration energy [2.2]. They have not, however, addressed the extent to which the observations reported represent a generic (*i.e.*, general) description of IL-based metal ion extraction systems. One of the more commonly noted characteristics of ILs is their tunability, affording millions of IL cation and anion combinations [2.13]. Unfortunately, until a general description of IL-based LLX systems is developed, extensive and tedious extraction studies (such as those presented here) are required to understand metal ion partitioning in each new IL-based system.

For an IL-based extraction system to be regarded as a viable alternative to a traditional organic solvent-based system, it must extract metal ions either more efficiently (as reflected in the magnitude of the metal ion distribution ratios) or more selectively (as reflected in the observed separation factors). To date, only $C_n\text{mim}^+$ ILs have been systematically examined as solvents for LLX. Thus, it remains unclear if the choice of IL family (*e.g.*, 1, 3-dialkylimidazolium *vs.* quaternary ammonium *vs.* *N*-alkylpyridinium-based ILs) significantly alters either the extraction efficiency or the extraction selectivity. To address this issue, extensive studies of the extraction of several alkali and alkaline earth cations into a series of quaternary ammonium- (described in this chapter) and *N*-alkylpyridinium-based ILs (described in the next chapter) containing dicyclohexano-18-crown-6 (DCH18C6) were conducted. While various quaternary ammonium salts (*e.g.*, Aliquat 336) [2.14-2.19], have long been known as extractants, their use as extraction solvents represents a more recent development [2.20, 2.21]. This study then, in addition to facilitating the development of a general description of the fundamental aspects of the partitioning of metal ions into ILs, will provide much needed practical information on the behavior of quaternary ammonium salts as extraction solvents.

2.2 Experimental

2.2.1 Materials

Bromide salts of tetraalkylammonium ($N_{n,n,n,n}^+\text{Br}^-$ where $n = 8, 10, \text{ or } 12$; Sigma-Aldrich, Milwaukee, WI) and trimethylalkylammonium ($N_{n,111}^+\text{Br}^-$, where $n = 8, 10, \text{ or } 12$; TCI America, Portland, OR) salts were purchased and used without further purification. For metathesis of the bromide salts to the desired anion form, the lithium salts of *bis*[(trifluoromethyl)sulfonyl]imide, $\text{Li}^+\text{Tf}_2\text{N}^-$, (TCI America, Portland, OR) and *bis*[(perfluoroethyl)sulfonyl]imide, Li^+BETI^- , (3M, St. Paul, MN) were employed. Commercially available radiotracers $^{133}\text{BaCl}_2$ (Isotope Products

Laboratories, Burbank, CA), $^{22}\text{NaCl}$ (Isotope Products Laboratories), and $^{85}\text{SrCl}_2$ (Perkin Elmer, Waltham, MA) were used for extraction studies. The neutral extractant employed was a mixture of the *cis-syn-cis* (A) and *cis-anti-cis* (B) isomers of dicyclohexano-18-crown-6 (DCH18C6, Parish Chemical Company, Orem, UT). Acid solutions were prepared from trace-metal grade concentrated nitric or hydrochloric acid (OptimaTM, Fisher, Fair Lawn, NJ) and were standardized by titration with standard sodium hydroxide (Ricca, Arlington, TX) using phenolphthalein indicator (Ricca, Arlington, TX). All aqueous solutions were prepared with deionized water with a specific resistance of at least 18 M Ω /cm.

2.2.2 Instruments

A Mettler Toledo AL204 balance was employed for all weighing. Karl Fischer titrations to measure the ionic liquid water content were performed on a Metrohm 870 KF Titrino Plus volumetric titrator. Due to the absence of a chromophore in the quaternary ammonium structure, the water solubility could not be determined spectrophotometrically. Instead, the solubility was determined using an Agilent 1200 series HPLC system with no column installed acting as a sample introduction system to a Varian 380-LC Evaporative Light Scattering Detector (ELSD). Radiometric assays were done *via* gamma spectroscopy on a Perkin Elmer Model 2480 Automatic Gamma Counter using standard procedures. In studies of the extraction of metal ions from water, nitrate concentrations were measured with a Dionex ICS-1000 ion chromatograph equipped with a conductivity detector, a Dionex IonPac AG12A column (4 \times 50 mm), and a Dionex ASRS 300 (4mm) conductivity suppressor. A mobile phase comprising 3.2 mM Na_2CO_3 and 1.0 mM NaHCO_3 (flow rate of 0.80 mL/min) was employed. An example ion chromatogram is provided in the Appendix.

2.2.3 Methods

Ionic liquid synthesis. The quaternary ammonium-based ionic liquids used in these studies were prepared from their bromide salts using established methods [2.22, 2.23]. Aqueous solutions of each quaternary ammonium bromide salt was combined with an aqueous solution (3% molar excess) of the lithium salt of *bis*[(trifluoromethyl)sulfonyl]imide, $\text{Li}^+\text{Tf}_2\text{N}^-$ or *bis*[(perfluoroethyl)sulfonyl]imide, Li^+BETf . This mixture was then left to stir overnight, during which time the product IL appeared as a separate phase. The aqueous phase was then removed and the water-insoluble ionic liquid remaining was washed with at least five aliquots of water. Each wash was tested with silver nitrate to determine if halide was present. Washing was continued until the formation of a silver halide precipitate was no longer observed.

Density measurements. The mass of an empty pipet tip was recorded and a known volume of IL was drawn up into the tip using an automatic pipette. The mass of the IL was determined in triplicate by subtracting the mass of the empty tip from the total mass of the IL sample in the tip. This value was then divided by the volume to determine the density of each IL.

Water solubility and content. A 1 mL aliquot of each trimethylalkylammonium-based IL was preconditioned three times by contacting the IL with 2 mL of water. This mixture was vortexed and then centrifuged, and the aqueous phase was removed and discarded. Once the IL phase had been preconditioned, 1 mL of water was added to it and the mixture was vortexed. After standing undisturbed overnight, the mixture was centrifuged to disengage the phases. The aqueous phase was then removed to determine the concentration of the IL present by evaporative light scattering. The concentration of water present in the IL phase was then determined by Karl Fischer titration.

Determination of metal ion distribution ratios. The extent of metal ion extraction, as reflected in values of the metal ion distribution ratios (D_M , defined as $[M_{org}] / [M_{aq}]$ at equilibrium), was determined for barium, sodium and strontium radiometrically using commercial radiotracers. All extraction experiments employing an acidic aqueous phase were conducted with 0.1 M DCH18C6 in the ionic liquid phase. Extraction from water was conducted according to previous reports [2.7, 2.3] with 0.2 M DCH18C6 in the ionic liquid phase. This higher crown ether concentration for systems employing water as the aqueous phase is necessitated by the absence of added nitric acid/nitrate, which results in reduced D_M values.

Extraction from water. The percentage of metal ion extracted from water ($\%E_M$) was measured by preconditioning an aliquot of IL containing 0.2 M DCH18C6 two times with twice its volume of water. After preconditioning, an equivolume aliquot of 0.0310 M $M^{n+}(\text{NO}_3^-)_n$ solution (nominal, where $M^{n+} = \text{Na}^+$, Ba^{2+} , or Sr^{2+}) was added to the IL phase. Sodium-22, barium-133 or strontium-85 radiotracer was then introduced and the mixture vortexed. After standing for 15 minutes to allow equilibrium to be reached, the mixture was centrifuged to disengage the phases. The separated aqueous and IL phases were then sampled and counted.

The percentage of nitrate extracted from water ($\%E_{\text{NO}_3^-}$) was determined by conducting the same liquid-liquid extraction as described in the determination of $\%E_M$ without addition of the radiotracer. The concentration of nitrate in the 0.0310 M $M^{n+}(\text{NO}_3^-)_n$ stock solution (where $M^{n+} = \text{Na}^+$, Ba^{2+} , or Sr^{2+}) and the aqueous phase following extraction were measured by ion chromatography. Dividing the difference in the nitrate concentration of the metal nitrate stock solution and the aqueous phase after extraction by the concentration of the metal nitrate stock solution gives the percentage of nitrate extracted from the aqueous phase.

Extraction from acid. Distribution ratios (D_M) were measured by preconditioning an aliquot of IL containing 0.1 M DCH18C6 twice with various nitric and hydrochloric acid solutions. After preconditioning was complete, an equivolume aliquot of the acid solution was added to the IL phase. Sodium-22, barium-133 or strontium-85 radiotracer was then introduced and the mixture vortexed and allowed to equilibrate for 15 minutes. Following centrifugation to disengage the phases, the aqueous and IL phases were separated and sampled for counting.

2.3 Results and Discussion

2.3.1 Physical properties

The measured physical properties of the ILs studied are listed in Table 2.1. Consistent with previous observations for other ILs [2.24, 2.25], the density of the quaternary ammonium ILs decreases as their alkyl chain length increases. An increase in the alkyl chain length for a homologous series of ILs (*e.g.*, $N_{8,111}^+Tf_2N^-$, $N_{10,111}^+Tf_2N^-$, and $N_{12,111}^+Tf_2N^-$) also results in a decrease in water content and water solubility for the Tf_2N^- ILs, again in agreement with prior observations for other IL families [2.25]. Unexpectedly, the water content of the $N_{n,111}^+BETI^-$ IL series actually rises as the alkyl chain length is increased, despite the fact that the hydrophobicity of the IL cation is increasing. While the reason for this is unclear at present, it is worth noting that a similar observation has been reported previously for the $BETI^-$ form of a series of C_nmim^+ ILs [2.4].

Primary alcohols are regarded as the industry standard for LLX systems and thus a benchmark against which to compare ILs. The physical properties of a series of primary alcohols are therefore included in Table 2.1 for comparison. A slight increase in density is observed as the alkyl chain length is increased, while the water content and water solubility decreases. The density

Table 2.1
Physical properties of ILs studied^a

	Density - "dry" (g/mL)	Water content - "wet" (ppm)	Water solubility ([IL], μM)
$\text{N}_{8,111}\text{Tf}_2\text{N}$	1.253 ± 0.010	9350 ± 64	3450 ± 369
$\text{N}_{10,111}\text{Tf}_2\text{N}$	1.234 ± 0.003	8144 ± 177	693 ± 58
$\text{N}_{12,111}\text{Tf}_2\text{N}$	1.225 ± 0.004	6701 ± 350	276 ± 51
$\text{N}_{8,111}\text{BETI}$	1.320 ± 0.007	4655 ± 255	3690 ± 362
$\text{N}_{10,111}\text{BETI}$	1.294 ± 0.016	5543 ± 290	670 ± 141
$\text{N}_{12,111}\text{BETI}$	1.253 ± 0.018	6099 ± 208	317 ± 20
$\text{N}_{7,7,7,7}\text{Tf}_2\text{N}$	NM ^b	4585 ± 393	NM ^b
$\text{N}_{8,8,8,8}\text{Tf}_2\text{N}$	NM ^b	3474 ± 83	NM ^b
$\text{N}_{10,10,10,10}\text{Tf}_2\text{N}$	NM ^b	2949 ± 155	NM ^b
1-hexanol	0.8136^c	65200^d	68200^d
1-heptanol	0.8219^c	15835^d	66300^d
1-octanol	0.8262^c	3760^d	43500^d

^a Uncertainties are reported at the 95% confidence level.

^b Due to availability of IL, value was not measured.

^c Values obtained from the 84th edition of the CRC Handbook of Chemistry and Physics

^d Values obtained from reference [2.26].

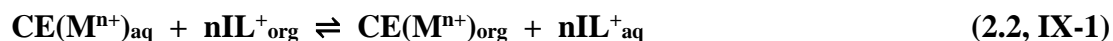
of the ILs studied here is greater than the primary alcohols, which has its benefits on a small scale, as the more viscous organic phase will be the bottom phase during LLX studies. This is particularly beneficial during the preconditioning of the IL phase, as the less viscous aqueous phase can be easily removed without significant loss of the IL. Density considerations are less of a concern from an industrial standpoint given the ability to design LLX processes to accommodate the denser organic phase. It is obvious that the ILs have lower mutual solubility with water compared to the primary alcohols. This is advantageous for LLX systems as it reduces the need to replace the solvent inventory and could lead to reduced phase carryover in an IL-based system.

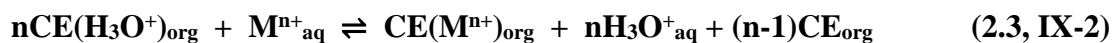
2.3.2 Three-path model of metal ion extraction

As is well known, the extraction of alkali and alkaline earth cations by a neutral extractant such as a crown ether into a traditional (*i.e.*, molecular) organic solvent involves the partitioning of a neutral complex / ion pair (Equation 2.1) [2.3].



Previous studies have shown that when ILs are substituted for traditional organic solvents in these systems, other modes of partitioning arise, namely ion-exchange processes [2.6]. This has led to the development of a so-called “three-path model” to explain the acid dependencies observed for IL-based solvent extraction systems (Figure 2.1) [2.9]. This model incorporates two forms of ion exchange in addition to neutral complex / ion pair extraction, one in which the IL cation is exchanged for the charged metal-extractant (*i.e.*, crown ether) complex (IX-1, Equation 2.2) and a second form involving exchange of the metal ion for a proton present in a protonated extractant molecule produced during acid preconditioning of the IL phase (IX-2, Equation 2.3).





Both forms of ion exchange are detrimental to the recovery of the IL phase for subsequent reuse, as both involve loss of the cationic component of the IL to the aqueous phase. All three modes of metal ion partitioning are in competition with each other, and the experimental conditions are expected to dictate which mode(s) are favored for a given system. Prior work in our laboratory has shown that among the more important factors governing the relative contributions of the paths are the IL cation [2.7] and anion [2.27] hydrophobicity and the hydration energy of the aqueous phase anion [2.2]. The specific role of each in quaternary ammonium IL-based extraction systems is described in detail in the following sections.

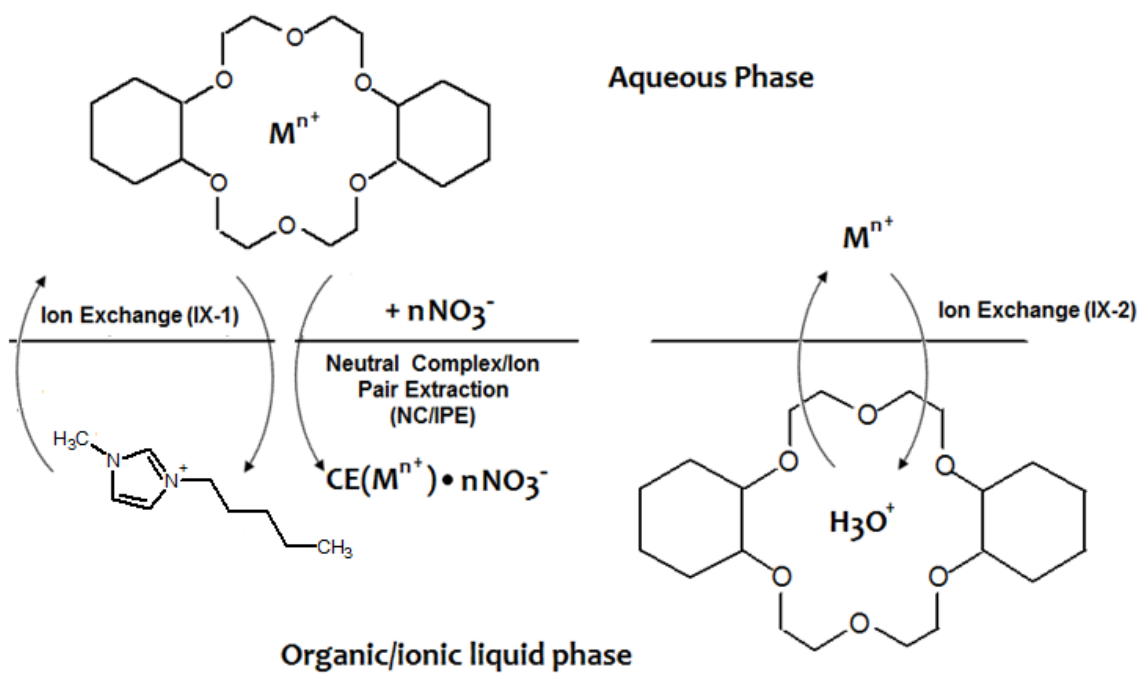


Figure 2.1. Three pathway model of metal ion extraction for a system comprising a neutral extractant (DCH18C6) dissolved in a $C_n\text{mim}^+$ -based IL in contact with nitric acid.

2.3.3 Extraction from water

Prior work [2.3, 2.7, 2.9] has shown that efforts to understand the metal ion partitioning process in IL-based extraction systems are facilitated by studies involving extraction from water. As a first step toward understanding the extraction of metal ions into ILs, the extraction of nitrate ($\%E_{NO_3^-}$) and the metal ions of interest ($\%E_M$) from water (*i.e.*, in the absence of nitric acid in the aqueous phase) was determined. Studying the extraction from water eliminates one of the three possible modes of partitioning, specifically, IX-2 (which requires a protonated crown ether molecule), thereby simplifying interpretation of the extraction data. Measurement of the extraction percentages for the various quaternary ammonium-based ILs according to a published method [2.7] yielded the results shown in Table 2.2.

If neutral complex / ion pair extraction is the predominant mode of partitioning, the ratio of $\%E_M$ and $\%E_{NO_3^-}$ (hereafter referred to as the extraction ratio, R) will approach unity. Values of $\%E_{NO_3^-}$ much lower than $\%E_M$, resulting in large values of R, indicate that some metal ion extraction is occurring without nitrate co-extraction (*i.e.*, NC/IPE), and thus are indicative of the presence of ion-exchange processes [2.7]. Consistent with a trend seen previously for $C_n\text{mim}^+$ -based IL systems [2.3, 2.7] the results show that as the hydrophobicity of the IL cation increases, there is a shift towards neutral complex / ion pair extraction, as indicated by the decrease in the value of R. In other words, extraction of metal ions into ILs with a longer alkyl chain length from water tends to proceed by NC/IPE more so than an IL with a shorter alkyl chain, suggesting that high IL cation hydrophobicity is preferred for IL-based LLX systems.

Table 2.2
Effect of IL structure on metal ion and nitrate extraction from water by DCH18C6 (0.2 M)
into various $N_{n,111}^+$ ILs ^{a, b}

Metal	IL	%E_M	%E_{NO₃⁻}	R	Predominant partitioning mode
Sr	N _{8,111} Tf ₂ N	46.4	16.5 ± 0.3	2.81	cation exchange
	N _{10,111} Tf ₂ N	15.7	12.1 ± 0.6	1.30	neutral complex
	N _{12,111} Tf ₂ N	8.2	8.2 ± 0.9	1.00	neutral complex
	N _{8,111} BETI	45.5	4.7 ± 0.2	9.68	cation exchange
	N _{10,111} BETI	6.6	3.1 ± 0.3	2.13	mixed
	N _{12,111} BETI	2.6	1.3 ± 0.1	2.00	mixed
Ba	N _{8,111} Tf ₂ N	57.2	17.5 ± 0.2	3.27	cation exchange
	N _{10,111} Tf ₂ N	19.8	13.2 ± 0.4	1.50	neutral complex
	N _{12,111} Tf ₂ N	7.3	7.0 ± 0.9	1.04	neutral complex
	N _{8,111} BETI	27.2	6.4 ± 0.3	4.25	cation exchange
	N _{10,111} BETI	5.6	4.9 ± 0.2	1.14	neutral complex
	N _{12,111} BETI	2.5	2.4 ± 0.1	1.04	neutral complex
Na	N _{8,111} Tf ₂ N	59.9	2.4 ± 0.6	25.0	cation exchange
	N _{10,111} Tf ₂ N	24.4	5.0 ± 0.1	4.88	cation exchange
	N _{12,111} Tf ₂ N	9.3	8.1 ± 0.4	1.15	neutral complex
	N _{8,111} BETI	51.2	0.8 ± 0.4	64.0	cation exchange
	N _{10,111} BETI	9.4	1.2 ± 0.5	7.83	cation exchange
	N _{12,111} BETI	3.0	2.2 ± 0.5	1.36	neutral complex

^a Uncertainties are reported at the 95% confidence level. %E values reported without uncertainties represent the average of duplicate measurements.

^b Initial metal salt concentrations were 0.031 M.

2.3.4 Effect of IL cation hydrophobicity on extraction from acidic nitrate media

Metal ion extraction from nitric acid solutions into a series of quaternary ammonium-based ILs incorporating four equivalent alkyl chains (*i.e.*, $N_{n,n,n,n}^+Tf_2N^-$ ILs) was next examined. The dependency of the extraction of Sr^{2+} by DCH18C6 (0.1 M) on nitric acid concentration into these ILs (Figure 2.2) follows the same *general* trend (*i.e.*, typically, increasing D_{Sr} with an increase in $[HNO_3]$) as seen for 1-octanol. This is promising because the shape of the acid dependency suggests that the desired mode of metal ion partitioning, namely NC/IPE, is the predominant path. Unfortunately, the D_{Sr} values are much lower at any given acidity than those observed for 1-octanol. That is to say, the tetraalkylammonium IL-based systems exhibit the correct mode of extraction, but are apparently not as efficient as extraction solvents as are more traditional organic diluents.

In contrast to prior reports describing extraction of strontium into $C_nmim^+Tf_2N^-$ ILs (where $n = 5, 6, 8,$ and 10) by the same extractant [2.3], there is little effect on the shape and direction of the dependency when the IL cation hydrophobicity is increased. Undoubtedly, this is due to the large carbon count in the quaternary ammonium ILs (28, 32, and 40 for $N_{n,n,n,n}^+Tf_2N^-$ ILs *vs.* 10, 13, and 15 for the $C_nmim^+Tf_2N^-$ ILs), which results in a very hydrophobic IL cation that is not prone to ion-exchange processes. Although these ILs demonstrate again that high IL hydrophobicity results in a shift away from ion exchange [2.3], they provide unacceptably low strontium distribution ratios. In addition, their high viscosity and tendency towards phase inversion make them difficult to handle. As a result, no further work was done using these symmetrical tetraalkylammonium-based ILs.

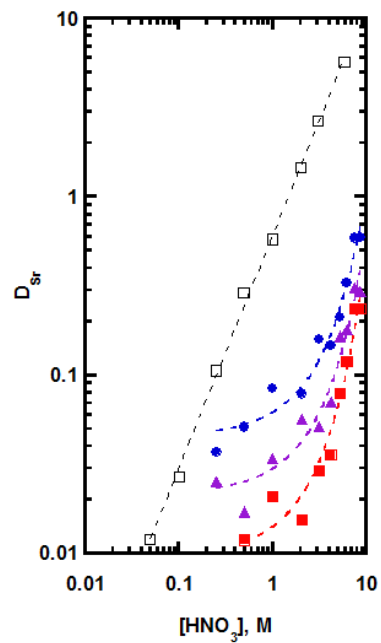


Figure 2.2. Effect of HNO_3 concentration on the extraction of Sr^{2+} by 0.1 M DCH18C6 into 1-octanol (open, black squares), $N_{7,7,7,7}^+Tf_2N^-$ (solid, blue circles), $N_{8,8,8,8}^+Tf_2N^-$ (solid, red squares) and $N_{10,10,10,10}^+Tf_2N^-$ (solid, purple triangles).

Figure 2.3 shows the nitric acid dependency of the extraction of representative alkali (Na^+) and alkaline earth (Sr^{2+} and Ba^{2+}) metal ions into several members of another group of quaternary ammonium-based ILs, designated as $\text{N}_{n,111}^+\text{Tf}_2\text{N}^-$ ILs, in which three of the four alkyl substituents are methyl groups. For Sr^{2+} (middle panel), extraction into the shortest chain IL ($\text{N}_{8,111}^+\text{Tf}_2\text{N}^-$) seems to favor ion exchange for $[\text{HNO}_3] < 2 \text{ M}$, as indicated by the decrease in D_{Sr} as the acid concentration increases. For HNO_3 concentrations above 2 M, an upturn is observed, whereby D_{Sr} rises with acid concentration, consistent with increased partitioning of a neutral complex / ion pair. When the alkyl chain length of the IL cation is increased, a downward shift in distributions ratios at low acid concentration is observed, consistent with increasing cation hydrophobicity and thus, greater difficulty of ion exchange processes involving the cation. For extraction into both $\text{N}_{10,111}^+\text{Tf}_2\text{N}^-$ and $\text{N}_{12,111}^+\text{Tf}_2\text{N}^-$, increasing D_{Sr} with acidity is observed up to *ca.* 1 M HNO_3 (suggesting that NC/IPE predominates), after which a downturn, possibly due to competition for the extractant by the acid present, is observed.

A similar shift from ion exchange towards neutral complex / ion pair extraction is seen for Ba^{2+} (right panel) when the hydrophobicity of the IL cation is increased. For Ba^{2+} , however, an upturn in extraction into $\text{N}_{8,111}^+\text{Tf}_2\text{N}^-$ at high acid concentration, such as was seen with Sr^{2+} , is not observed. This is likely due to the lower charge density of Ba^{2+} which disfavors NC/IPE because the formation of a stable metal-nitrato-crown complex is more difficult (ionic radii of Sr^{2+} and Ba^{2+} are 127 and 143 pm, respectively [2.28]). This agrees with results reported previously for $\text{C}_n\text{mim}^+\text{Tf}_2\text{N}^-$ ILs [2.3]. Due to its even lower charge density, sodium (left panel) partitions almost entirely *via* ion exchange (ionic radius of Na^+ is 98 pm [2.28]). Not unexpectedly though, in the low acid region ($< 0.5 \text{ M HNO}_3$), a downward shift in the extraction at any given acidity is observed as the alkyl chain length of the IL cation is increased.

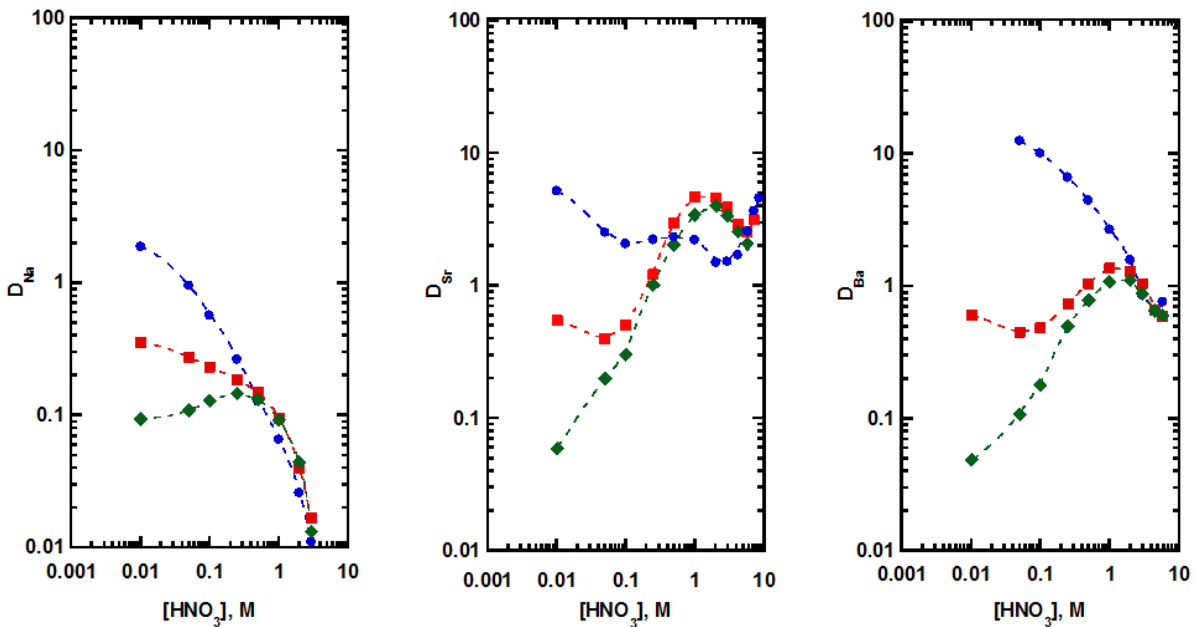


Figure 2.3. Effect of HNO_3 concentration on the extraction of Na^+ (left), Sr^{2+} (middle) and Ba^{2+} (right) by 0.1 M DCH18C6 into $\text{N}_{8,111}^+\text{Tf}_2\text{N}^-$ (solid, blue circles), $\text{N}_{10,111}^+\text{Tf}_2\text{N}^-$ (solid, red squares), $\text{N}_{12,111}^+\text{Tf}_2\text{N}^-$ (solid, green diamonds).

Overall, several similarities between the nitric acid dependencies of metal ion extraction into $N_{n,111}^+Tf_2N^-$ ILs and those seen previously for $C_nmim^+Tf_2N^-$ ILs [2.3] are apparent. That is, for divalent metal ions, there is a shift in the mode of partitioning from ion exchange towards neutral complex / ion pair extraction as the hydrophobicity of the IL cation increases. A similar shift is observed for Na^+ at low acidities ($[HNO_3] < 0.5$ M), above which the acid dependencies are nearly identical and ion exchange predominates.

2.3.5 Effect of IL anion hydrophobicity on extraction from acidic nitrate media

Previous work examining IL anion effects on metal ion extraction into ILs has compared C_nmim^+ ILs incorporating PF_6^- , Tf_2N^- and $BETI^-$ anions [2.4, 2.27, 2.29, 2.30] Unfortunately, the hexafluorophosphate (PF_6^-) forms of trimethylalkylammonium salts were found to be solids with melting points well above ambient temperature, thus precluding extraction studies with them. For this reason, our studies were restricted to ILs incorporating Tf_2N^- or $BETI^-$ anions, which generally have melting points lower than those observed for the corresponding PF_6^- ILs [2.30]. Mass action considerations, as described by Luo *et al.* [2.27], indicate that increasing IL anion hydrophobicity will favor extraction by ion exchange. That is, as the hydrophobicity of the IL anion increases, less IL cation will be initially present in the aqueous phase, favoring ion exchange processes. Therefore, ion exchange should be more prevalent for the $BETI^-$ form of a given IL than for the analogous Tf_2N^- form.

Figure 2.4 shows the nitric acid dependency of Na^+ , Sr^{2+} and Ba^{2+} extraction into $N_{n,111}^+$ (where $n = 8, 10,$ and 12) ILs incorporating the $BETI^-$ anion. As was the case for the Tf_2N^- analogs of these ILs, if the hydrophobicity of the IL cation increases, a shift from ion exchange towards neutral complex / ion pair extraction occurs for the divalent metal ions. A similar shift is also observed for Na^+ below $[HNO_3]$ of 0.5 M.

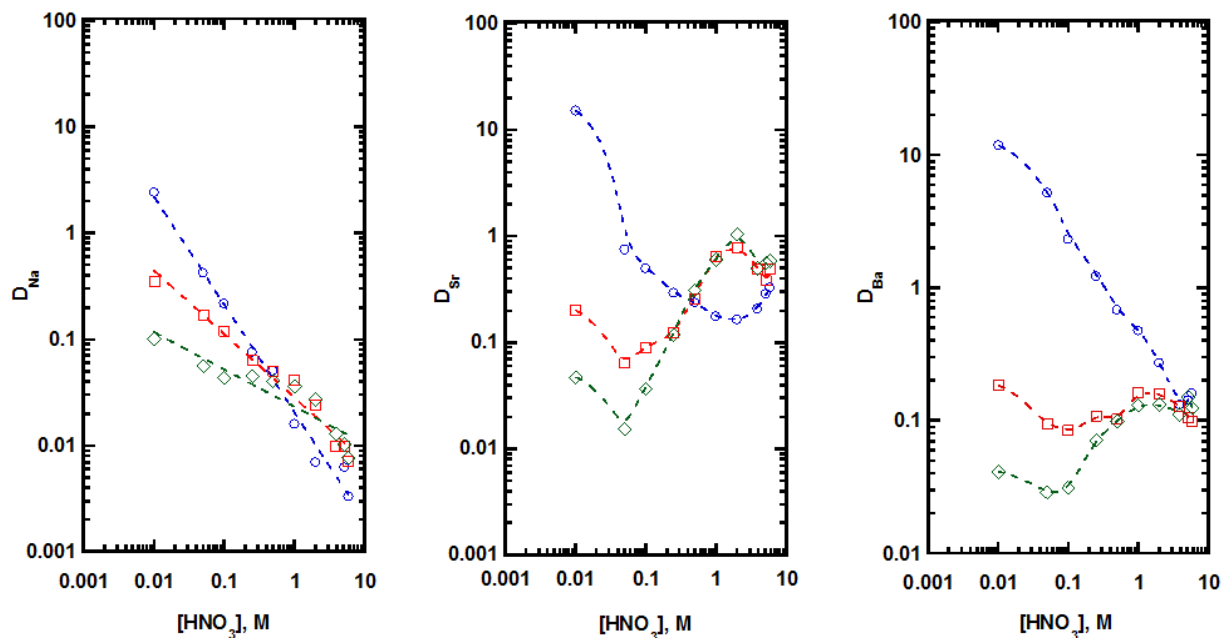


Figure 2.4. Effect of HNO_3 concentration on the extraction of Na^+ (left), Sr^{2+} (middle) and Ba^{2+} (right) by 0.1 M DCH18C6 into $\text{N}_{8,111}^+\text{BETI}^-$ (open, blue circles), $\text{N}_{10,111}^+\text{BETI}^-$ (open, red squares), $\text{N}_{12,111}^+\text{BETI}^-$ (open, green diamonds).

2.3.6 Effect of IL cation hydrophobicity on extraction from acidic chloride media

Although nitric acid is the most common aqueous phase for these types of extraction systems, other aqueous phases, specifically hydrochloric acid, have been employed as an alternative to broaden the applicability of IL-based metal ion extraction [2.2, 2.31, 2.32]. Prior studies of the effect of aqueous phase anion (*e.g.*, NO_3^- vs. Cl^-) on the extraction of alkali and alkaline earth metal ions into various C_nmim^+ -based ILs by DCH18C6 [2.2] have shown that the influence of the aqueous phase anion can be significant, and that ion exchange processes tend to predominate for aqueous anions exhibiting a high hydration enthalpy. For neutral complex / ion pair extraction to occur, the aqueous phase anion must transfer from the aqueous phase to the organic phase. If the energy required for this process is too high (*i.e.*, as is apparently the case for Cl^- at low $[\text{HCl}]$), ion exchange will be favored.

Consistent with this observation is the fact that for the quaternary ammonium-based ILs of interest here, extraction of divalent metal ions from HCl (Figure 2.5) is dominated by ion exchange at low acid concentrations. As the cation chain length is increased, a drop in the magnitude of the distribution ratio, instead of a shift in partitioning mode, at any given acidity is observed, a result of the greater difficulty in transferring a more hydrophobic IL cation into the aqueous phase. This greater difficulty is also evident from the acidities at which the upturn of the metal ion distribution ratios occurs. That is, for ILs incorporating more hydrophobic IL cations, the upturn (*i.e.*, the transition from ion exchange to neutral complex / ion pair extraction as the predominant mode of extraction) occurs at lower acidities (*e.g.*, 2 M for $\text{N}_{8,111}^+\text{Tf}_2\text{N}^-$ vs. 1 M for $\text{N}_{10,111}^+\text{Tf}_2\text{N}^-$ vs. 0.5 M for $\text{N}_{12,111}^+\text{Tf}_2\text{N}^-$ for Sr^{2+}). For Na^+ , as seen in nitric acid-based systems, ion exchange predominates under all conditions. In addition, again as in nitric acid-based systems, a slight downward shift in the acid dependency is observed for HCl concentrations below 3 M.

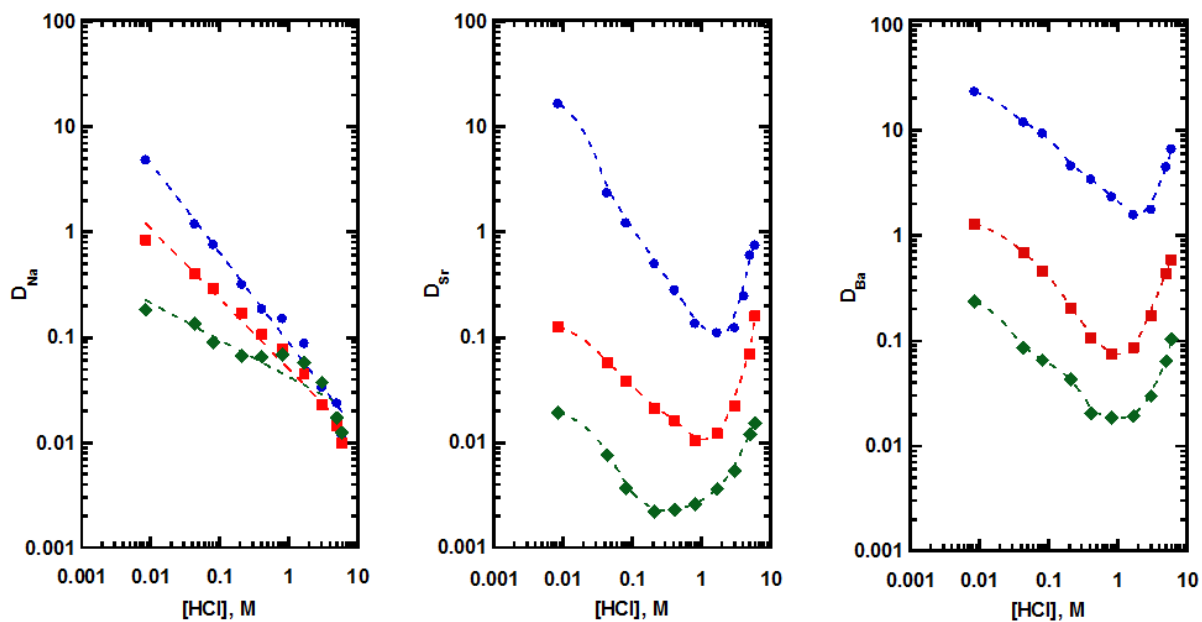


Figure 2.5. Effect of HCl concentration on the extraction of Na^+ (left), Sr^{2+} (middle) and Ba^{2+} (right) by 0.1 M DCH18C6 into $N_{8,111}^+Tf_2N^-$ (solid, blue circles), $N_{10,111}^+Tf_2N^-$ (solid, red squares), $N_{12,111}^+Tf_2N^-$ (solid, green diamonds).

2.3.7 Effect of IL anion hydrophobicity on extraction from acidic chloride media

As was the case for the Tf_2N^- forms of these ILs, extraction of metal ions from acidic chloride media into $\text{N}_{n,111}^+\text{BETI}^-$ ILs is dominated by ion exchange (Figure 2.6) an observation consistent with the greater hydration enthalpy of the chloride anion versus nitrate, making partitioning of the aqueous phase anion as part of a metal-crown complex more difficult. At any given acidity, a drop in the magnitude of distribution ratios is again observed for the divalent metal ions with IL cation hydrophobicity. For the representative monovalent cation, Na^+ , extraction also exhibits a slight downward shift with IL cation alkyl chain length at low $[\text{HCl}]$ ($< 2 \text{ M}$), due to the IL cation becoming more hydrophobic and thus, more difficult to exchange into the aqueous phase. Above acid concentrations of 2 M , the trends in extraction are nearly identical. As noted above, ion exchange should predominate for ILs with a highly hydrophobic IL anion. Consistent with this, the upturn in the acid dependencies observed for the divalent metal ions occurs at acid concentrations higher than those seen for their Tf_2N^- analogs (*i.e.*, 4 M for $\text{N}_{8,111}^+\text{BETI}^-$ and 2 M for $\text{N}_{10,111}^+\text{BETI}^-$ for Sr^{2+}).

Comparison of the acid dependencies for the extraction of strontium into $\text{N}_{10,111}^+\text{Tf}_2\text{N}^-$ and $\text{N}_{10,111}^+\text{BETI}^-$ (Figure 2.7), further illustrates that the BETI^- IL exhibits a greater tendency toward ion exchange, as evidenced by a more negative slope in the acid region from 0.01 M to 2 M HCl . It can also be seen that under most conditions, the metal ion distribution ratios are lower for the BETI^- ILs compared to their Tf_2N^- analogs. In other words, extraction into Tf_2N^- forms of the ILs exhibit less extraction by ion exchange processes and is more efficient than the BETI^- forms.

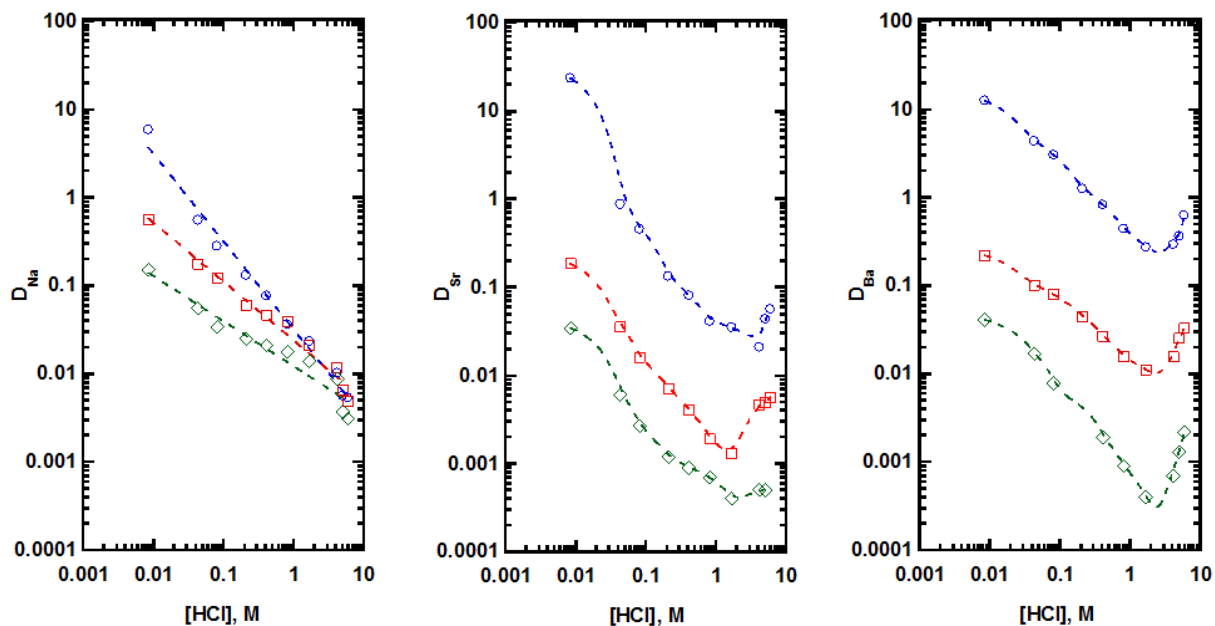


Figure 2.6. Effect of HCl concentration on the extraction of Na^+ (left), Sr^{2+} (middle) and Ba^{2+} (right) by 0.1 M DCH18C6 into $N_{8,111}^+BETI^-$ (solid, blue circles), $N_{10,111}^+BETI^-$ (solid, red squares), $N_{12,111}^+BETI^-$ (open, green diamonds).

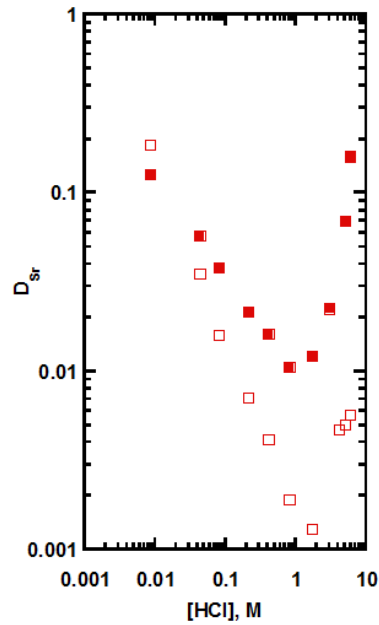


Figure 2.7. Comparison of the effect of HNO₃ concentration on the extraction of Sr²⁺ by 0.1 M DCH18C6 into N_{10,111}⁺Tf₂N⁻ (solid, red squares), N_{10,111}⁺BETI⁻ (open, red squares).

2.3.8 Extraction selectivity of $N_{n,111}^+Tf_2N^-$ and $N_{n,111}^+BETF^-$ ILs

A complete evaluation of any IL as an extraction solvent requires consideration not only of the magnitude of the D_M values obtained (*i.e.*, the extraction efficiency), but also the metal ion selectivity (*i.e.*, separation factors). In several of the applications for which ILs are being investigated as alternative solvents (*e.g.*, treatment of nuclear waste streams, analysis of soil leachates and biological samples), Sr^{2+} is the metal ion of interest. Therefore, high selectivity *vs.* other metal ions (*e.g.*, Ba^{2+} , Ca^{2+} , Na^+ , K^+ and Cs^+) present in the sample matrix in the typical working range of 1-3 M acid is desired [2.33, 2.34]. Separation factors (α_{M_1/M_2}) for the extraction of strontium from nitric acid into several traditional organic solvents, the ILs studied in this work, and the ‘best’ $C_n\text{mim}^+$ IL (determined as comprising a combination of the most hydrophobic IL cation studied – $C_{10}\text{mim}^+$ and the anion with less propensity towards ion exchange processes – Tf_2N^-) are shown in Table 2.3.

It can be seen that large variations in the separation factors of strontium over sodium and barium are observed for different types of organic solvents ($\alpha_{Sr/Na}$: cyclohexane < primary alcohols < toluene << chloroform; $\alpha_{Sr/Ba}$: cyclohexane < primary alcohols < chloroform < toluene). In addition, when comparing a homologous series of organic solvents with an increasing chain length (*i.e.*, primary alcohols), values of $\alpha_{Sr/Na}$ decrease by nearly a factor of 4 as the chain length increases from five to ten. In other words, a decrease in the hydrophobicity of the solvent favors selective extraction of strontium. In contrast, $\alpha_{Sr/Ba}$ values increase slightly as the hydrophobicity of the alcohol is increased. Although some of the separation factors obtained using traditional organic solvents are quite impressive (> 1000 for chloroform), the volatility and toxicity of these solvents make ionic liquids of interest as substitutes.

Table 2.3
Effect of HNO₃ concentration on $\alpha_{\text{Sr}/\text{Ba}}$ (= $D_{\text{Sr}} / D_{\text{Ba}}$) and $\alpha_{\text{Sr}/\text{Na}}$ (= $D_{\text{Sr}} / D_{\text{Na}}$) values for various traditional organic solvents, N_{*n*,111}Tf₂N ILs, N_{*n*,111}BETI ILs, and C₁₀mimTf₂N from extraction data for 0.1 M DCH18C6 in the specified organic or IL phase.

[HNO ₃]	1 M		2 M		3 M	
	$\alpha_{\text{Sr}/\text{Na}}$	$\alpha_{\text{Sr}/\text{Ba}}$	$\alpha_{\text{Sr}/\text{Na}}$	$\alpha_{\text{Sr}/\text{Ba}}$	$\alpha_{\text{Sr}/\text{Na}}$	$\alpha_{\text{Sr}/\text{Ba}}$
cyclohexane	0.67	1.74	0.73	0.37	1.04	0.21
toluene	77.6	14.7	47.5	13.1	22.6	10.2
chloroform	2370	2.56	2450	2.76	1200	3.11
1-pentanol ^a	12.3	1.39	21.2	1.61	37.0	1.70
1-hexanol ^a	11.8	1.36	17.3	1.70	32.6	1.82
1-octanol ^a	7.35	1.52	8.22	1.82	14.2	2.03
1-decanol ^a	3.88	1.75	5.07	2.09	9.18	2.32
C ₁₀ mimTf ₂ N ^a	25.8	1.15	42.6	1.17	68.4	1.38
N _{8,111} Tf ₂ N	33.8	0.83	57.4	0.94	137	1.77
N _{10,111} Tf ₂ N	49.3	3.43	116	3.55	233	3.71
N _{12,111} Tf ₂ N	37.1	3.16	90.3	3.58	256	3.84
N _{8,111} BETI	11.0	0.37	23.8	0.61	NM	NM
N _{10,111} BETI	15.6	4.00	32.6	4.99	NM	NM
N _{12,111} BETI	16.7	4.61	38.6	7.92	NM	NM

^a Data from reference [2.3].

Table 2.4
Effect of HCl concentration on $\alpha_{\text{Sr/Ba}}$ ($= D_{\text{Sr}} / D_{\text{Ba}}$) and $\alpha_{\text{Sr/Na}}$ ($= D_{\text{Sr}} / D_{\text{Na}}$) values for $\text{N}_{n,111}\text{Tf}_2\text{N}$ ILs, $\text{N}_{n,111}\text{BETI}$ ILs, $\text{C}_{10}\text{mimTf}_2\text{N}$, and 1-octanol from extraction data for 0.1 M DCH18C6 in the organic or IL phase.

[HCl]	1 M		2 M		3 M	
	$\alpha_{\text{Sr/Na}}$	$\alpha_{\text{Sr/Ba}}$	$\alpha_{\text{Sr/Na}}$	$\alpha_{\text{Sr/Ba}}$	$\alpha_{\text{Sr/Na}}$	$\alpha_{\text{Sr/Ba}}$
1-octanol ^a	0.58	0.58	0.78	0.65	0.78	0.57
$\text{C}_{10}\text{mimTf}_2\text{N}$ ^a	0.08	0.15	0.08	0.12	0.29	0.11
$\text{N}_{8,111}\text{Tf}_2\text{N}$	0.90	0.06	1.25	0.07	3.67	0.07
$\text{N}_{10,111}\text{Tf}_2\text{N}$	0.13	0.14	0.27	0.14	0.98	0.13
$\text{N}_{12,111}\text{Tf}_2\text{N}$	0.04	0.14	0.06	0.19	0.15	0.18
$\text{N}_{8,111}\text{BETI}$	1.14	0.09	1.52	0.13	2.04	0.07
$\text{N}_{10,111}\text{BETI}$	0.05	0.12	0.06	0.12	0.40	0.30
$\text{N}_{12,111}\text{BETI}$	0.04	0.78	0.02	0.75	0.06	0.71

^a Data from reference [2.3].

Because ILs incorporating the more hydrophobic IL anion (*i.e.*, BETI⁻) exhibit a greater propensity to ion exchange (an undesirable process), the separation factors of the Tf₂N⁻ forms of the quaternary ammonium-based ILs were evaluated to determine the strontium selectivity of this IL family *vs.* other extraction solvents. Like most of the traditional organic solvents and C₁₀mim⁺Tf₂N⁻, the separation factors for the N_{*n*,111}⁺Tf₂N⁻ IL systems increase as the acid concentration increases. Interestingly all three N_{*n*,111}⁺Tf₂N⁻ ILs exhibit $\alpha_{\text{Sr/Na}}$ values greater than those observed for either C₁₀mim⁺Tf₂N⁻ or most of the organic solvents. These favorable separation factors are a result of both higher D_{Sr} and lower D_{Ba} and D_{Na} values at these acid concentrations, and indicate that DCH18C6 in N_{*n*,111}⁺Tf₂N⁻ IL-based systems is generally more selective than in the corresponding C_{*n*}mim⁺ IL-based systems. These systems also compare favorably with conventional organic solvents. For example, the $\alpha_{\text{Sr/Ba}}$ values for N_{10,111}⁺Tf₂N⁻ and N_{12,111}⁺Tf₂N⁻ are bested only by toluene. Also, as the carbon chain length of the N_{*n*,111}⁺Tf₂N⁻ ILs increases from eight to ten, a roughly two-fold increase in $\alpha_{\text{Sr/Na}}$ values is observed, much more favorable than the trend observed for the primary alcohols, for which a four-fold decrease from 1-pentanol to 1-decanol is seen. Additionally, $\alpha_{\text{Sr/Ba}}$ values increase by almost a factor of four for 1 M and 2 M nitric acid conditions and more than a factor of two for 3 M nitric acid conditions. Taken together, these data demonstrate the superior selectivity for Sr²⁺ extraction of the N_{*n*,111}⁺ family of ILs over C_{*n*}mim⁺ ILs, as well as over many conventional organic solvents.

Table 2.4 shows the separation factors for extraction of metal ions from hydrochloric acid into the ILs studied in this work, C₁₀mim⁺Tf₂N⁻ and the ‘benchmark’ organic solvent, 1-octanol. It can be seen that for nearly all systems and acidities (N_{8,111}⁺BETI⁻ being a notable exception), extraction of sodium and barium is favored over the extraction of strontium. Together with the fact that the predominant mode of extraction from hydrochloric acid media is ion exchange (due

to the high hydration enthalpy of chloride making its transfer to the IL phase more difficult), this poor strontium selectivity indicates that efficient and selective extraction of strontium from acidic chloride media by DCH18C6 in the quaternary ammonium ILs is simply not feasible.

2.4 Conclusions

The results of this work show that the trends reported previously in the extraction of Sr^{2+} , Ba^{2+} , and Na^+ by DCH18C6 from nitric and hydrochloric acids into 1,3-dialkylimidazolium-based ILs are also observed when quaternary ammonium-based ILs are employed as the extraction solvent, including a shift towards ion exchange with increasing IL cation hydrophobicity when extracting divalent metal ions from nitric acid and the predominance of ion exchange in the extraction of Na^+ under all conditions. Similarly, when the hydrophobicity of the IL anion is increased, a greater propensity towards ion exchange is observed. Also as seen previously, extraction into HCl continues to be dominated by ion exchange and exhibits unfavorable Sr^{2+} selectivity. It appears then that the so-called “three-path model” of metal ion extraction that arose from studies of 1,3-dialkylimidazolium-based ILs also applies to quaternary ammonium-based ILs. While additional work to confirm this is needed, these results suggest that the three-path model may represent a general description of metal ion extraction by neutral extractants into a range of ionic liquids. On a less fundamental level, the results demonstrate that extraction by DCH18C6 from nitric acid into trimethylalkylammonium-based ILs shows marked improvements in efficiency and selectivity for Sr^{2+} compared to a number of alternative extraction solvents, including C_nmim^+ -based ILs. Thus, proper selection of IL cation and anion could prove crucial in determining the feasibility of a given extraction process. To further confirm that these observations are generic and therefore apply to ILs as a whole, a systematic study of another family

of ILs, namely *N*-alkylpyridinium salts, was conducted. The results obtained are presented in the next chapter.

2.5 References

- [2.1] Dietz, M.L.; Garvey, S.L.; Hawkins, C.A. Mechanisms of Metal Ion Transfer into RTILs: Implications for Their Use as Extraction Solvents. *Proceedings of the 19th International Solvent Extraction Conference, Santiago, Chile, Chapter X*, **2011**, 208-213.
- [2.2] Garvey, S.L.; Hawkins, C.A.; Dietz, M.L., Effect of Aqueous Phase Anion on the Mode of Facilitated Ion Transfer into Room-Temperature Ionic Liquids. *Talanta*, **2012**, 95, 25-30.
- [2.3] Hawkins, C.A.; Garvey, S.L.; Dietz, M.L., Structural Variations in Room-Temperature Ionic Liquids: Influences on Metal Ion Partitioning Modes and Extraction Selectivity. *Separation and Purification Technology*, **2012**, 89, 31-38.
- [2.4] Garvey, S.L.; Dietz, M.L., Ionic Liquid Anion Effects in the Extraction of Metal Ions by Macrocyclic Polyethers. *Separation and Purification Technology*, **2014**, 123, 145-152.
- [2.5] Dietz, M.L.; Dzielawa, J.A., Ion-Exchange as a Mode of Cation Transfer into Room-Temperature Ionic Liquids Containing Crown Ethers: Implications for the “Greenness” of Ionic Liquids as Diluents in Liquid-Liquid Extraction. *Chemical Communications*, **2001**, 2124-2125.
- [2.6] Jensen, M.P.; Dzielawa, J.A.; Rickert, P.; Dietz, M.L., EXAFS Investigations of the Mechanism of Facilitated Ion Transfer into a Room-Temperature Ionic Liquid. *Journal of the American Chemical Society*, **2002**, 124, 10664-10665.
- [2.7] Dietz, M.L.; Dzielawa, J.A.; Laszak, I.; Young, B.A.; Jensen, M.P., Influence of Solvent Structural Variations on the Mechanism of Facilitated Ion Transfer into Room-Temperature Ionic Liquids. *Green Chemistry*, **2003**, 5, 682-685.
- [2.8] Stepinski, D.C.; Jensen, M.P.; Dzielawa, J.A.; Dietz, M.L., Synergistic Effects in the Facilitated Transfer of Metal Ions into Room-Temperature Ionic Liquids. *Green Chemistry*, **2005**, 7, 151-158.
- [2.9] Dietz, M.L.; Stepinski, D. C., A Ternary Mechanism for the Facilitated Transfer of Metal Ions into Room-Temperature Ionic Liquids (RTILs): Implications for the “Greenness” of RTILs as Extraction Solvents. *Green Chemistry*, **2005**, 7, 747-750.
- [2.10] Dietz, M.L.; Stepinski, D.C., Anion Concentration-Dependent Partitioning Mechanism in the Extraction of Uranium into Room-Temperature Ionic Liquids. *Talanta*, **2008**, 75, 598-603.
- [2.11] Dai, S.; Ju, Y.H.; Barnes, C.E., Solvent Extraction of Strontium Nitrate by a Crown Ether Using Room-Temperature Ionic Liquids. *Dalton Transactions*, **1999**, 8, 1201-1202.
- [2.12] Visser, A.E.; Swatlowki, R.P.; Reichert, W.M.; Griffin, S.T.; Rogers, R.D., Traditional Extractants in Nontraditional Solvents: Groups 1 and 2 Extraction by Crown Ethers in Room-Temperature Ionic Liquids. *Industrial and Engineering Chemistry Research*, **2000**, 39, 3596-3604.
- [2.13] Plechkova, N.V.; Seddon, K.R., Applications of Ionic Liquids in the Chemical Industry. *Chemical Society Reviews*, **2008**, 37, 123-150.

- [2.14] Petrom, H.G.; Allen, R.J., Radiochemical Determination of Actinium in Uranium Mill Effluents. *Analytical Chemistry*, **1963**, 35, 747-749.
- [2.15] Churchward, P.E.; Bridges, D.W., Tungsten Recovery from Low-Grade Concentrates. *Bureau of Mines Report of Investigations*, **1966**, 6845, 16-17.
- [2.16] Van Ooyen, J., Quaternary Ammonium Nitrates as Extractants for Trivalent Actinides. *Solvent Extraction Chemistry, Proceedings of the International Conference*, Goteborg **1967**, 485-492.
- [2.17] Barbano, P.G.; Rigali-Camen, L., Solvent Extraction of Polonium and Bismuth from Nitrate Solutions. *Radiochimica Acta*, **1967**, 8, 214-215.
- [2.18] McDonald, C.; Mahayni, M.; Kanjo, M., Solvent Extraction Studies of Lead Using Alamine 336 and Aliquat 336-S. *Separation Science and Technology*, **1978**, 13, 429-437.
- [2.19] Rajec, P.; Macasek, F.; Belan, J., Membrane Extraction of Pertechetate with Quaternary Ammonium Salts Comparison with Solvent Extraction, *Journal of Radioanalytical and Nuclear Chemistry*, **1986**, 101, 71-76.
- [2.20] Ouadi, A.; Klimchuk, O.; Gaillard, C.; Billard, I., Solvent Extraction of U(VI) by Task Specific Ionic Liquids Bearing Phosphoryl Groups. *Green Chemistry*, **2007**, 9, 1160-1162
- [2.21] Kumano, M.; Yabutani, T.; Motonaka, J.; Mishima, Y., Recovery and Extraction of Heavy Metal Ions Using Ionic Liquid as Green Solvent. *International Journal of Modern Physics B*, **2006**, 20, 4051-4056.
- [2.22] Kilaru, P.; Baker, G.A.; Scovazzo, P., Density and Surface Tension Measurements of Imidazolium-, Quaternary, Phosphonium-, Ammonium-Based Room-Temperature Ionic Liquids: Data and Correlations. *Journal of Chemistry and Engineering Data*, **2007**, 52, 2306-2314.
- [2.23] Liang, M.; Kaintz, A.; Baker, G.A.; Maroncelli, M., Bimolecular Electron Transfer in Ionic Liquids: Are Reaction Rates Anomalously High? *Journal of Physical Chemistry B*, **2012**, 116, 1370-1384.
- [2.24] Kilaru, P.; Baker, G.A.; Scovazzo, P., Density and Surface Tension Measurement of Imidazolium-, Quaternary Phosphonium-, and Ammonium-Based Room-Temperature Ionic Liquids: Data and Correlations. *Journal of Chemical and Engineering Data*, **2007**, 52, 2306-2314.
- [2.25] Huddleston, J.G.; Visser, A.E.; Reichert, W.M.; Willauer, H.D.; Broker, G.A.; Rogers, R.D., Characterization and Comparison of Hydrophilic and Hydrophobic Room-Temperature Ionic Liquids Incorporating the Imidazolium Cation. *Green Chemistry*, **2001**, 3, 156-164.
- [2.26] Stephenson, R.; Stuart, J.; Tabak, M., Mutual Solubility of Water and Aliphatic Alcohols. *Journal of Chemical and Engineering Data*, **1984**, 29, 287-290.

- [2.27] Luo, H.; Dai, S.; Bonnesen, P.V.; Haverlock, T.J.; Moyer, B.A.; Buchanan III, A.C., A Striking Effect of Ionic-Liquid Anions in the Extraction of Sr^{2+} and Cs^+ by Dicyclohexano-18-Crown-6. *Solvent Extraction and Ion Exchange*, **2006**, 24, 19-31.
- [2.28] Chang, R.; Overby, J., *General Chemistry: The Essential Concepts*, 6th edition; McGraw-Hill: New York, 2011.
- [2.29] Jensen, M.P.; Neufeind, J.; Beitz, J.V.; Skanthakumar, S.; Soderholm, L., Mechanisms of Metal Ion Transfer into Room Temperature Ionic Liquids: The Role of Anion Exchange. *Journal of the American Chemical Society*, **2003**, 125, 15466-15473.
- [2.30] Ngo, H.L.; LeCompte, K.; Hargens, L.; McEwen, A.B., Thermal Properties of Imidazolium Ionic Liquids. *Thermochimica Acta*, **2000**, 357-358, 97-102.
- [2.31] Panigrahi, M.; Grabda, M.; Kozak, D.; Dorai, A.; Shibata, E.; Kawamura, J.; Nakamura, T., Liquid-liquid Extraction of Neodymium Ions from Aqueous Solutions of NdCl_3 by Phosphonium-Based Ionic Liquids. *Separation and Purification Technology*, **2016**, 171, 263-269.
- [2.32] Parmentier, D.; Hoogerstraete, T.V; Metz, S.J.; Binnemans, K.; Kroon, M.C., Selective Extraction of Metals from Chloride Solutions with the Tetroctylphosphonium Oleate Ionic Liquid. *Industrial & Engineering Chemistry Research*, **2015**, 54, 5149-5158.
- [2.33] Horwitz, E.P.; Dietz, M.L.; Fisher, D.E., Separation and Preconcentration of Strontium from Biological, Environmental, and Nuclear Waste Samples by Extraction Chromatography Using a Crown Ether. *Analytical Chemistry*, **1991**, 63, 522-525.
- [2.34] Horwitz, E.P.; Chiarizia, R.; Dietz, M.L., A Novel Strontium-Selective Extraction Chromatographic Resin. *Solvent Extraction and Ion Exchange*, **1992**, 10, 313-336.

Chapter 3:
Mechanistic implications of micellization in the extraction of metal ions into *N*-alkylpyridinium-based ILs by DCH18C6

3.1 Introduction

As noted above, the majority of studies aimed at understanding the extraction of metal ions into ILs have employed 1, 3-dialkylimidazolium-based ILs [3.1-3.10]. The results presented in Chapter 2 demonstrated that trends observed for the extraction of several alkali and alkaline earth metal cations into quaternary ammonium-based ILs by DCH18C6 are in agreement with those seen previously for 1, 3-dialkylimidazolium IL-based systems. This suggests that the observations made for these two IL families could represent general characteristics of IL-based extraction systems and thus, might provide a basis for the rational design of these systems. To further investigate the generality of these trends and to confirm that the choice of IL family (*e.g.*, 1, 3-dialkylimidazolium *vs.* trimethylalkylammonium *vs.* *N*-alkylpyridinium) can have a substantial influence on metal ion extraction efficiency (*i.e.*, the magnitude of the distribution ratio) and selectivity (*i.e.*, separation factors), a systematic study of the extraction of several alkali and alkaline earth metal ions from acidic media into *N*-alkylpyridinium-based ILs (abbreviated as $C_n\text{pyr}^+$) by DCH18C6 was undertaken. *N*-alkylpyridinium-based ILs have been used previously in applications ranging from the catalytic reduction of sulfoxides [3.11] to the separation of aromatic molecules from aliphatic hydrocarbons [3.12] and additives for protein refolding [3.13], among others [3.14, 3.15]. The work presented here explores the use of these ILs as extraction solvents, and focuses on the major factors that dictate which modes of metal ion partitioning predominate.

3.2 Experimental

3.2.1 Materials

The *N*-alkylpyridinium, *N*-alkyl-4-ethylpyridinium and 1, 3-dialkylimidazolium ionic liquids used in this study were synthesized by a two-step process. The bromide forms of the $C_n\text{pyr}^+$ (where $n = 4, 6, 7, 8, 10, 12$ and 14), $C_n\text{etpyr}^+$ (where $n = 6, 8, 10,$ and 12) and $C_n\text{mim}^+$ (where $n = 10, 12$ and 14) ILs were first prepared by microwave synthesis according to established methods [3.16], followed by metathesis to the desired anion [3.17]. Commercially available pyridine (Alfa Aesar, Ward Hill, MA), 1-ethylpyridine (Acros Organics, New Jersey), 1-methylimidazole (Acros Organics) and several 1-bromoalkanes (*i.e.*, 1-bromobutane (Acros Organics), 1-bromohexane (Acros Organics), 1-bromoheptane (Sigma Aldrich, Milwaukee, Wisconsin), 1-bromooctane (Acros Organics), 1-bromodecane (Sigma Aldrich), 1-bromododecane (Acros Organics), and 1-bromotetradecane (Alfa Aesar)) were purchased and used without further purification. Lithium salts of *bis*[(trifluoromethyl)sulfonyl]imide, $\text{Li}^+\text{Tf}_2\text{N}^-$, (TCI America, Portland, OR) and *bis*[(perfluoroethyl)sulfonyl]imide, Li^+BETI^- , (3M, St. Paul, MN) were employed to convert the bromide salts of the ILs by metathesis to Tf_2N^- and BETI^- forms. The $N_{n,111}^+\text{Tf}_2\text{N}^-$ (where $n = 10$ and 12) ILs used were those prepared in conjunction with the work described in Chapter 2. In addition, $N_{14,111}^+\text{Tf}_2\text{N}^-$ was prepared from $N_{14,111}^+\text{Br}^-$ (myristyltrimethylammonium bromide (Sigma Aldrich)) by metathesis. *N*-alkyl-4-dimethylaminopyridinium ionic liquids ($C_n\text{dmapyr}^+\text{Tf}_2\text{N}^-$, where $n = 8$ and 12) were generously provided for this work by Dr. James F. Wishart of Brookhaven National Laboratory and used without further purification.

The dicyclohexano-18-crown-6 (DCH18C6, Parish Chemical Company, Orem, UT) used was a mixture of the *cis-syn-cis* (A) and *cis-anti-cis* (B) isomers. Acid solutions were prepared from trace-metal grade concentrated nitric or hydrochloric acid (Optima™, Fisher, Fair Lawn, NJ)

and were standardized by titration with standard sodium hydroxide (Ricca, Arlington, TX) using phenolphthalein indicator (Ricca, Arlington, TX). Commercially available radiotracers $^{133}\text{BaCl}_2$ (Isotope Products Laboratories, Burbank, CA), $^{22}\text{NaCl}$ (Isotope Products Laboratories), and $^{85}\text{SrCl}_2$ (Perkin Elmer, Waltham, MA) were used for extraction studies. All aqueous solutions were prepared with deionized water with a specific resistance of at least 18 M Ω /cm.

3.2.2 Instruments

A Mettler Toledo AL204 balance was employed for all weighing. Karl Fischer titrations to measure the ionic liquid water content were performed on a Metrohm 870 KF Titrino Plus volumetric titrator. The solubility of each C_npyr^+ IL in water was measured on a double-beam Shimadzu UV-2450 UV-VIS Spectrophotometer using quartz cuvettes. Radiometric assays were done *via* gamma spectroscopy on a Perkin Elmer Model 2480 Automatic Gamma Counter using standard procedures. Phase changes of $\text{C}_{14}\text{pyr}^+\text{Tf}_2\text{N}^-$ and $\text{N}_{14,111}^+\text{Tf}_2\text{N}^-$ were measured with a TA Instruments Differential Scanning Calorimeter (DSC) Q20 using T-zero pans and hermetic lids (TA, New Castle, DE). In studies of the extraction of metal ions from water, nitrate concentrations were measured with a Dionex ICS-1000 ion chromatograph equipped with a conductivity detector, a Dionex IonPac AG18 guard column (4 \times 50 mm) and AS18 analytical column (4 \times 250 mm), and a Dionex ASRS 300 (4mm) conductivity suppressor. A 37mM NaOH mobile phase (flow rate of 1.00 mL/min) was employed. An example ion chromatogram is provided in the Appendix. A Fisher Scientific Surface Tensiomat 21 equipped with a du Noüy platinum-iridium ring (CSC Scientific, Fairfax, VA) was employed for the surface tension studies.

3.2.3 Methods

Ionic liquid synthesis. The *N*-alkylpyridinium ($C_n\text{pyr}^+$, where $n = 4, 6, 7, 8, 10, 12,$ and 14) ionic liquids used in this study were synthesized by a two-step process. In the first step, the bromide form of each IL was prepared by microwave irradiation of a mixture of an appropriate alkyl bromide (5% excess) and pyridine according to established methods [3.16]. The bromide form of the IL was then converted to the desired Tf_2N^- or BETI^- form *via* an established anion metathesis reaction [3.18]. Aqueous solutions of each *N*-alkylpyridinium bromide salt were combined with an aqueous solution (3% molar excess) of the lithium salt of *bis*[(trifluoromethyl)sulfonyl]imide, $\text{Li}^+\text{Tf}_2\text{N}^-$ or *bis*[(perfluoroethyl)sulfonyl]imide, Li^+BETI^- . After overnight stirring, the aqueous phase was removed and the water-insoluble ionic liquid remaining was washed with at least five aliquots of water of equal or greater volume. Each wash was tested with silver nitrate to determine if bromide ion was present. Washing was continued until the formation of a silver bromide precipitate was no longer observed. The identity of the final product was confirmed by $^1\text{H-NMR}$ and/or elemental analysis, as appropriate. In a similar manner, the Tf_2N^- forms of 1-alkyl-3-methylimidazolium ($C_n\text{mim}^+$, where $n = 12$ and 14) ILs were prepared. $\text{N}_{14,111}^+\text{Br}^-$ was converted to the desired Tf_2N^- form by metathesis in the same way.

Density measurements. The mass of an empty pipet tip was recorded and a known volume of IL was drawn up into the tip using an automatic pipette. The mass of the IL was determined in triplicate by subtracting the mass of the empty tip from the total mass of the IL sample in the tip. This value was then divided by the volume to determine the density of each IL.

Water solubility and content. A 1 mL aliquot of each *N*-alkylpyridinium-based IL was preconditioned three times by contacting the IL with 2 mL of water. This mixture was vortexed and then centrifuged, and the aqueous phase was removed and discarded. Once the IL phase had been preconditioned, 1 mL of water was added to it and the mixture was vortexed. After standing undisturbed overnight, the mixture was centrifuged to disengage the phases. The aqueous phase was then removed to determine the concentration of the IL dissolved by UV/VIS spectroscopy. The concentration of water present in the IL phase was then determined by Karl Fischer titration.

Thermal studies. To determine the thermal properties (especially the melting points) of ionic liquids found to be solid at room temperature, a small portion of IL that had been dried under vacuum was placed into a tared Tzero aluminum pan and hermetically sealed using a die press provided with the DSC system. The sample masses ranged from 2.5 to 4.5 mg. To start the measurements, all samples were cooled to -75°C, held there for 5 minutes, and then ramped at a rate of 10°C/min to 100°C. The phase transitions were identified through TA Universal Analysis software.

Determination of metal ion distribution ratios. Metal ion distribution ratios (D_M , defined as $[M_{org}] / [M_{aq}]$ at equilibrium), was determined for barium, sodium and strontium radiometrically using commercial radiotracers. All extraction experiments employing an acidic aqueous phase were conducted with 0.1 M DCH18C6 in the ionic liquid phase. Extraction from water was conducted according to previous reports [3.3, 3.7] with 0.2 M DCH18C6 in the ionic liquid phase. This higher crown ether concentration for systems employing water as the aqueous phase is necessitated by the absence of added nitric acid/nitrate, which results in reduced D_M values.

Extraction from water. The percentage of metal ion extracted from water ($\%E_M$) was measured by preconditioning an aliquot of IL containing 0.2 M DCH18C6 two times with twice its volume

of water. After preconditioning, an equivolume aliquot of 0.0310 M $M^{n+}(\text{NO}_3^-)_n$ solution (nominal, where $M^{n+} = \text{Na}^+, \text{Ba}^{2+}, \text{or Sr}^{2+}$) was added to the IL phase. Sodium-22, barium-133 or strontium-85 radiotracer was then introduced and the mixture vortexed. After standing for 15 minutes to allow equilibrium to be reached, the mixture was centrifuged to disengage the phases. The separated aqueous and IL phases were then sampled and counted.

The percentage of nitrate extracted from water ($\%E_{\text{NO}_3^-}$) was determined by conducting the same liquid-liquid extraction as described in the determination of $\%E_M$ without addition of the radiotracer. The concentration of nitrate in the 0.0310 M $M^{n+}(\text{NO}_3^-)_n$ stock solution (where $M^{n+} = \text{Na}^+, \text{Ba}^{2+}, \text{or Sr}^{2+}$) and the aqueous phase following extraction were measured by ion chromatography. Dividing the difference in the nitrate concentration of the metal nitrate stock solution and the aqueous phase after extraction by the concentration of the metal nitrate stock solution gives the percentage of nitrate extracted from the aqueous phase.

Extraction from acid. Distribution ratios (D_M) were measured by preconditioning an aliquot of IL containing 0.1 M DCH18C6 twice with various nitric and hydrochloric acid solutions. After preconditioning was complete, an equivolume aliquot of the acid solution was added to the IL phase. Sodium-22, barium-133 or strontium-85 radiotracer was then introduced and the mixture vortexed and allowed to equilibrate for 15 minutes. Following centrifugation to disengage the phases, the aqueous and IL phases were separated and sampled for counting.

It should be noted that $\text{C}_{14}\text{pyr}^+\text{Tf}_2\text{N}^-$ and $\text{N}_{14,111}^+\text{Tf}_2\text{N}^-$ exhibit phase changes at 30 °C and 42 °C/49 °C, respectively, so they are solid at room temperature. Liquid-liquid extraction experiments using them were therefore conducted at 50 ± 2 °C to ensure that the IL phase was liquid. According to Horwitz *et al.* [3.19], metal ion distribution ratios (D_M) observed for solvent extraction systems employing DCH18C6 and traditional organic solvents are little changed when

the temperature is increased from 25 °C to 50 °C. To confirm that these observations apply to IL-based systems, extraction studies of selected room temperature ionic liquids were conducted at 50 °C and compared to those completed at room temperature. Figure 3.1 summarizes the results of such a study for the extraction of strontium into several $C_n\text{pyr}^+\text{Tf}_2\text{N}^-$ ILs (where $n = 4, 7$ and 10). As can be seen, there is little change in the acid dependency when the temperature is increased. Slight differences in the distribution ratios are observed, but the general trends and therefore, the mechanism of strontium extraction is unchanged. This, it should be noted, also rules out the possibility that the elevated temperature is the cause of the observations discussed in the following sections.

Surface tension. An approximately 2-mL aliquot of each “water-insoluble” ionic liquid was preconditioned with three aliquots of water (4 mL), and then allowed to stand in contact with ~25 mL of water for one week with a brief (several minute) daily vortex mixing. The aqueous phase was then removed and centrifuged to disengage the phases. The initial concentration of the IL in the aqueous phase was measured using a double-beam Shimadzu UV-2450 UV-VIS Spectrophotometer with quartz cuvettes. Following measurement of the initial surface tension, aliquots of water were successively added to dilute the solution and the surface tension measurements were repeated. In this way, a plot of surface tension vs. IL concentration in the aqueous phase was constructed from the most concentrated to the least concentrated solution.

Extraction studies typically involve preconditioning with two aliquots of water, but an additional aliquot was used in the surface tension studies to ensure not only that preconditioning of the IL phase was complete, but also that any water-soluble contaminants that might be present in trace amounts due to the IL synthesis, namely precursors or halide forms of the IL, were removed.

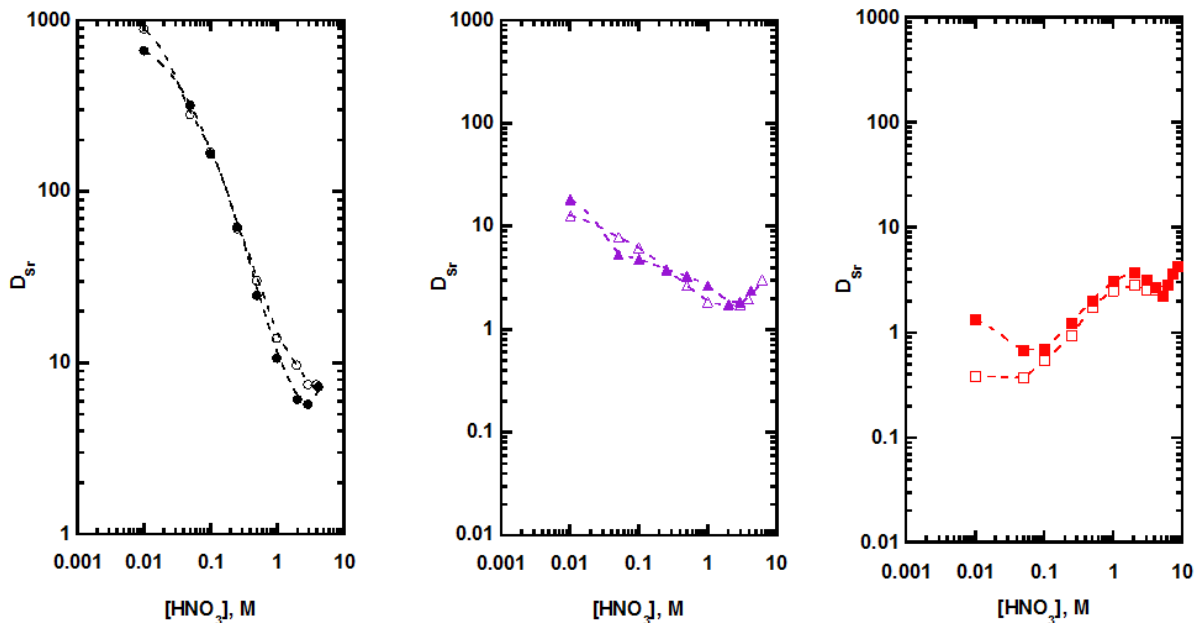


Figure 3.1. Effect of temperature on the extraction of Sr^{2+} by 0.1 M DCH18C6 into $C_4pyr^+Tf_2N^-$ (room temperature – solid, black circles and 50 °C – open, black circles), $C_7pyr^+Tf_2N^-$ (room temperature – solid, purple triangles and 50 °C – open, purple triangles) and $C_{10}pyr^+Tf_2N^-$ (room temperature – solid, red squares and 50 °C – open, red squares).

3.3 Results and Discussion

3.3.1 Physical properties

The measured physical properties of the $C_n\text{pyr}^+$ ILs are presented in Table 3.1. As can be seen, as the alkyl chain length of the *N*-alkylpyridinium ILs is increased, the density decreases, consistent with observations by others for $C_n\text{pyr}^+\text{Tf}_2\text{N}^-$ [3.18] and other IL families [3.20, 3.21]. Prior observations for a homologous series of ILs (*e.g.*, $C_5\text{mim}^+\text{Tf}_2\text{N}^-$, $C_6\text{mim}^+\text{Tf}_2\text{N}^-$, $C_8\text{mim}^+\text{Tf}_2\text{N}^-$, etc.) indicate that a decrease in water content and water solubility should accompany an increase in the alkyl chain length [3.21]. Indeed, results for the *N*-alkylpyridinium ILs follow this expected trend, except for $C_{14}\text{pyr}^+\text{Tf}_2\text{N}^-$ and $C_{14}\text{pyr}^+\text{BETf}^-$, which have higher than expected values. Considering again the physical properties observed for traditional organic solvents used in LLX systems, namely the primary alcohols (Table 2.1), density increases as the alkyl chain length increases and water content and solubility both decrease. As stated in Chapter 2, when compared to primary alcohols, the density difference of ILs makes them easier to use in benchtop studies, and as was seen for the $N_{n,111}^+$ ILs, $C_n\text{pyr}^+$ ILs have lower water contents and solubility, resulting in a reduced phase carryover.

3.3.2 Extraction from water

As noted in Chapter 2, studying the extraction of metal ions from water simplifies the extraction system by eliminating contributions from IX-2. Our studies of $C_n\text{pyr}^+$ -based ILs thus began with an examination of the extraction of the nitrate salts of Sr^{2+} , Ba^{2+} and Na^+ from water into a series of these ILs containing DCH18C6. Table 3.2 summarizes the results obtained for a representative group of $C_n\text{pyr}^+$ (where $n = 4, 7, 10,$ and 14) ILs that incorporate either Tf_2N^- or

Table 3.1
Physical properties of ILs studied^a

	Density - "dry" (g/mL)	Water content - "wet" (ppm)	Water solubility (ppm)
C ₄ pyrTf ₂ N	1.466 ± 0.005	14150 ± 245	7710 ± 55
C ₆ pyrTf ₂ N	1.391 ± 0.005	11240 ± 356	2990 ± 140
C ₇ pyrTf ₂ N	1.362 ± 0.007	10270 ± 655	1390 ± 20
C ₈ pyrTf ₂ N	1.344 ± 0.004	9460 ± 165	835 ± 8
C ₁₀ pyrTf ₂ N	1.297 ± 0.004	8660 ± 149	282 ± 6
C ₁₂ pyrTf ₂ N	1.265 ± 0.008	7980 ± 568	111 ± 1
C ₁₄ pyrTf ₂ N	NM ^b	8590 ± 189	171 ± 2
C ₄ pyrBETI	1.543 ± 0.004	8260 ± 870	1866 ± 7
C ₇ pyrBETI	1.442 ± 0.005	6400 ± 316	210 ± 3
C ₁₀ pyrBETI	1.364 ± 0.011	5425 ± 133	121 ± 2
C ₁₄ pyrBETI	1.288 ± 0.010	4801 ± 253	1098 ± 4

^a Uncertainties are reported at the 95% confidence level.

^b Due to difficulty in sampling, value was not measured.

Table 3.2
Effect of IL structure on metal ion and nitrate extraction from water by DCH18C6 (0.2 M)
into various C_npyr⁺ ILs^{a, b}

Metal	IL	%E_M	%ENO₃⁻	R	Predominant partitioning mode
Sr	C ₄ pyrTf ₂ N	97.7	5.6 ± 0.6	17.4	cation exchange
	C ₇ pyrTf ₂ N	56.1	13.6 ± 0.5	4.13	cation exchange
	C ₁₀ pyrTf ₂ N	20.7	10.3 ± 0.4	2.01	cation exchange
	C ₁₄ pyrTf ₂ N	17.4	6.5 ± 0.3	2.68	cation exchange
	C ₄ pyrBETI	98.4	2.8 ± 0.4	35.1	cation exchange
	C ₇ pyrBETI	36.6	5.1 ± 0.3	7.18	cation exchange
	C ₁₀ pyrBETI	17.8	3.7 ± 1.2	4.81	cation exchange
	C ₁₄ pyrBETI	56.0	4.1 ± 1.1	13.7	cation exchange
Ba	C ₄ pyrTf ₂ N	98.4	5.7 ± 0.2	17.3	cation exchange
	C ₇ pyrTf ₂ N	72.9	20.4 ± 0.2	3.57	cation exchange
	C ₁₀ pyrTf ₂ N	22.3	17.5 ± 0.2	1.27	mixed
	C ₁₄ pyrTf ₂ N	21.2	11.1 ± 0.1	1.91	cation exchange
	C ₄ pyrBETI	93.1	2.7 ± 0.3	34.5	cation exchange
	C ₇ pyrBETI	48.2	8.4 ± 1.7	5.74	cation exchange
	C ₁₀ pyrBETI	17.0	5.6 ± 0.7	3.04	cation exchange
	C ₁₄ pyrBETI	55.1	5.6 ± 0.4	9.84	cation exchange
Na	C ₄ pyrTf ₂ N	94.5	1.3 ± 0.2	72.7	cation exchange
	C ₇ pyrTf ₂ N	55.2	3.5 ± 0.7	15.8	cation exchange
	C ₁₀ pyrTf ₂ N	12.9	6.2 ± 0.4	2.08	cation exchange
	C ₁₄ pyrTf ₂ N	16.5	5.6 ± 0.5	2.95	cation exchange
	C ₄ pyrBETI	95.3	ND		
	C ₇ pyrBETI	42.9	2.5 ± 0.8	17.2	cation exchange
	C ₁₀ pyrBETI	17.3	3.6 ± 0.6	4.81	cation exchange
	C ₁₄ pyrBETI	71.5	1.8 ± 0.5	39.7	cation exchange

^a Uncertainties are reported at the 95% confidence level. %E values reported without uncertainties represent the average of duplicate measurements.

^b Initial metal salt concentrations were 0.031 M.

ND indicates no measurable change in nitrate concentration.

BETI⁻ as the anion. If neutral complex / ion pair extraction is the only mode of partitioning present in a system, the ratio of %E_M to %E_{NO₃⁻} (R) will equal unity. If the percentage of metal ion extracted is greater than the corresponding value for nitrate ion, neutral complex / ion pair extraction cannot be the only mode of partitioning present, and therefore cation-exchange (IX-1) must also be occurring. Thus, the magnitude of R (*i.e.*, how much larger than 1 it is) is a direct reflection of the extent to which ion-exchange (as IX-1) contributes to the overall partitioning.

As can be seen from Table 3.2, cation-exchange is the predominant mode of partitioning under nearly all conditions, regardless of the metal ion being extracted, IL anion or cation. If the alkyl chain length is increased from four to seven to ten, however, a decrease in R is observed, indicative of a decrease in the contribution of cation exchange to the overall extraction. Such a decrease with increasing IL cation alkyl chain length is consistent with previous studies of analogous systems employing C_nmim⁺ or N_{n,111}⁺-based ILs [3.3, 3.7]. For ionic liquids incorporating the C₁₄pyr⁺ cation, however, the further increase in IL cation alkyl chain length leads to an unexpected increase in the ratio, consistent with a greater contribution to the overall extraction by cation exchange than would be expected on the basis of chain length alone. In every case, larger R values (*i.e.*, greater contributions from ion exchange) are observed for ILs incorporating the more hydrophobic BETI⁻ anion when compared to their homologous Tf₂N⁻-bearing IL. This is consistent with observations seen previously [3.4, 3.7] for metal ion extraction from an acidic aqueous phase when BETI⁻-based ILs are employed.

3.3.3 Extraction of Sr²⁺ from nitric acid media into C_npyr⁺Tf₂N⁻ ILs

Figure 3.2 shows the dependence of the strontium distribution ratio (D_{Sr}) on the concentration of nitric acid, [HNO₃], for a homologous series of C_npyr⁺ ILs (where *n* = 4, 6, 7, 8, 10, 12, and 14). As is known from previous work [3.1, 3.3, 3.7], a downward slope in the

dependency (*i.e.*, a decrease in D_M as $[\text{HNO}_3]$ increases) is indicative of the predominance of ion-exchange processes under the experimental conditions. In contrast, when distribution ratios rise with an increase in acid concentration, neutral complex / ion pair extraction predominates, as is observed for metal ion extraction by neutral extractants into traditional organic solvents [3.3]. The left panel of Figure 3.2 shows the acid dependencies for $C_n\text{pyr}^+\text{Tf}_2\text{N}^-$ ILs, where $n = 4, 6, 7, 8,$ and 10 . For the shorter chain ($n = 4-7$) ILs, a decrease in D_{Sr} is observed as the $[\text{HNO}_3]$ increases until high acid concentration (2-4 M) is reached, above which an upturn occurs. This change in the shape / direction of the acid dependency is consistent with observations made for other families of ILs, and suggests a shift from ion-exchange to neutral complex / ion pair extraction as the predominant mode of strontium extraction.

The behavior of the short-chain $C_n\text{pyr}^+$ ILs is also characterized by a significant decrease in the distribution ratios at low acidities (*i.e.*, ≤ 0.1 M HNO_3) as the alkyl chain length of the cation increases, an observation consistent with ion-exchange involving the cationic component of the IL as the predominant mode of partitioning in this region. That is, the distribution ratio falls because it becomes progressively more difficult to transfer an IL cation into the aqueous phase as its length (*i.e.*, hydrophobicity) increases. Such results too are consistent with those reported previously for both quaternary ammonium (Chapter 2) and $C_n\text{mim}^+$ ILs [3.3], which have been reproduced in Figure 3.3 for purposes of comparison.

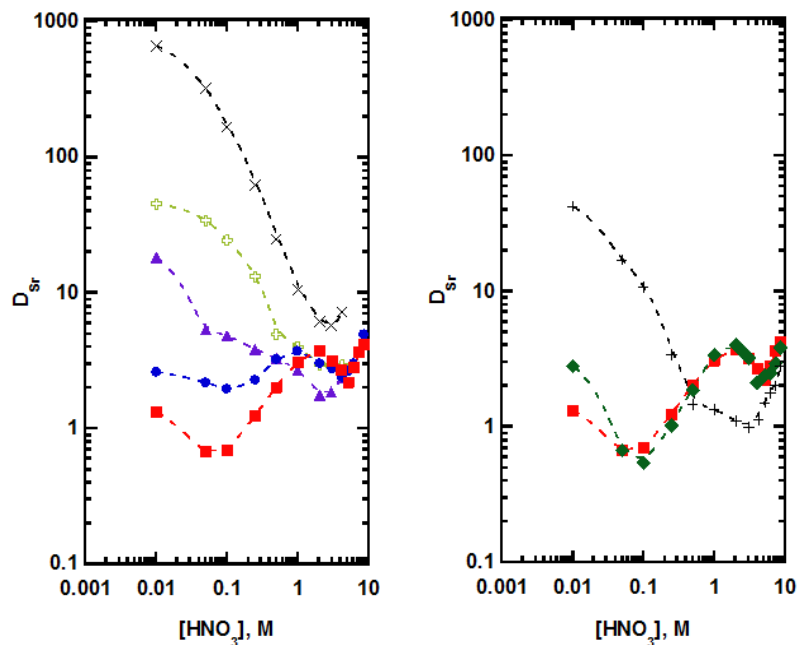


Figure 3.2. Effect of HNO_3 concentration on the extraction of Sr^{2+} by 0.1 M DCH18C6 into several $\text{C}_n\text{pyr}^+\text{Tf}_2\text{N}^-$ ILs. Left panel: $\text{C}_4\text{pyr}^+\text{Tf}_2\text{N}^-$ (black exes), $\text{C}_6\text{pyr}^+\text{Tf}_2\text{N}^-$ (open, green plus signs), $\text{C}_7\text{pyr}^+\text{Tf}_2\text{N}^-$ (solid, purple diamonds), $\text{C}_8\text{pyr}^+\text{Tf}_2\text{N}^-$ (solid, blue circles) and $\text{C}_{10}\text{pyr}^+\text{Tf}_2\text{N}^-$ (solid, red squares); Right panel: $\text{C}_{10}\text{pyr}^+\text{Tf}_2\text{N}^-$ (solid, red squares), $\text{C}_{12}\text{pyr}^+\text{Tf}_2\text{N}^-$ (solid, green diamonds), and $\text{C}_{14}\text{pyr}^+\text{Tf}_2\text{N}^-$ (black crosses).

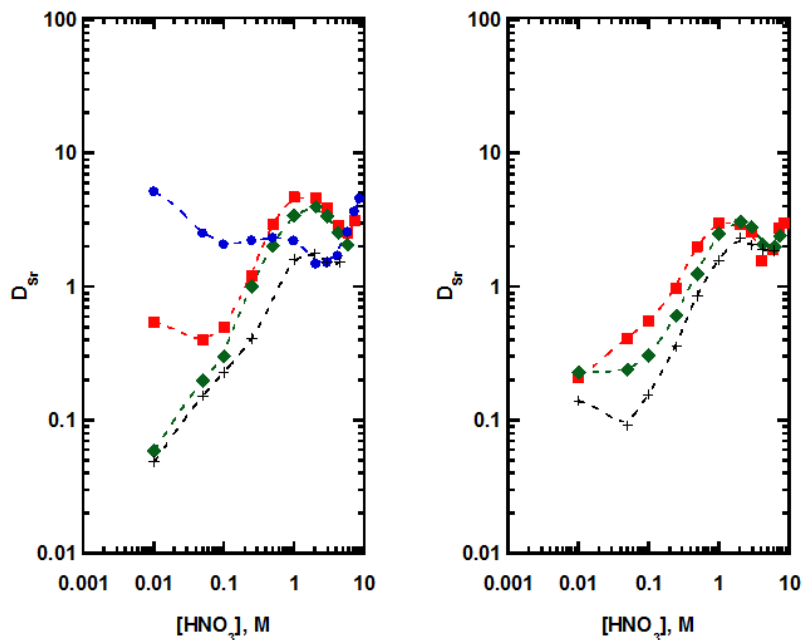


Figure 3.3. Effect of HNO₃ concentration on the extraction of Sr²⁺ by 0.1 M DCH18C6 into several ILs. Left panel: N_{8,111}⁺Tf₂N⁻ (solid, blue circles), N_{10,111}⁺Tf₂N⁻ (solid, red squares), N_{12,111}⁺Tf₂N⁻ (solid, green diamonds), and N_{14,111}⁺Tf₂N⁻ (black crosses); Right panel: C₁₀mim⁺Tf₂N⁻ (solid, red squares), C₁₂mim⁺Tf₂N⁻ (solid, green diamonds), and C₁₄mim⁺Tf₂N⁻ (black crosses).

What is not consistent with prior reports is the behavior of the long-chain $C_n\text{pyr}^+$ ILs, in particular, $C_{12}\text{pyr}^+\text{Tf}_2\text{N}^-$ and $C_{14}\text{pyr}^+\text{Tf}_2\text{N}^-$. Because of their greater alkyl chain length and the accompanying higher hydrophobicity, these cations should afford ILs exhibiting a greater contribution from neutral complex / ion pair extraction than is observed for the analogous $C_{10}\text{pyr}^+$ IL. It is obvious from Figure 3.2 (right panel), however, that this is not the case. Instead a shift back towards ion-exchange, which manifests itself here as a widening of the range of acidities over which a downward slope is observed for the acid dependency of D_{Sr} and / or an increase in D_{Sr} at a given nitric acid concentration in the low acidity region ($[\text{HNO}_3] < \sim 0.1 \text{ M}$), occurs.

Taken together with the higher than expected water content and water solubility of these ILs (Table 3.1), along with the observed predominance of ion exchange in the extraction of strontium from water, it is clear that the longest chain $C_n\text{pyr}^+\text{Tf}_2\text{N}^-$ ILs (most noticeably $C_{14}\text{pyr}^+\text{Tf}_2\text{N}^-$), which are ostensibly the most hydrophobic, are behaving as if they are more hydrophilic in nature.

3.3.4 Micelle formation by $C_n\text{pyr}^+$ ILs

In an earlier study examining the formation of an optically birefringent gel by $C_{10}\text{mim}^+\text{Br}^-$ upon addition of water, Firestone *et al.* [3.22] noted the resemblance of various IL cations to ordinary cationic surfactants (*i.e.*, amphiphilicity derived from a charged polar head group and a long hydrophobic tail; see Figure 3.4). A subsequent report by the same authors [3.23] reiterated this point, and went on to note that certain properties of ILs could be readily understood by drawing analogies to more conventional reagents, in particular, surfactants and liquid ion-exchangers. Since this time, it has become widely recognized that many ILs *are* surfactants, and this awareness has produced a voluminous literature on the subject of the fundamental chemistry and applied aspects of surface-active ILs [3.24, 3.25]. Not unexpectedly, with few exceptions (see, for

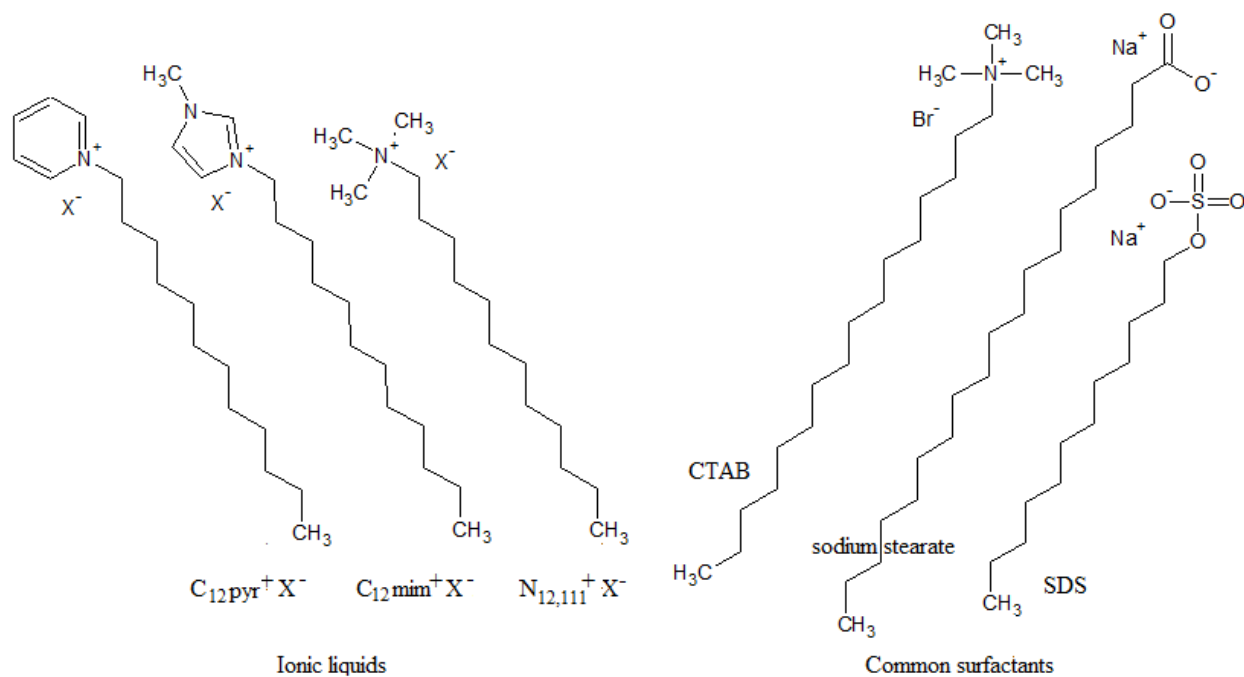


Figure 3.4. Structures of several representative ionic liquids and surfactants.

example, refs. [3.16, 3.27, 3.28]), studies of these ILs have focused on those exhibiting significant water solubility (*e.g.*, halide salts). The possibility that the surface activity of a *hydrophobic* IL might exert an influence on partitioning processes involving a biphasic IL-aqueous system has therefore not been systematically explored. To determine if self-association of the long-chain $C_n\text{pyr}^+$ ILs is the origin of the unexpected results obtained, it is necessary to establish if these ILs do, in fact, form micelles.

A number of techniques have been used to detect the formation of micelles, including the measurement of surface tension [3.29-3.31], conductivity [3.29, 3.32], fluorescence [3.29, 3.31, 3.33], and ^1H NMR spectra [3.29, 3.30, 3.33] at various concentrations of IL in an aqueous phase. These techniques typically involve measurements over a relatively wide range of IL concentrations. Given the low water solubility of long-chain $C_n\text{pyr}^+$ ILs bearing hydrophobic Tf_2N^- and BETI^- anions compared to their halide analogs, the working range over which micelle formation can be probed in these systems is somewhat limited. Nonetheless, if the water solubility of the IL is such as to exceed the critical micellar concentration (CMC) (*i.e.*, the concentration of IL required in the aqueous phase for micelle formation to occur) of the IL cation, a CMC determination is obviously feasible. It is now well-established that for many non-micelle forming ILs, the surface tension of the aqueous phase will fall as the concentration of the IL in the aqueous phase rises. If micelles are present in the aqueous phase, however, the surface tension of the solution will eventually become independent of IL concentration, and a plateau will be observed above the critical micellar concentration.

For the previously studied $C_n\text{mim}^+$ ILs (where $n = 10-14$) (Figure 3.5, panel A), increasing aqueous concentrations of the IL are accompanied by a decrease in the surface tension, consistent with the resemblance of the IL cations to conventional cationic surfactants [3.23], related studies

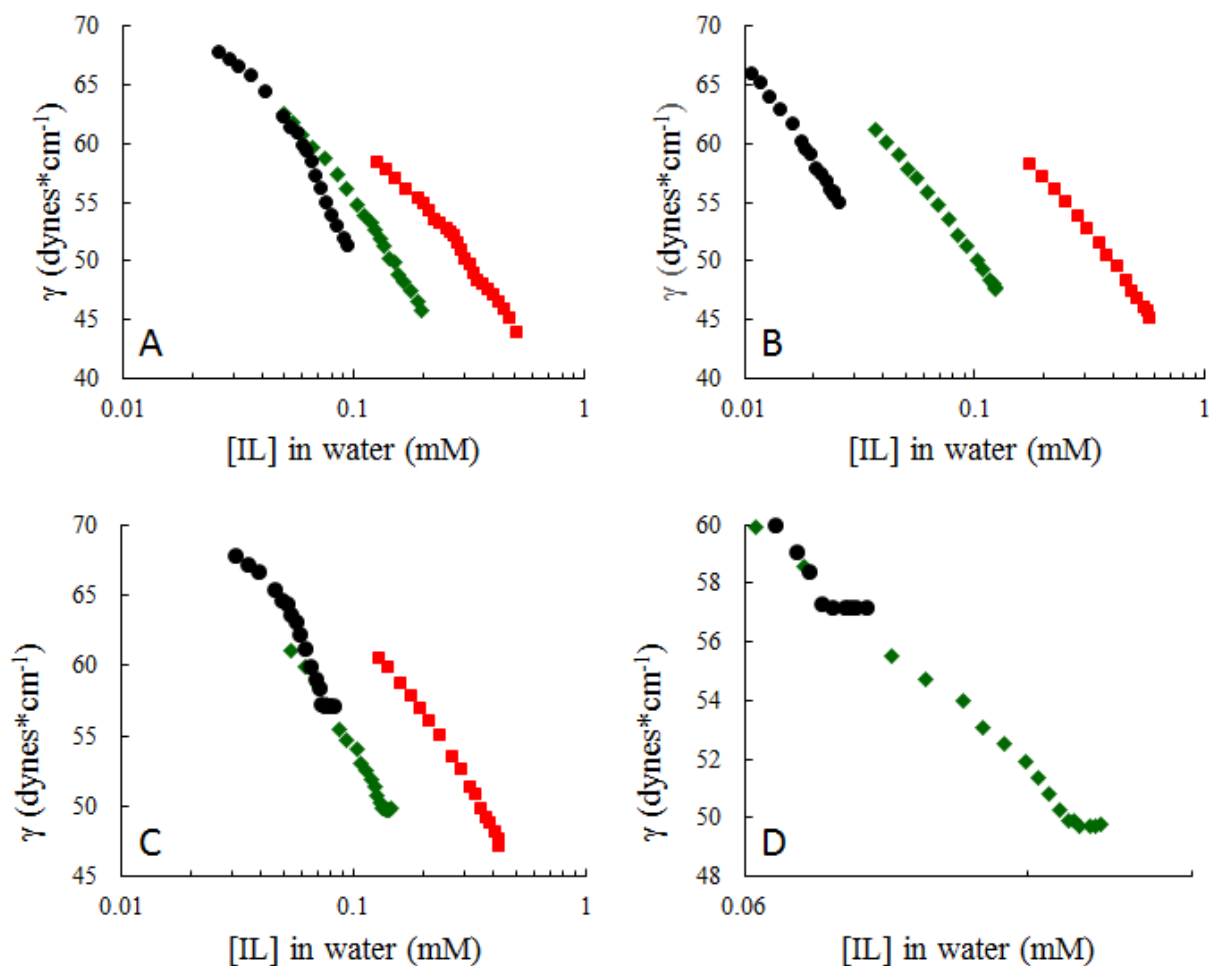


Figure 3.5. Aqueous phase surface tension at various concentrations of IL. Panel A: $C_{10}mim^+Tf_2N^-$ (solid, red squares), $C_{12}mim^+Tf_2N^-$ (solid, green diamonds), and $C_{14}mim^+Tf_2N^-$ (solid, black circles); Panel B: $N_{10,111}^+Tf_2N^-$ (solid, red squares), $N_{12,111}^+Tf_2N^-$ (solid, green diamonds) and $N_{14,111}^+Tf_2N^-$ (solid, black circles); Panel C: $C_{10}pyr^+Tf_2N^-$ (solid, red squares), $C_{12}pyr^+Tf_2N^-$ (solid, green diamonds), and $C_{14}pyr^+Tf_2N^-$ (solid, black circles); Panel D: $C_{12}pyr^+Tf_2N^-$ (solid, green diamonds), and $C_{14}pyr^+Tf_2N^-$ (solid, black circles).

employing water-soluble analogs (*e.g.*, halide salts) of these same IL cations [3.34-3.37], and published data for $C_n\text{mim}^+\text{Tf}_2\text{N}^-$ ILs [3.33]. Note, that for none of the three ILs is a concentration reached at which a plateau in the surface tension plot is observed. Similar results are observed (panel B) for the $N_{n,111}^+\text{Tf}_2\text{N}^-$ ILs ($n = 10-14$), as might be anticipated from the surface activity of related hydrophilic (*e.g.*, Cl^-) salts [3.33, 3.38]. For the $C_n\text{pyr}^+$ ILs ($n = 10-14$, panel C), increasing aqueous concentrations of the IL are again accompanied by declining surface tension. In this case, however, the surface tension plot exhibits a plateau region for both the C_{12} - and C_{14} -ILs (panel D) at sufficiently high concentrations, indicative of the formation of micelles [3.39].

The observation of micelle formation in these systems is somewhat unexpected. As has been noted previously in an examination of the surface tension of $C_{10}\text{mim}^+\text{X}^-$ ILs, where $\text{X} = \text{Cl}^-$, PF_6^- , or Tf_2N^- , the latter two ions are likely too large to fit in the surface region of a micelle (*i.e.*, the Stern layer). Moreover, the low aqueous solubility of ILs incorporating a relatively hydrophobic anion suggests that the systems will undergo phase separation before any bulk aggregation can occur [3.33]. On the other hand, however, the relatively strong binding of a hydrophobic anion to the IL cation and the anion hydrophobicity itself could lead to a decrease in the electrostatic repulsion between head groups on the IL cation, lowering the critical micelle concentration and thus, promoting micelle formation. Apparently then it is the balance between two opposing tendencies, that is, for anion bulk to disfavor micelle formation while anion hydrophobicity favors it, that determines whether phase separation or micelle formation is observed in a given instance. In practical terms, this means that if the CMC is reached before the concentration at which phase separation occurs is exceeded, then micelle formation will be observed. Here the surface tension data yield CMC values of 0.133 mM and 0.072 mM, respectively, for $C_{12}\text{pyr}^+\text{Tf}_2\text{N}^-$ and its C_{14} -analog. These values are significantly less than those

reported previously for the corresponding bromide and chloride ILs (9.3 mM and 2.2 mM for the respective $C_n\text{pyr}^+$ bromides ($n = 12$ and 14) [3.29]; 16.43 mM and 4.01 mM for the corresponding $C_n\text{pyr}^+$ chlorides) [3.37], consistent with reports suggesting that for a given IL cation, the CMC declines with the size of the counter anion [3.33].

Due to the unexpected nature of these observations (*i.e.*, the formation of micelles by ILs with very hydrophobic IL anions) it is important to ensure that impurities, namely the halide precursors which are known to form micelles, are not the cause of these observations. As mentioned in Section 3.2.3, an additional preconditioning step was conducted in order to remove any trace amounts of water-soluble precursors. In addition, elemental analysis of $C_{12}\text{pyr}^+\text{Tf}_2\text{N}^-$ and $C_{14}\text{pyr}^+\text{Tf}_2\text{N}^-$ was conducted and the results show that the actual percent masses of carbon, hydrogen and nitrogen match the theoretical values (Table 3.3). Furthermore, if the observed micelles were a result of contaminant halide form of the IL, the CMC values measured should agree with those observed previously for the halide forms.

Table 3.3
Results of carbon, hydrogen, and nitrogen elemental analysis of $C_{12}\text{pyr}^+\text{Tf}_2\text{N}^-$ and $C_{14}\text{pyr}^+\text{Tf}_2\text{N}^-$

	% C		% H		% N	
	<i>Theoretical</i>	<i>Actual</i>	<i>Theoretical</i>	<i>Actual</i>	<i>Theoretical</i>	<i>Actual</i>
$C_{12}\text{pyrTf}_2\text{N}$	43.2	43.4	5.72	5.80	5.30	5.32
$C_{14}\text{pyrTf}_2\text{N}$	45.3	45.5	6.16	6.17	5.03	5.03

Uncertainty of measured values is $\pm 0.5\%$.

3.3.5 Mechanistic implications of micelle formation

As already noted, the accepted three-path model of metal ion partitioning into ILs in the presence of a neutral extractant implies that increasing IL cation hydrophobicity will be accompanied by a decreasing contribution from ion-exchange processes. Although this model explains well the extraction behavior reported for both 1, 3-dialkylimidazolium and quaternary ammonium ILs, it clearly does not account for several aspects of the behavior of long-chain $C_n\text{pyr}^+$ ILs, in particular their unexpectedly high water content and water solubility and the significant contribution of ion-exchange to the extraction of Sr^{2+} by DCH18C6. Recognition of the fact that micelle formation occurs for the long-chain $C_n\text{pyr}^+$ ILs, however, suggests a simple modification of the model that fully accounts for the new observations (Figure 3.6).

That is, in those cases in which the IL cation is known to exhibit micellization, it is not sufficient to represent the ion-exchange processes, IX-1 or IX-2, as merely an exchange of the IL cation for the cationic metal-extractant complex or the hydronium ion. Rather, it must be denoted that these exchange processes are accompanied by self-association of the IL cation. This aggregation has the effect of both driving the ion-exchange processes and raising the concentration of IL cation in the aqueous phase above that expected on the basis of alkyl chain length considerations alone. Thus, micellization does not introduce a new path for metal ion partitioning, but it does promote an existing one, unfortunately, an undesirable one from the perspective of the development of “green” IL-based separation processes. Stated another way, micelle formation in these systems restricts our ability to increase the contribution of neutral complex / ion pair partitioning simply by increasing the hydrophobicity of the IL cation, an observation that contrasts with behavior previously reported for $C_n\text{mim}^+$ [3.3] and quaternary ammonium-based ILs (Chapter 2).

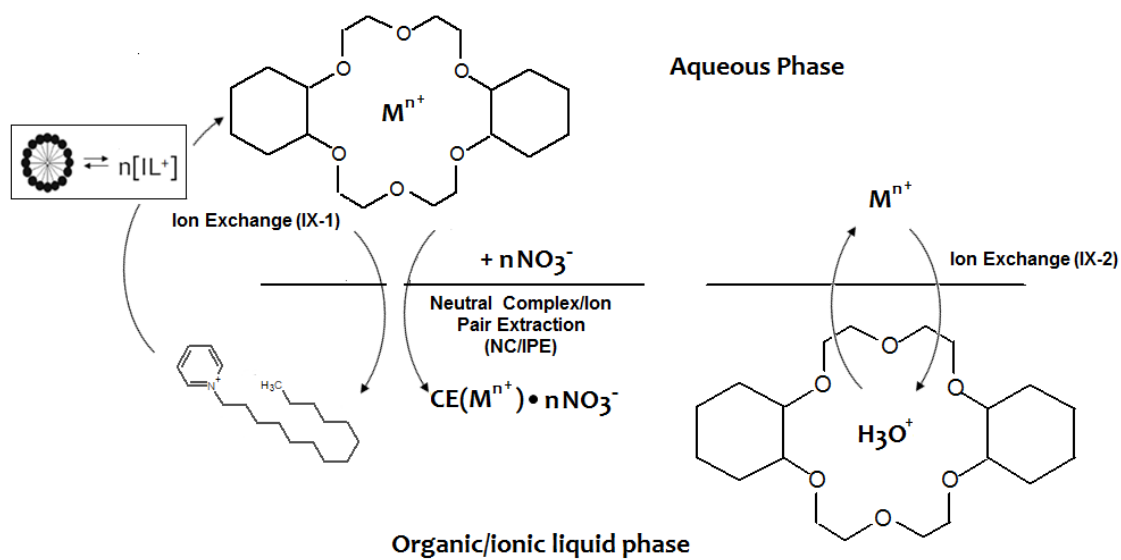


Figure 3.6. Three-path model of metal ion extraction for a system comprising a neutral extractant (*e.g.*, DCH18C6) dissolved in a micelle-forming IL (*e.g.*, $C_{14}pyr^+Tf_2N^-$) in contact with a nitric acid solution.

3.3.6 Effect of IL cation hydrophobicity on extraction from acidic nitrate media

Anticipating the continued effects of micelle formation, the remaining metal ion extraction studies were conducted with a representative group of $C_n\text{pyr}^+\text{X}^-$ ILs (where $n = 4, 7, 10$ and 14 and $\text{X}^- = \text{Tf}_2\text{N}^-$ and BETf^-) that includes one IL that forms micelles and three that do not. The nitric acid dependencies of Na^+ and Ba^{2+} extraction into $C_n\text{pyr}^+\text{Tf}_2\text{N}^-$ ILs are presented in Figure 3.7. It is evident from the effect of nitric acid concentration on the extraction of Ba^{2+} that the ability of $C_{14}\text{pyr}^+\text{Tf}_2\text{N}^-$ to form micelles reduces the amount of neutral complex / ion pair extraction present and causes the IL to behave as if it is unexpectedly hydrophilic, which is indicated by greater than expected prevalence of ion exchange. In contrast, the short-chain, non-micelle-forming ILs behave as expected, that is, according to the trends observed previously for $C_n\text{mim}^+$ and $N_{n,111}^+$ IL families [3.3] (*i.e.*, a downward shift in the Ba^{2+} acid dependency as the alkyl chain length on the IL cation is increased). Extraction of Na^+ into these three ILs is dominated by ion-exchange and, again, follows trends similar to those observed previously for other IL families [3.3], namely a slight downward shift of distribution ratios below 1 M HNO_3 , above which all of the dependencies are nearly the same.

3.3.7 Effect of IL anion hydrophobicity on extraction from acidic nitrate media

As noted in Chapter 2, an increase in the IL anion hydrophobicity has been shown to lead to an increased tendency towards ion-exchange [3.3, 3.4], due to mass action considerations [3.40]. That is, as the hydrophobicity of the anion increases, less IL dissolves initially in the aqueous phase, thus allowing more IL cation to exchange into the aqueous phase. Comparing the extraction of Na^+ , Sr^{2+} , and Ba^{2+} from nitric acid into $C_n\text{pyr}^+\text{Tf}_2\text{N}^-$ (Figures 3.2 and 3.7) and $C_n\text{pyr}^+\text{BETf}^-$ (Figure 3.8) ILs, it is clear that metal ion extraction into the BETf^- forms is more prone to ion-

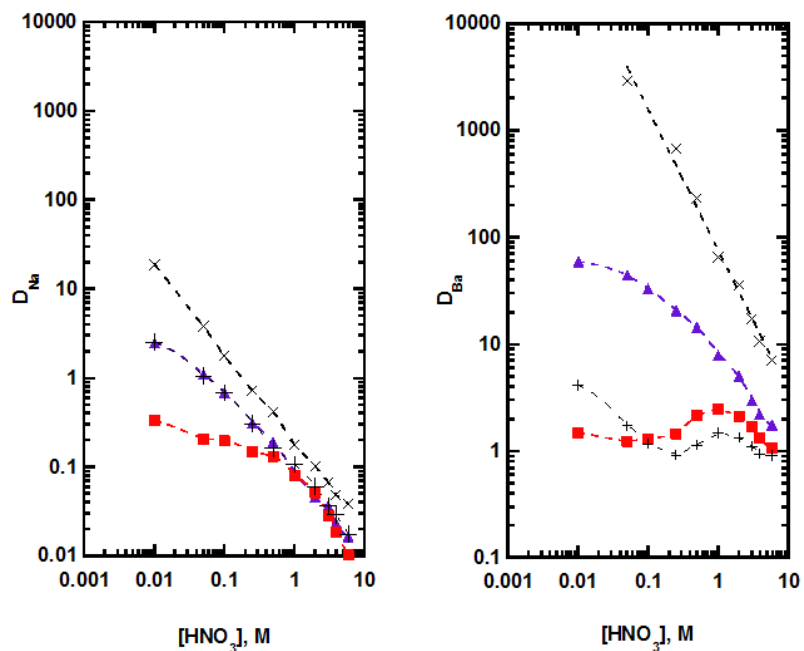


Figure 3.7. Effect of HNO_3 concentration on the extraction of Na^+ (left) and Ba^{2+} (right) by 0.1 M DCH18C6 into $C_4pyr^+Tf_2N^-$ (black exes), $C_7pyr^+Tf_2N^-$ (solid, purple triangles), $C_{10}pyr^+Tf_2N^-$ (solid, red squares) and $C_{14}pyr^+Tf_2N^-$ (black crosses).

exchange, as is evident from the more steeply negative slopes of the acid dependencies. As was seen for the extraction of Sr^{2+} and Ba^{2+} into $\text{C}_n\text{pyr}^+\text{Tf}_2\text{N}^-$ ILs, there is a shift from ion-exchange towards neutral complex / ion pair extraction when these divalent metal ions are extracted into $\text{C}_n\text{pyr}^+\text{BETI}^-$ ILs by DCH18C6 as the hydrophobicity of the IL cation is increased. The extraction of Na^+ continues to be dominated by ion exchange processes when $\text{C}_n\text{pyr}^+\text{BETI}^-$ ILs are employed. It is obvious when analyzing the acid dependencies of all three metal ions that the contributions from ion exchange are greater than one would expect when considering IL cation hydrophobicity alone for $\text{C}_{14}\text{pyr}^+\text{BETI}^-$.

A surface tension study (Figure 3.9) of C_{10}^- and $\text{C}_{14}\text{pyr}^+\text{BETI}^-$ shows a plateau at sufficiently high concentrations of $\text{C}_{14}\text{pyr}^+\text{BETI}^-$, indicating that it too forms micelles (CMC = 1.07 mM). Elemental analysis confirms that impurities are not responsible for the observed behavior (Table 3.4). It is unclear at present why an ostensibly more hydrophobic IL anion yields in an *increase* in the value of the CMC, but ILs bearing the BETI^- anion have exhibited unexpected behavior before [3.4]. It is important to consider, though, that the nature (*i.e.*, shape and size) of the micelles forming in these systems is not known. Thus, further studies utilizing small-angle X-ray scattering (SAXS) or small-angle neutron scattering (SANS), for example, will be required to fully explain our observations.

Table 3.4
Results of carbon, hydrogen, and nitrogen elemental analysis of $\text{C}_{14}\text{pyr}^+\text{BETI}^-$

	% C		% H		% N	
	<i>Theoretical</i>	<i>Actual</i>	<i>Theoretical</i>	<i>Actual</i>	<i>Theoretical</i>	<i>Actual</i>
$\text{C}_{14}\text{pyrBETI}$	42.1	41.9	5.22	5.04	4.27	4.33

Uncertainty of measured values is $\pm 0.5\%$.

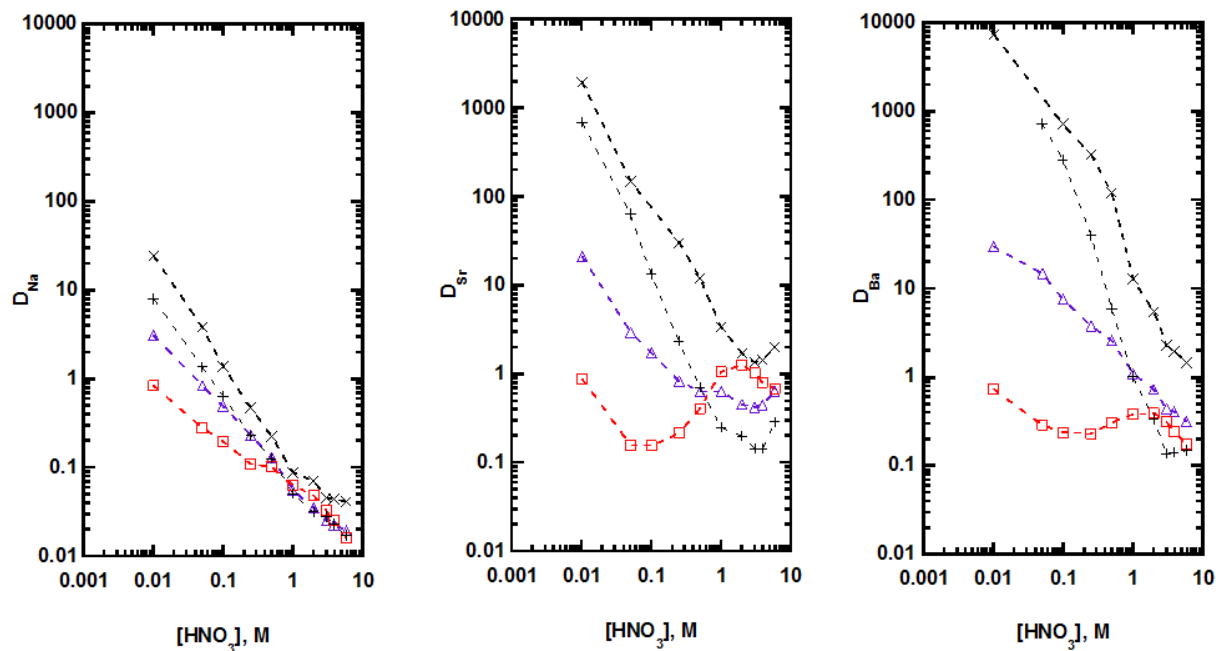


Figure 3.8. Effect of HNO_3 concentration on the extraction of Na^+ (left), Sr^{2+} (middle) and Ba^{2+} (right) by 0.1 M DCH18C6 into C₄pyr⁺BETI⁻ (black exes), C₇pyr⁺BETI⁻ (open, purple triangles), C₁₀pyr⁺BETI⁻ (open, red squares) and C₁₄pyr⁺BETI⁻ (black crosses).

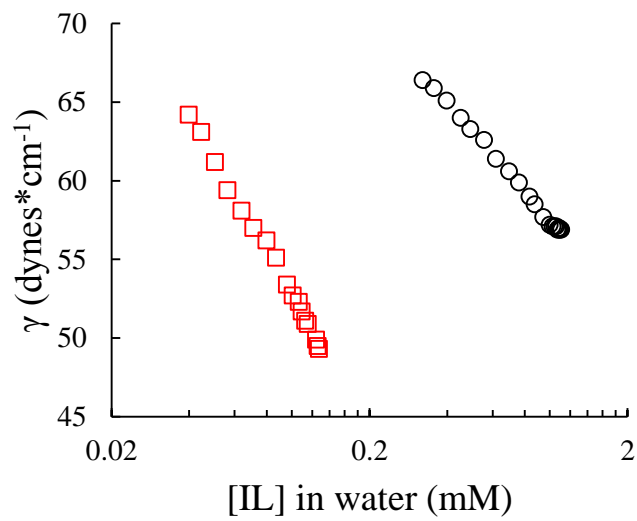


Figure 3.9 Aqueous phase surface tension at various concentrations of C₁₀pyr⁺BETI⁻ (open, red squares) and C₁₄pyr⁺BETI⁻ (open, black circles).

3.3.8 Effect of IL cation hydrophobicity on extraction from acidic chloride media

The extraction of alkali and alkaline earth metals from acidic chloride media into $C_n\text{mim}^+$ and $N_{n,111}^+$ ILs is dominated by ion-exchange processes due to the comparatively high hydration enthalpy of the chloride anion compared to nitrate (-381 kJ/mol and -314 kJ/mol, respectively) [3.41], thus making the transfer of a neutral complex / ion pair more difficult [3.2]. The acid dependencies of Na^+ , Sr^{2+} and Ba^{2+} into $C_n\text{pyr}^+\text{Tf}_2\text{N}^-$ are presented in Figure 3.10. It is evident that ion-exchange processes predominate in these systems as well. Extraction of Na^+ from HCl strongly resembles extraction from HNO_3 , that is, a slight downward shift in distribution ratios up to 1 M [HCl]. In contrast, the effect of IL cation hydrophobicity on the extraction of the divalent metal ions does not present itself as a shift from ion-exchange to neutral complex / ion pair extraction, but as a decrease in the magnitude of the distribution ratios, observations which agree with other IL-based systems [3.2]. Micelle formation clearly continues to affect extraction, even when the aqueous phase is hydrochloric acid, as indicated by higher than expected distribution ratios when $C_{14}\text{pyr}^+\text{Tf}_2\text{N}^-$ is employed.

3.3.9 Effect of IL anion hydrophobicity on extraction from acidic chloride media

The effect of IL anion hydrophobicity observed for nitric acid media (*i.e.*, that a more hydrophobic IL anion will facilitate ion-exchange processes) is evident when examining divalent metal ion extraction into $C_n\text{pyr}^+\text{BETI}^-$ ILs (Figure 3.11). Here, a slight increase in the acid concentration where the upturn in the distribution ratios occurs. For example, the acid dependency of Sr^{2+} extraction into $C_{10}\text{pyr}^+\text{Tf}_2\text{N}^-$ exhibits an upturn at 2 M HCl whereas the upturn occurs at 3 M HCl for $C_{10}\text{pyr}^+\text{BETI}^-$. As expected, the effect of micelle formation is again apparent in the extraction of metal ions from HCl into $C_{14}\text{pyr}^+\text{BETI}^-$, resulting in distribution ratios that are higher than expected based on the IL cation hydrophobicity alone.

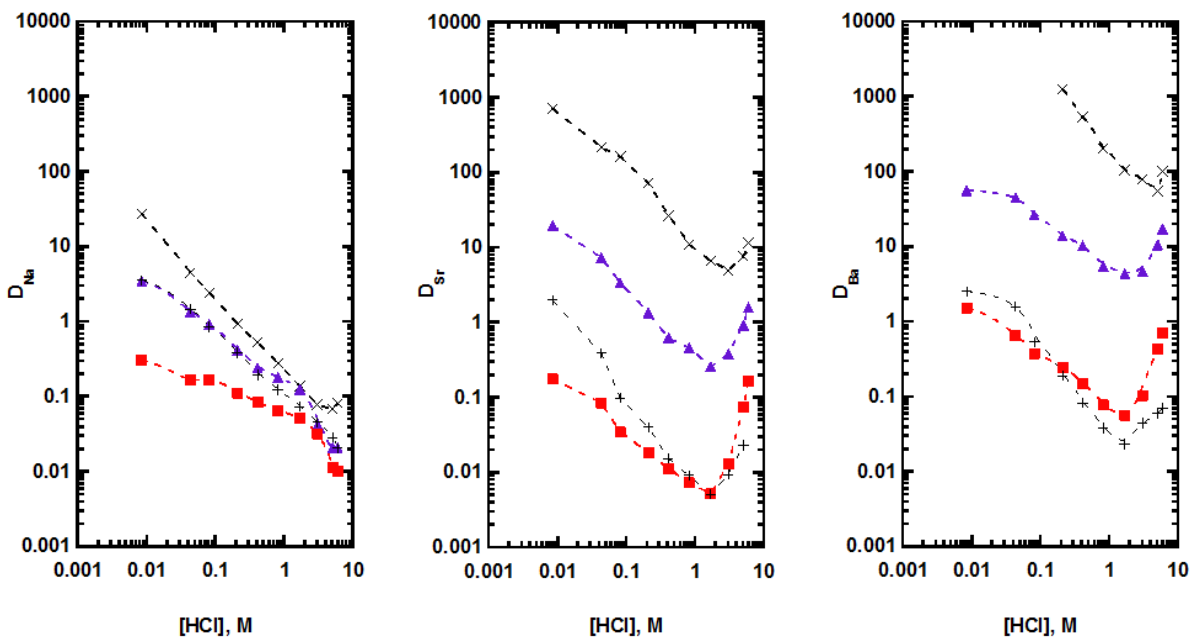


Figure 3.10. Effect of HCl concentration on the extraction of Na^+ (left), Sr^{2+} (middle) and Ba^{2+} (right) by 0.1 M DCH18C6 into $C_4pyr^+Tf_2N^-$ (black exes), $C_7pyr^+Tf_2N^-$ (solid, purple triangles), $C_{10}pyr^+Tf_2N^-$ (solid, red squares) and $C_{14}pyr^+Tf_2N^-$ (black crosses).

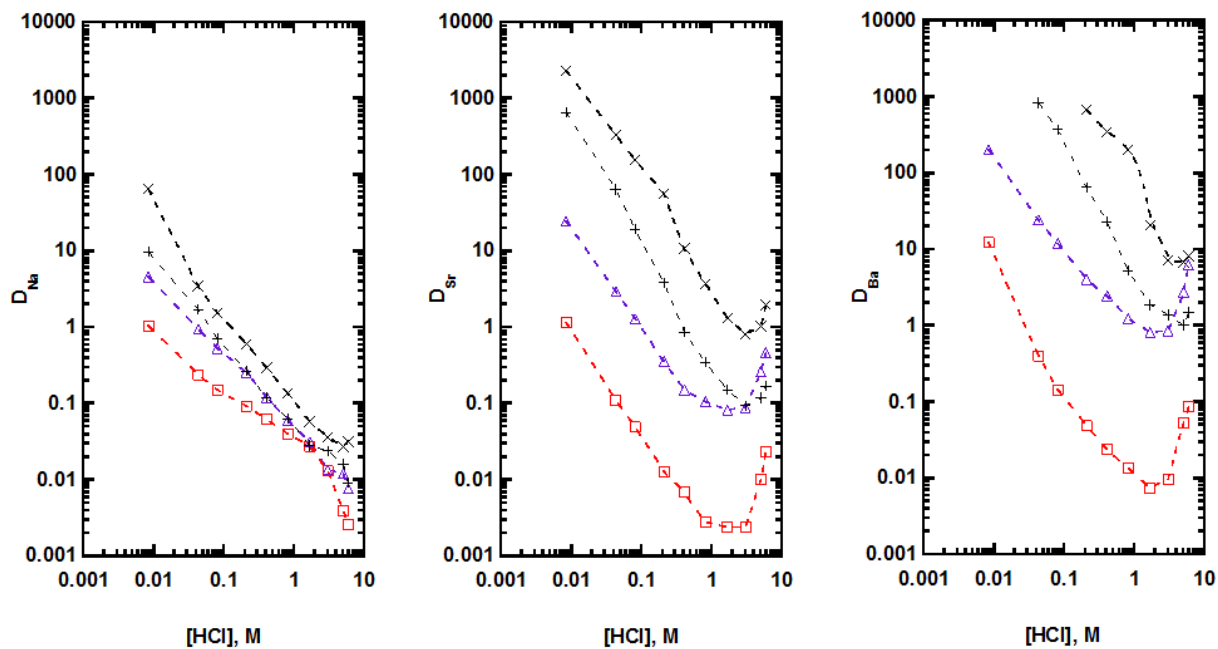


Figure 3.11. Effect of HCl concentration on the extraction of Na^+ (left), Sr^{2+} (middle) and Ba^{2+} (right) by 0.1 M DCH18C6 into $C_4pyr^+BETI^-$ (black exes), $C_7pyr^+BETI^-$ (open, purple triangles), $C_{10}pyr^+BETI^-$ (open, red squares) and $C_{14}pyr^+BETI^-$ (black crosses).

3.3.10 Extraction selectivity

For ILs to be of practical value in either liquid-liquid extraction or extraction chromatographic systems for metal ion separations (*e.g.*, separation and preconcentration of trace radionuclides from soil leachates or biological samples), the partitioning of the metal ion of interest in the 1-3 M acid range must be highly selective *vs.* other metal ions present, particularly matrix ions such as Ca^{2+} and Na^+ [3.19, 3.42]. To assess the selectivity of *N*-alkylpyridinium IL-based systems, separation factors (α_{M_1/M_2}) were calculated from the extraction data presented above and the results presented in Table 3.5 (HNO_3) and Table 3.6 (HCl). As has been shown, neutral complex / ion pair extraction (*i.e.*, the preferred, “green” mode of metal ion partitioning) is favored for non-micelle-forming ILs comprising a hydrophobic cation and a somewhat hydrophilic anion. This suggests that $\text{C}_{10}\text{pyr}^+\text{Tf}_2\text{N}^-$, which is the longest chain C_npyr^+ IL that does not form micelles, is the most appropriate choice of the *N*-alkylpyridinium ILs to compare to previously studied solvents (1-octanol, $\text{C}_{10}\text{mim}^+\text{Tf}_2\text{N}^-$, and $\text{N}_{12,111}^+\text{Tf}_2\text{N}^-$) to determine if this IL family affords any improvement in extraction selectivity.

When nitric acid-containing aqueous phases are employed (Table 3.5), $\text{C}_{10}\text{pyr}^+\text{Tf}_2\text{N}^-$ is more selective (as reflected in larger values of $\alpha_{\text{Sr}/\text{Ba}}$ and $\alpha_{\text{Sr}/\text{Na}}$) than $\text{C}_{10}\text{mim}^+\text{Tf}_2\text{N}^-$ and provides higher $\alpha_{\text{Sr}/\text{Na}}$ values than 1-octanol, but it is outperformed by $\text{N}_{12,111}^+\text{Tf}_2\text{N}^-$ under nearly all conditions. Moreover, examination of the respective acid dependencies makes it clear that $\text{C}_{10}\text{pyr}^+\text{Tf}_2\text{N}^-$ is more prone to ion-exchange than either $\text{C}_{10}\text{mim}^+\text{Tf}_2\text{N}^-$ or $\text{N}_{12,111}^+\text{Tf}_2\text{N}^-$ (based on the shape of their dependencies) [3.3]. Unfortunately, as pointed out above, micelle formation restricts our ability to further increase the hydrophobicity of the IL cation to reduce the prevalence of ion-exchange processes. Extraction from hydrochloric acid (Table 3.6) tends to favor Na^+ partitioning over Sr^{2+} , except for some ILs known to extract predominately by ion exchange

Table 3.5
Effect of HNO₃ concentration on $\alpha_{\text{Sr/Ba}}$ ($= D_{\text{Sr}} / D_{\text{Ba}}$) and $\alpha_{\text{Sr/Na}}$ ($= D_{\text{Sr}} / D_{\text{Na}}$) values for C_npyr⁺Tf₂N⁻ ILs, C_npyr⁺BETI⁻ ILs, C₁₀mim⁺Tf₂N⁻, N_{12,111}⁺Tf₂N⁻ and 1-octanol from extraction data for 0.1 M DCH18C6 in the specified organic or IL phase

[HNO ₃]	1 M		2 M		3 M	
	$\alpha_{\text{Sr/Na}}$	$\alpha_{\text{Sr/Ba}}$	$\alpha_{\text{Sr/Na}}$	$\alpha_{\text{Sr/Ba}}$	$\alpha_{\text{Sr/Na}}$	$\alpha_{\text{Sr/Ba}}$
1-octanol ^a	7.35	1.52	8.22	1.82	14.2	2.03
C ₁₀ mimTf ₂ N ^a	25.8	1.15	42.6	1.17	68.4	1.38
N _{12,111} Tf ₂ N ^b	37.1	3.16	90.3	3.58	256.0	3.84
C ₄ pyrTf ₂ N	59.3	0.16	59.9	0.17	84.0	0.33
C ₇ pyrTf ₂ N	32.2	0.34	38.0	0.35	52.0	0.63
C ₁₀ pyrTf ₂ N	38.1	1.26	72.0	1.76	111	1.88
C ₁₄ pyrTf ₂ N	12.4	0.91	18.0	0.82	27.0	0.89
C ₄ pyrBETI	38.5	0.26	24.1	0.31	30.0	0.60
C ₇ pyrBETI	11.4	0.57	12.8	0.62	16.7	0.95
C ₁₀ pyrBETI	16.5	2.75	25.9	3.21	31.3	3.27
C ₁₄ pyrBETI	4.90	0.25	6.30	0.59	5.18	1.06

^a Data from reference [3.3].

^b Data from Table 2.3.

Table 3.6
Effect of HCl concentration on $\alpha_{\text{Sr}/\text{Ba}}$ ($= D_{\text{Sr}} / D_{\text{Ba}}$) and $\alpha_{\text{Sr}/\text{Na}}$ ($= D_{\text{Sr}} / D_{\text{Na}}$) values for $\text{C}_n\text{pyr}^+\text{Tf}_2\text{N}^-$ ILs, $\text{C}_n\text{pyr}^+\text{BETI}^-$ ILs, $\text{C}_{10}\text{mim}^+\text{Tf}_2\text{N}^-$, $\text{N}_{12,111}^+\text{Tf}_2\text{N}^-$ and 1-octanol from extraction data for 0.1 M DCH18C6 in the organic or IL phase

[HCl]	1 M		2 M		3 M	
	$\alpha_{\text{Sr}/\text{Na}}$	$\alpha_{\text{Sr}/\text{Ba}}$	$\alpha_{\text{Sr}/\text{Na}}$	$\alpha_{\text{Sr}/\text{Ba}}$	$\alpha_{\text{Sr}/\text{Na}}$	$\alpha_{\text{Sr}/\text{Ba}}$
1-octanol ^a	0.58	0.58	0.78	0.65	0.78	0.57
$\text{C}_{10}\text{mimTf}_2\text{N}^{\text{a}}$	0.08	0.15	0.08	0.12	0.29	0.11
$\text{N}_{12,111}\text{Tf}_2\text{N}^{\text{b}}$	0.04	0.14	0.06	0.19	0.15	0.18
$\text{C}_4\text{pyrTf}_2\text{N}$	40.2	0.05	47.1	0.06	62.4	0.06
$\text{C}_7\text{pyrTf}_2\text{N}$	2.54	0.08	2.05	0.06	9.21	0.08
$\text{C}_{10}\text{pyrTf}_2\text{N}$	0.11	0.09	0.10	0.09	0.41	0.13
$\text{C}_{14}\text{pyrTf}_2\text{N}$	0.07	0.24	0.07	0.22	0.20	0.21
$\text{C}_4\text{pyrBETI}$	27.3	0.02	22.8	0.06	22.4	0.11
$\text{C}_7\text{pyrBETI}$	1.76	0.08	2.63	0.10	6.61	0.11
$\text{C}_{10}\text{pyrBETI}$	0.07	0.21	0.09	0.32	0.18	0.25
$\text{C}_{14}\text{pyrBETI}$	5.52	0.07	5.32	0.08	3.91	0.07

^a Data from reference [3.3].

^b Data from Table 2.4.

processes. Also, Ba^{2+} is preferentially extracted (*vs.* Sr^{2+}) under all conditions, and therefore, solvent extraction systems employing HCl may not be of particular value if Sr^{2+} selectivity is desired. It appears then that the use of the $\text{N}_{n,111}^+$ IL family is preferred over the C_npyr^+ family due to the lack of micelle formation and more favorable strontium selectivity over barium and sodium when acidic nitrate media are employed.

3.3.11 Effect of IL cation structure on the formation of micelles

It should be obvious at this point that the ability of long chain C_npyr^+ ILs to form micelles in the aqueous phase is detrimental in IL-based solvent extraction systems employing DCH18C6 (and by analogy, other neutral extractants) because of the accompanying increase in the contribution of ion-exchange processes to the overall partitioning. Although this family of ILs represents the only one for which this phenomenon has been observed to date, it is nonetheless worthwhile to determine if it will be possible to eliminate micellization were it to arise in studies of other IL families. As indicated above, the stability of a micelle depends on several factors, including head group repulsion [3.43]. That is, an amphiphile whose head group repulsions are too great will not be able to undergo micellization. This suggests that the structure of the hydrophilic head group could be modified to block micelle formation of the IL cation. Additionally, previous work on the surface activity of mono- and dicationic imidazolium-based ILs demonstrates the effect of each alkyl chain length on the CMC [3.44]. It was found that ILs bearing a methyl- group opposite the alkyl chain had lower CMCs compared to ILs with similar total carbon number, but bearing a butyl- group opposite the alkyl chain (*e.g.*, 1-decyl-3-methyl imidazolium bromide – total C = 14 and CMC = 20 mM; 1-butyl-3-octyl imidazolium bromide – total C = 15 and CMC = 41 mM). That is, for ILs with similar or the same total carbon number, an increase in the number of carbons on the side of the ring opposite that of the main alkyl chain

results in an increase in the CMC, implying that micelle formation is more difficult. With this in mind, extraction studies were conducted with IL cations incorporating an ethyl- or dimethylamino-substituent at the 4-position on the pyridinium ring (Figure 3.12).

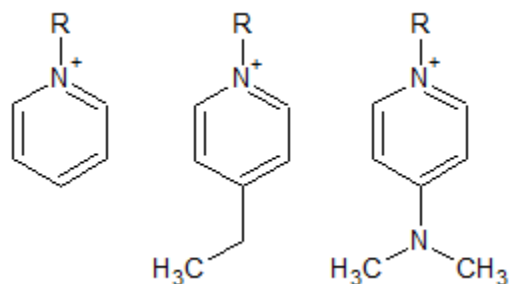


Figure 3.12. Structures of *N*-alkylpyridinium ($C_n\text{pyr}^+$), *N*-alkyl-4-ethylpyridinium ($C_n\text{etpyr}^+$) and *N*-alkyl-4-(dimethyl)aminopyridinium ($C_n\text{dmapyr}^+$) IL cations.

Figure 3.13 shows the nitric acid dependencies for Sr^{2+} extraction into $C_n\text{etpyr}^+\text{Tf}_2\text{N}^-$ ILs by DCH18C6 (left panel), as well as surface tension measurements at various concentrations of the same IL in water (right panel). As is evident from a comparison of the extraction data to that observed for the $C_n\text{pyr}^+\text{Tf}_2\text{N}^-$ ILs (Figure 3.2), the presence of an ethyl- group appears to enhance ion exchange processes in these systems compared to ILs bearing the unsubstituted ring. In fact, all four $C_n\text{etpyr}^+\text{Tf}_2\text{N}^-$ IL-based systems exhibit acid dependencies with regions that have steep negative slopes, suggesting substantial contributions from ion exchange. Despite the presence of a downward shift in the distributions ratios as the alkyl chain length is increased, which has been reported previously for $C_n\text{mim}^+$ [3.1-3.3], $N_{n,111}^+$ (Chapter 2), and $C_n\text{pyr}^+$ ILs that do not form micelles, the surface tension measurements show that the longest chain IL ($C_{12}\text{etpyr}^+\text{Tf}_2\text{N}^-$) does in fact form micelles (CMC = 0.478mM). $C_{14}\text{pyr}^+\text{Tf}_2\text{N}^-$ represents the unsubstituted $C_n\text{pyr}^+$ IL with the same total carbon as $C_{12}\text{etpyr}^+\text{Tf}_2\text{N}^-$. As expected, the ‘shift’ of an ethyl- group from the main alkyl chain to the opposite side of the IL cation ring results in an increase in the CMC (0.307

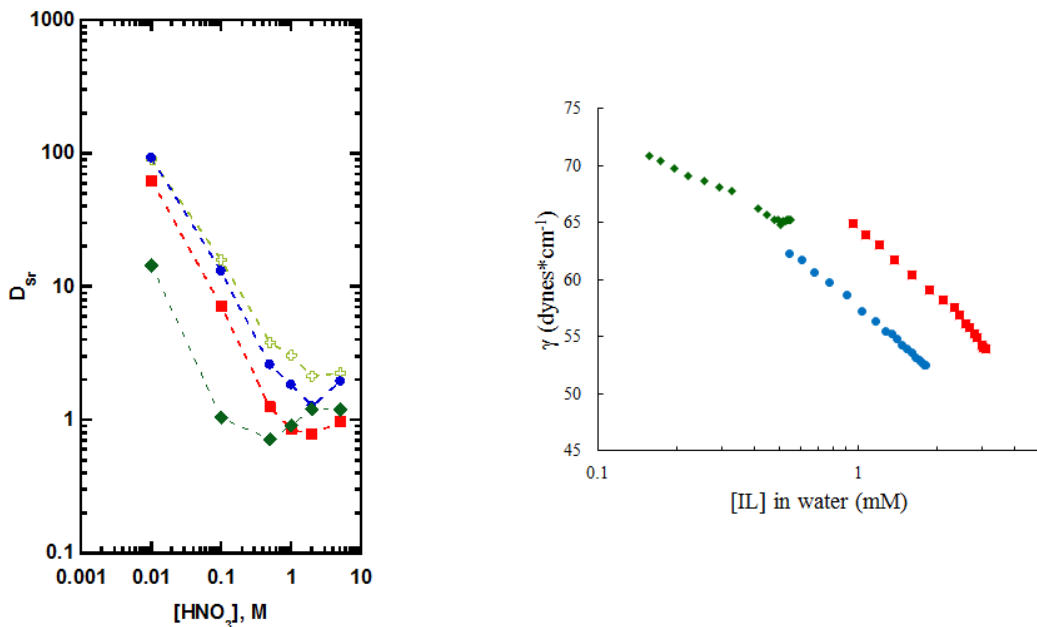


Figure 3.13. Left panel: Effect of HNO_3 concentration on the extraction of Sr^{2+} by 0.1 M DCH18C6 into C_6 etpyr $^+Tf_2N^-$ (open, green crosses), C_8 etpyr $^+Tf_2N^-$ (solid, blue circles), C_{10} etpyr $^+Tf_2N^-$ (solid, red squares) and C_{12} etpyr $^+Tf_2N^-$ (solid, green diamonds). Right panel: Aqueous phase surface tension at various concentrations of C_8 etpyr $^+Tf_2N^-$ (solid, blue circles), C_{10} etpyr $^+Tf_2N^-$ (solid, red squares) and C_{12} etpyr $^+Tf_2N^-$ (solid, green diamonds).

mM and 0.478 mM for $C_{14}\text{pyr}^+\text{Tf}_2\text{N}^-$ and $C_{12}\text{etpyr}^+\text{Tf}_2\text{N}^-$, respectively). In addition, $C_{10}\text{etpyr}^+\text{Tf}_2\text{N}^-$ does not form micelles whereas $C_{12}\text{pyr}^+\text{Tf}_2\text{N}^-$ does (CMC = 0.133 mM).

It is clear that the presence of the ethyl- group on the *N*-alkylpyridinium ring favors extraction by ion exchange processes. This effect is obvious when the nitric acid dependencies for the extraction of Sr^{2+} of ILs with the same total carbon count are compared (Figure 3.14). Based only on the shape of their acid dependencies, $C_{12}\text{etpyr}^+\text{Tf}_2\text{N}^-$ and $C_{14}\text{pyr}^+\text{Tf}_2\text{N}^-$ appear to incorporate comparable contributions from ion exchange. Why a more dramatic effect is not observed in the extraction behavior for $C_{12}\text{etpyr}^+\text{Tf}_2\text{N}^-$ can be explained by the higher water solubilities observed for ethyl-bearing ILs compared to those with the same carbon count without the ethyl- group (Table 3.7). It appears then, that although the addition of an ethyl- group to the *N*-alkylpyridinium ring makes micelle formation more difficult by raising the CMC of ILs with the same total carbon count, the increased water solubility of the ethyl-containing ILs promotes ion exchange processes.

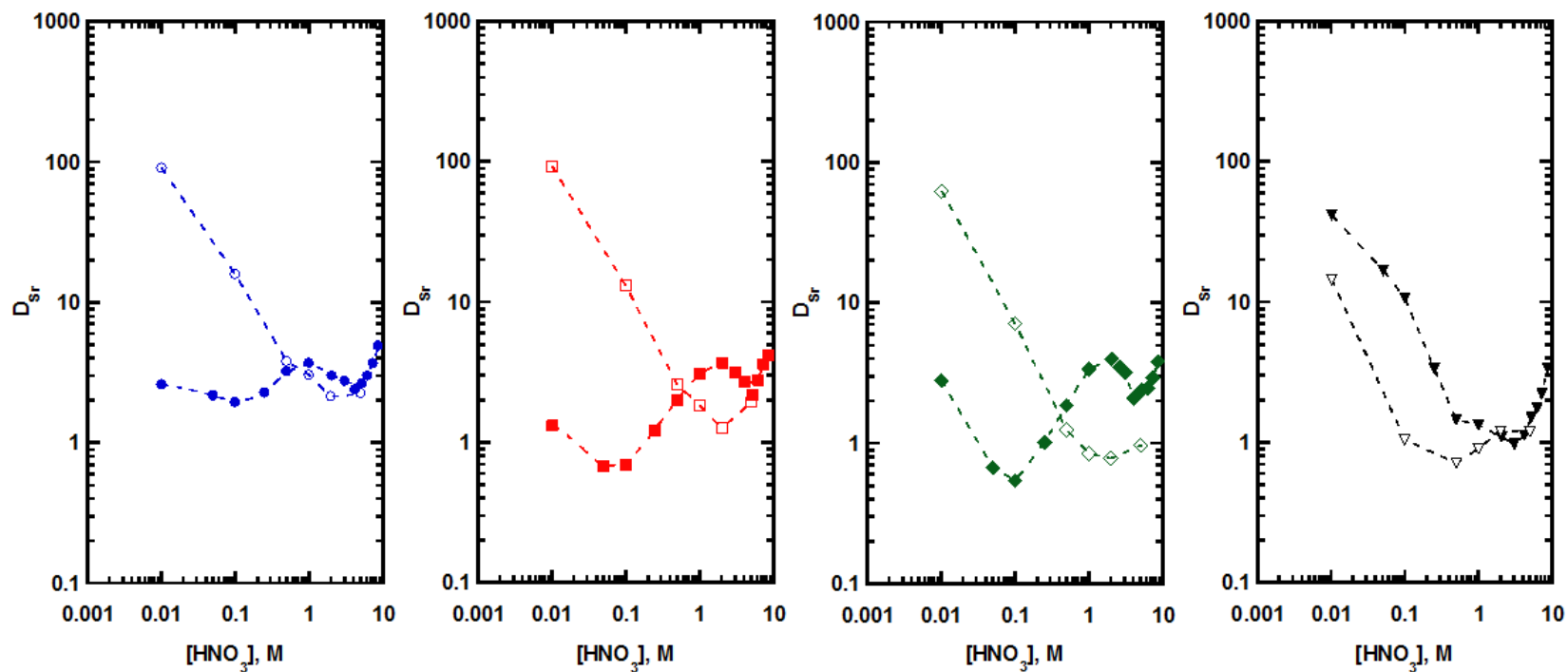


Figure 3.14. Effect of HNO_3 concentration on the extraction of Sr^{2+} by 0.1 M DCH18C6. Panel A: $\text{C}_8\text{pyr}^+\text{Tf}_2\text{N}^-$ (solid, blue circles) and $\text{C}_6\text{etpyr}^+\text{Tf}_2\text{N}^-$ (open, blue circles). Panel B: $\text{C}_{10}\text{pyr}^+\text{Tf}_2\text{N}^-$ (solid, red squares) and $\text{C}_8\text{etpyr}^+\text{Tf}_2\text{N}^-$ (open, red squares). Panel C: $\text{C}_{12}\text{pyr}^+\text{Tf}_2\text{N}^-$ (solid, green diamonds) and $\text{C}_{10}\text{etpyr}^+\text{Tf}_2\text{N}^-$ (open, green diamonds). Panel D: $\text{C}_{14}\text{pyr}^+\text{Tf}_2\text{N}^-$ (solid, black triangles) and $\text{C}_{12}\text{etpyr}^+\text{Tf}_2\text{N}^-$ (open, black triangles).

Table 3.7
Comparison of IL water solubilities

Carbon Count	Ionic liquid	Water solubility (ppm)
15	C ₁₀ pyrTf ₂ N	282
	C ₈ etpyrTf ₂ N	2026
	C ₈ dmapTf ₂ N	243
17	C ₁₂ pyrTf ₂ N	111
	C ₁₀ etpyrTf ₂ N	3387
19	C ₁₄ pyrTf ₂ N	171
	C ₁₂ etpyrTf ₂ N	1334
	C ₁₂ dmapTf ₂ N	46

The dimethylamino- group represents not only a larger substituent compared to ethyl-, but also a more polar one due to the presence of the electron withdrawing nitrogen atom, which should increase the CMC. In addition, work conducted at Brookhaven National Laboratory has shown that ILs incorporating this substituent group are relatively stable in the presence of radiation compared to similar ILs [3.45], which is an advantageous attribute for ILs given the intended applications of these solvents. Strontium extraction data (left panel) and surface tension measurements (right panel) for $C_8\text{dmapyr}^+\text{Tf}_2\text{N}^-$ and $C_{12}\text{dmapyr}^+\text{Tf}_2\text{N}^-$ are presented in Figure 3.15. Unlike the ethyl-bearing ILs, the incorporation of the dimethylamino- group actually reduces the contributions from ion exchange compared to the non-substituted analogs. Additionally, the water solubility of these ILs was found to be less than both the ethyl- containing ILs and those comprising unsubstituted IL cations (Table 3.7). Figure 3.16 shows a comparison of the nitric acid dependencies for the extraction of Sr^{2+} into $C_n\text{pyr}^+\text{Tf}_2\text{N}^-$ and $C_n\text{dmapyr}^+\text{Tf}_2\text{N}^-$ ILs with the same total carbon count. Not only do $C_n\text{dmapyr}^+\text{Tf}_2\text{N}^-$ IL-based systems exhibit favorable strontium extraction data, but based on measurements of surface tension at various concentrations of IL in water, they do not form micelles under these conditions. Surfactants bearing a dimethylamino- group that form micelles have been described previously [3.46], but the CMC of the ILs in these particular systems has increased enough to eliminate micellization.

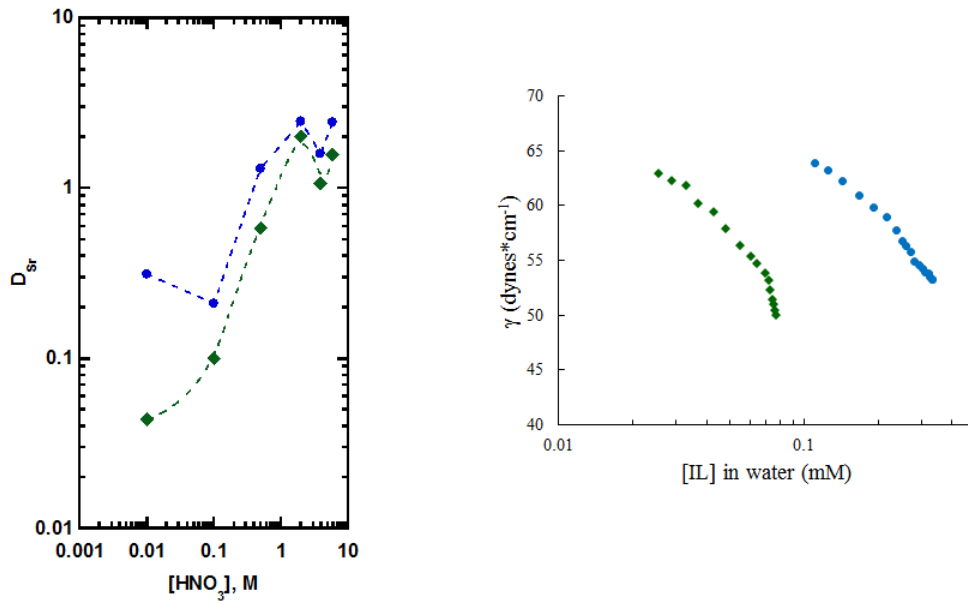


Figure 3.15. Left panel: Effect of HNO_3 concentration on the extraction of Sr^{2+} by 0.1 M DCH18C6 into C_8 mapyr $^+Tf_2N^-$ (solid, blue circles) and C_{12} mapyr $^+Tf_2N^-$ (solid, green diamonds). Right panel: Aqueous phase surface tension at various concentrations of C_8 mapyr $^+Tf_2N^-$ (solid, blue circles) and C_{12} mapyr $^+Tf_2N^-$ (solid, green diamonds).

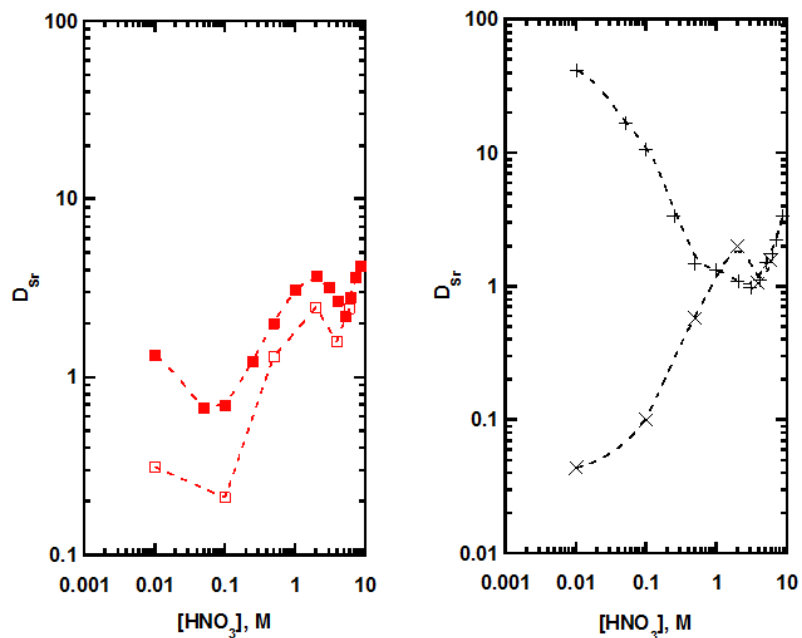


Figure 3.16. Effect of HNO_3 concentration on the extraction of Sr^{2+} by 0.1 M DCH18C6. Left panel: $C_{10}pyr^+Tf_2N^-$ (solid, red squares) and $C_8dmapyr^+Tf_2N^-$ (open, red squares). Right panel: $C_{14}pyr^+Tf_2N^-$ (black plus signs) and $C_{12dmapyr^+Tf_2N^-}$ (black exes).

3.4 Conclusions

This work has confirmed that the effects of IL cation and anion hydrophobicity and the hydration enthalpy of the aqueous phase anion on metal ion extraction reported for other IL families *are* general. It has also revealed that aggregation of the IL cation in the aqueous phase represents yet another complexity of IL-based extraction systems that must be taken into account when considering their use as alternatives to traditional organic solvents in these applications. Micelle formation by the IL cation facilitates undesirable ion-exchange processes and prevents the exploitation of a highly hydrophobic IL cation to enhance neutral complex / ion pair extraction. Despite this, the so-called ‘three-path model’ does appear to represent a general description of the partitioning of a metal ion into an ionic liquid in the presence of a neutral extractant. That is, micelle formation does not represent a new extraction mechanism; rather it is a driving force for cation exchange involving the IL cation. Lastly, the incorporation of a dimethylamino- group into the *N*-alkylpyridinium ring effectively blocks micelle formation and facilitates strontium extraction via neutral complex / ion pair formation by reducing the contributions from ion exchange processes. We expect that a variety of other substituents will eventually be found to serve this same purpose.

3.5 References

- [3.1] Dietz, M.L.; Garvey, S.L.; Hawkins, C.A. Mechanisms of Metal Ion Transfer into RTILs: Implications for Their Use as Extraction Solvents. *Proceedings of the 19th International Solvent Extraction Conference, Santiago, Chile, Chapter X*, **2011**, 208-213.
- [3.2] Garvey, S.L.; Hawkins, C.A.; Dietz, M.L., Effect of Aqueous Phase Anion on the Mode of Facilitated Ion Transfer into Room-Temperature Ionic Liquids. *Talanta*, **2012**, 95, 25-30.
- [3.3] Hawkins, C.A.; Garvey, S.L.; Dietz, M.L., Structural Variations in Room-Temperature Ionic Liquids: Influences on Metal Ion Partitioning Modes and Extraction Selectivity. *Separation and Purification Technology*, **2012**, 89, 31-38.
- [3.4] Garvey, S.L.; Dietz, M.L., Ionic Liquid Anion Effects in the Extraction of Metal Ions by Macrocyclic Polyethers. *Separation and Purification Technology*, **2014**, 123, 145-152.
- [3.5] Dietz, M.L.; Dzielawa, J.A., Ion-Exchange as a Mode of Cation Transfer into Room-Temperature Ionic Liquids Containing Crown Ethers: Implications for the “Greenness” of Ionic Liquids as Diluents in Liquid-Liquid Extraction. *Chemical Communications*, **2001**, 2124-2125.
- [3.6] Jensen, M.P.; Dzielawa, J.A.; Rickert, P.; Dietz, M.L., EXAFS Investigations of the Mechanism of Facilitated Ion Transfer into a Room-Temperature Ionic Liquid. *Journal of the American Chemical Society*, **2002**, 124, 10664-10665.
- [3.7] Dietz, M.L.; Dzielawa, J.A.; Laszak, I.; Young, B.A.; Jensen, M.P., Influence of Solvent Structural Variations on the Mechanism of Facilitated Ion Transfer into Room-Temperature Ionic Liquids. *Green Chemistry*, **2003**, 5, 682-685.
- [3.8] Stepinski, D.C.; Jensen, M.P.; Dzielawa, J.A.; Dietz, M.L., Synergistic Effects in the Facilitated Transfer of Metal Ions into Room-Temperature Ionic Liquids. *Green Chemistry*, **2005**, 7, 151-158.
- [3.9] Dietz, M.L.; Stepinski, D. C., A Ternary Mechanism for the Facilitated Transfer of Metal Ions into Room-Temperature Ionic Liquids (RTILs): Implications for the “Greenness” of RTILs as Extraction Solvents. *Green Chemistry*, **2005**, 7, 747-750.
- [3.10] Dietz, M.L.; Stepinski, D.C., Anion Concentration-Dependent Partitioning Mechanism in the Extraction of Uranium into Room-Temperature Ionic Liquids. *Talanta*, **2008**, 75, 598-603.
- [3.11] Bagherzadeh, M.; Ghazali-Esfahani, S., Efficient Recyclable Catalytic System for Deoxygenation of Sulfoxides: Catalysis of Ionic Liquid-Molybdenum Complexes in Ionic Liquid Solution. *New Journal of Chemistry*, **2012**, 36, 971-976.
- [3.12] Kim, M.J.; Shin, S.H.; Kim, Y.J.; Cheong, M.; Lee, J.S.; Kim, H.S., Role of Alkyl Group in the Aromatic Extraction Using Pyridinium-Based Ionic Liquids. *Journal of Physical Chemistry B*, **2013**, 117, 14827-14834.

- [3.13] Yamamoto, E.; Yamaguchi, S.; Nagamune, T., Protein Refolding by N-Alkylpyridinium and N-Alkyl-N-Methylpyrrolidinium Ionic Liquids. *Applied Biochemistry and Biotechnology*, **2011**, 164, 957-967.
- [3.14] Papaiconomou, N.; Lee, J-M.; Salminen, J.; Von Stosch, M.; Prausnitz, J.M., Selective Extraction of Copper, Mercury, Silver and Palladium Ions from Water Using Hydrophobic Ionic Liquids. *Industrial and Engineering Chemistry Research*, **2008**, 47, 5080-5086.
- [3.15] Wu, W.; Wu, G.; Zhang, M., Highly Selective Synthesis of 2,6-Dimethylnaphthalene by Green Catalysts—N-alkyl-pyridinium Halides-Ammonium Chloride Ionic Liquids. *Applied Catalysis A: General*, **2007**, 326, 189-193.
- [3.16] Deetlefs, M.; Seddon, K.R., Improved Preparations of Ionic Liquids Using Microwave Irradiation. *Green Chemistry*, **2003**, 5, 181-186.
- [3.17] Bonhote, P.; Dias, P.; Papageorgiou, N.; Kalyanasundaram, K.; Gratzel, M., Hydrophobic, Highly Conductive Ambient-Temperature Molten Salts. *Inorganic Chemistry*, **1996**, 35, 1168-1178.
- [3.18] Yunus, N.M.; Mutalib, M.I.A.; Man, Z.; Bustam, M.A.; Murugesan, T., Thermophysical Properties of 1-Alkylpyridinium Bis(trifluoromethylsulfonyl)imide Ionic Liquids. *Journal of Chemical Thermodynamics*, **2010**, 42, 491-495.
- [3.19] Horwitz, E.P.; Dietz, M.L.; Fisher, D.E., Separation and Preconcentration of Strontium from Biological, Environmental, and Nuclear Waste Samples by Extraction Chromatography Using a Crown Ether. *Analytical Chemistry*, **1991**, 63, 522-525.
- [3.20] Kilaru, P.; Baker, G.A.; Scovazzo, P., Density and Surface Tension Measurements of Imidazolium-, Quaternary, Phosphonium-, Ammonium-Based Room-Temperature Ionic Liquids: Data and Correlations. *Journal of Chemistry and Engineering Data*, **2007**, 52, 2306-2314.
- [3.21] Huddleston, J.G.; Visser, A.E.; Reichert, W.M.; Willauer, H.D.; Broker, G.A.; Rogers, R.D., Characterization and Comparison of Hydrophilic and Hydrophobic Room Temperature Ionic Liquids Incorporating the Imidazolium Cation. *Green Chemistry*, **2001**, 3, 156-162.
- [3.22] Firestone, M.A.; Dzielawa, J.A.; Zapol, P.; Curtiss, L.A.; Seifert, S.; Dietz, M.L., Lyotropic Liquid-Crystalline Gel Formation in a Room-Temperature Ionic Liquid. *Langmuir*, **2002**, 18, 7258-7260.
- [3.23] Dietz, M.L.; Dzielawa, J.A.; Jensen, M.P.; Firestone, M.A., "Conventional aspects of unconventional solvents: Room-temperature ionic liquids as ion exchangers and ionic surfactants", in *Ionic Liquids as Green Solvents: Progress and Prospects*, (R.D. Rogers and K.L. Seddon, Eds.) American Chemical Society, Washington, DC, **2003**, 526-543.
- [3.24] Sharma, R.; Mahajan, R.K., Influence of Various Additives on the Physicochemical Properties of Imidazole-Based Ionic Liquids: A Comprehensive Review. *RSC Advances*, **2014**, 4, 748-774.

- [3.25] Tariq, M.; Freire, M.G.; Saramago, B.; Coutinho, J.A.P.; Canongia Lopes, J.N.; Rebelo, L.P.N., Surface Tension of Ionic Liquids and Ionic Liquid Solutions. *Chemical Society Review*, **2012**, 41, 829-868.
- [3.26] Freire, M.G.; Carvalho, P.J.; Fernandes, A.M.; Marrucho, I.M.; Queimada, A.J.; Coutinho, J.A.P., Surface Tension of Imidazolium-Based Ionic Liquids: Anion, Cation, Temperature and Water Effect. *Journal of Colloid and Interface Science*, **2007**, 314, 621-630.
- [3.27] Ghatee, M.H.; Zolghadr, A.R., Surface Tension Measurements of Imidazolium-Based Ionic Liquids at Liquid-Vapor Equilibrium. *Fluid Phase Equilibrium*, **2008**, 263, 168-175.
- [3.28] Ahosseini, A.; Sensenich, B.; Weatherly, L.R.; Scurto, A.M., Phase Equilibrium, Volumetric, and Interfacial Properties of the Ionic Liquid, 1-hexyl-3-methylimidazolium bis(trifluoromethylsulfonyl)amide and 1-octene. *Journal of Chemical and Engineering Data*, **2010**, 55, 1611-1617.
- [3.29] Cornellas, A.; Perez, L.; Comelles, F.; Ribosa, I.; Manresa, A.; Garcia, M.T., Self-Aggregation and Antimicrobial Activity of Imidazolium and Pyridinium Based Ionic Liquids in Aqueous Solution. *Journal of Colloid and Interface Science*, **2011**, 355, 164-171.
- [3.30] Sastry, N.V.; Vaghela, N.M.; Macwan, P.M.; Soni, S.S.; Aswal V.K.; Gibaud, A., Aggregation Behavior of Pyridinium Based Ionic Liquids in Water – Surface Tension, ¹H NMR Chemical Shifts, SANS and SAXS. *Journal of Colloid and Interface Science*, **2012**, 371, 52-61.
- [3.31] Garcia, M.T.; Ribosa, I.; Perez, L.; Manresa, A.; Comelles, F., Aggregation Behavior and Antimicrobial Activity of Ester-Functionalized Imidazolium- and Pyridinium-Based Ionic Liquids in Aqueous Solution. *Langmuir*, **2013**, 29, 2536-2545.
- [3.32] Jin-Yan, L.; Yong-juan, L.; Hai-Chao, L., Conductometry Properties of Mixed Reverse Micelles with Amphiphilic Ionic Liquids. *Advanced Materials Research*, **2012**, 455-456, 800-805.
- [3.33] Blesic, M.; Marques, M.H.; Plechkova, N.V.; Seddon, K.R.; Rebelo L.P.N.; Lopes, A., Self-Aggregation of Ionic Liquids: Micelle Formation in Aqueous Solution. *Green Chemistry*, **2007**, 9, 481-490.
- [3.34] Jungnickel, C.; Luczak, J.; Ranke, J.; Fernandez, J.F.; Muller, A.; Thöming, J., Micelle Formation of Imidazolium Ionic Liquids in Aqueous Solution. *Colloids and Surfaces A: Physicochemical Engineering Aspects*, **2008**, 316, 278-284.
- [3.35] Luczak, J.; Hupka, J.; Thöming, J.; Jungnickel, C., Self-Organization of Imidazolium Ionic Liquids in Aqueous Solution. *Colloids and Surfaces A: Physicochemical Engineering Aspects*, **2008**, 329, 125-133.

- [3.36] El Seoud, O.A.; Pires, P.A.R.; Abdel-Moghny, T.; Bastos, E.L., Synthesis and Micellar Properties of Surface-Active Ionic Liquids: 1-alkyl-3-methylimidazolium Chlorides. *Journal of Colloid and Interface Science*, **2007**, 313, 296-304.
- [3.37] Galgano, P.D., El Seoud, O.A., Surface Active Ionic Liquids: Study of the Micellar Properties of 1-(1-alkyl)-3-methylimidazolium Chlorides and Comparison with Structurally Related Surfactants. *Journal of Colloid and Interface Science*, **2011**, 361, 186-194.
- [3.38] Mata, J.; Varade, D.; Bahadur, P., Aggregation Behavior of Quaternary Salt-Based Cationic Surfactants. *Thermochimica. Acta*, **2005**, 428, 147-155.
- [3.39] Rosen, M.J., *Surfactants and Interfacial Phenomena*. 2nd ed., Wiley Interscience, Hoboken, NJ, 1989.
- [3.40] Luo, H.; Dai, S.; Bonnesen, P.V.; Haverlock, T.J.; Moyer, B.A.; Buchanan III, A.C., A Striking Effect of Ionic-Liquid Anions in the Extraction of Sr²⁺ and Cs⁺ by Dicyclohexano-18-Crown-6. *Solvent Extraction and Ion Exchange*, **2006**, 24, 19-31.
- [3.41] Smith, D.W., Ionic Hydration Enthalpies. *Journal of Chemical Education*, **1977**, 54, 540-542.
- [3.42] Horwitz, E.P.; Chiarizia, R.; Dietz, M.L., A Novel Strontium-Selective Extraction Chromatographic Resin. *Solvent Extraction and Ion Exchange*, **1992**, 10, 313-336.
- [3.43] Tanford, C., Thermodynamics of Micelle Formation: Prediction of Micelle Size and Size Distribution. *Proceedings of the National Academy of Sciences of the United States*, **1974**, 71, 1811-1815.
- [3.44] Baltazar, Q.Q.; Chandawalla, J.; Sawyer, K.; Anderson, J.L., Interfacial and Micellar Properties of Imidazolium-Based Monocationic and Dicationic Ionic Liquids. *Colloids and Surfaces A: Physicochemical Engineering Aspects*, **2007**, 302, 150-156.
- [3.45] Mincher, B.J.; Wishart, J.F., The Radiation Chemistry of Ionic Liquids: A Review. *Solvent Extraction and Ion Exchange*, **2014**, 32, 563-583.
- [3.46] Tiwari, A.K.; Sowmiya, S.M.; Saha, S.K., Study on Premicellar and Micellar Aggregates of Gemini Surfactants with Hydroxyl Substituted Spacers in Aqueous Solution Using a Probe Showing TICT Fluorescence Properties. *Journal of Photochemistry and Photobiology A: Chemistry*, **2011**, 223, 6-13.

Chapter 4:

Octanol-water distribution coefficients and their potential use in predicting extraction behavior

4.1 Introduction

The work described in Chapters 2 and 3 clearly illustrates the substantial effort required to systematically investigate the extraction of metal ions into ILs, as well as the many complexities of such systems. These studies focused on the extraction of only two types of metal ions (*i.e.*, alkali and alkaline earth cations) into two families of ILs (*i.e.*, quaternary ammonium and *N*-alkylpyridinium) with a single neutral extractant (*i.e.*, DCH18C6), which taken together represent only a minute fraction of all possible extraction systems. Although such studies have led to the elucidation of certain general trends in extraction behavior when ILs are employed as diluents for metal ion extraction, it would clearly be advantageous to develop means by which to predict the extraction behavior for as-yet unstudied systems without the need for extensive extraction studies. Ideally, a single parameter (*e.g.*, a chemical or physical property of the IL) could be used to predict extraction behavior in IL-based systems. Furthermore, if the parameter selected could be calculated theoretically, extraction behavior could be predicted entirely theoretically, prior to synthesis of the IL. Octanol-water distribution coefficients (D_{ow}) [4.1-4.7], water contents [4.8-4.11], densities [4.12] and melting points [4.13] are among the various properties of ILs that have been predicted using a theoretical approach, and all are thus potential candidates for the prediction of extraction behavior.

Previous work [4.14-4.21] and the preceding chapters describe several features of an IL-based extraction system that dictate the efficiency, selectivity, and mechanism of metal ion

partitioning. These factors include the IL cation [4.15, 4.19] and anion hydrophobicity [4.16], aqueous phase anion hydration enthalpies [4.14], and the charge density of the metal ion [4.15, 4.17-4.21], among others. Of these, the hydrophobicity of the IL has a particularly strong influence on the mechanism by which metal ions are extracted by the neutral extractant [4.15, 4.16, 4.19, 4.21]. That is, the extraction of divalent metal ions into ILs with cations bearing short alkyl chains, whose hydrophobicity is low, tends to proceed by ion exchange processes. Employing an IL with a long alkyl chain on the IL cation (which is thus more hydrophobic) favors neutral complex / ion pair extraction. Conversely, the more hydrophobic the IL anion, the greater the tendency for ion exchange processes to predominate in the system. Therefore, a single parameter that captures the *overall* hydrophobicity of the IL (*e.g.*, water content, water solubility, or D_{ow}) might prove useful in predicting the behavior of IL-based extraction systems.

Theoretical models have been proposed previously to predict extraction in desulfurization processes [4.22, 4.23], rare earth element (REE) separations [4.24], and the purification and isolation of pharmaceuticals [4.25]. These reports exploit various physical, chemical and thermodynamic properties (*e.g.*, melting point, viscosity, equilibrium constants, and analyte solubility) for the identification of suitable extraction solvents. Therefore, it is reasonable to expect that the use of parameters that embody the hydrophobicity of an IL, such as water content, water solubility, and D_{ow} , may provide the basis of theoretical predictions of extraction behavior for these systems.

The amount of aqueous phase that the organic phase can dissolve (*i.e.*, water content) or vice versa (*i.e.*, water solubility) play a major role in LLX systems, as the partitioning of analytes between the two phases occurs at their interface. Insufficient interaction between the phases may result in a less efficient extraction, while too much phase carryover can cause loss of the solvent

or poor phase separation. Rapid and simple techniques exist to measure the water content and solubility of ionic liquids (*e.g.*, Karl Fischer titration and UV/VIS). In fact, determinations of water content and water solubility are regularly performed in our laboratory as part of IL characterization, and these parameters have already been measured for many of the ILs synthesized, including those presented in Chapters 2 and 3. Additionally, several reports of the prediction of IL water contents and solubilities exist [4.8-4.11].

Octanol-water partition coefficients, K_{ow} defined in Equation 4.1, (or for ionizable species like ILs, octanol-water distribution coefficients, D_{ow} , Equation 4.2) are possibly the most well-established means by which to describe the hydrophobicity of a substance. Their widespread use, especially in the pharmaceutical field, is a result of the similarity between the dielectric properties of 1-octanol and a lipid phase. This resemblance has led to the use of D_{ow} values to model the transfer of solutes (*e.g.*, pharmaceuticals) across a biological membrane [4.26-4.29]. Additional applications include modelling of the environmental fate of organic chemicals [4.30], the mobility of radionuclides in groundwater [4.31], and the effectiveness of pesticides [4.32]. As is the case for water content and water solubility, a number of techniques exist for the measurement of octanol-water distribution coefficients, including the shake flask method [4.33], the slow stir method [4.34], and HPLC-based analysis [4.35], among others [4.36], but more reports of the prediction of D_{ow} values than solvent water solubility or water content values have appeared [4.1-4.7].

$$K_{ow} = \frac{[X]_{org}}{[X]_{aq}} \quad (4.1)$$

$$D_{ow} = \frac{[X_{ionized}]_{org} + [X_{un-ionized}]_{org}}{[X_{ionized}]_{aq} + [X_{un-ionized}]_{aq}} \quad (4.2)$$

Although D_{ow} values for a few $C_n\text{mim}^+\text{Tf}_2\text{N}^-$ ILs have been reported (see Table 4.2 below) and we have previously obtained certain of these values ourselves, analogous data for $C_n\text{pyr}^+\text{Tf}_2\text{N}^-$ and $N_{n,111}^+\text{Tf}_2\text{N}^-$ ILs are lacking. In this chapter, we describe our efforts to determine if a relationship exists between the hydrophobicity of an IL, as reflected in its octanol-water distribution coefficient, and its behavior as an extraction solvent. Furthermore, currently available models reported to predict D_{ow} values will be surveyed to determine the potential of D_{ow} values (and therefore, extraction behavior) to be predicted entirely theoretically. For this study, previous work conducted in our laboratory, which involved the development of an HPLC method for the quantification of ILs [4.37], has been modified to incorporate a mass spectrometer in place of a UV/VIS detector.

4.2 Experimental

4.2.1 Materials

$C_n\text{mim}^+$ (where $n = 2, 5, 6, 8, 10, 12, 14$), $C_n\text{pyr}^+$ (where $n = 4, 6, 7, 8, 10, 12, 14$) and $N_{n,111}^+$ (where $n = 8, 10, 12, 14$) ionic liquids bearing the *bis*[(trifluoromethyl)sulfonyl]imide, Tf_2N^- , anion were used in this study. All ionic liquids employed were already available and had been prepared previously according to the synthetic routes described in Sections 2.2.3 and 3.2.3 using commercially available precursors. Prior to use, the ionic liquids were dried under vacuum ($T = 80\text{ }^\circ\text{C}$ and $P = 15\text{ inHg}$) for a minimum of 3 days. Equal parts deionized water with a specific resistance of at least $18\text{ M}\Omega/\text{cm}$ and 1-octanol (Alfa Aesar, Ward Hill, MA) were left in contact for one week with gentle stirring to equilibrate the phases, which were then separated and used for sample preparation. The mobile phase used for LC-MS analysis was prepared using LC-MS grade acetonitrile (Fisher, Fair Lawn, NJ) and formic acid (Thermo Scientific, Rockford, IL).

4.2.2 Instruments

A Shimadzu LC-MS 2020 was employed to measure the IL⁺ concentration in the aqueous and organic phases by direct injection (no chromatographic column used). An internal standard (C₂mim⁺Tf₂N⁻) was utilized to account for matrix effects. The IL cation concentration of the IL of interest (various m/z ratios) and the internal standard (C₂mim⁺, m/z = 111.3) were measured as two events in single ion monitoring (SIM) positive mode. An identical amount of internal standard was added to all samples and standards prior to analysis. The Shimadzu LS-MS 2020 was equipped with a dual ion source (DUIS) comprising electrospray (ESI) and atmospheric pressure chemical (APCI) ionization modes. Additional instrument parameters, are presented in Table 4.1. A Mettler Toledo AL204 balance was employed for all weighing.

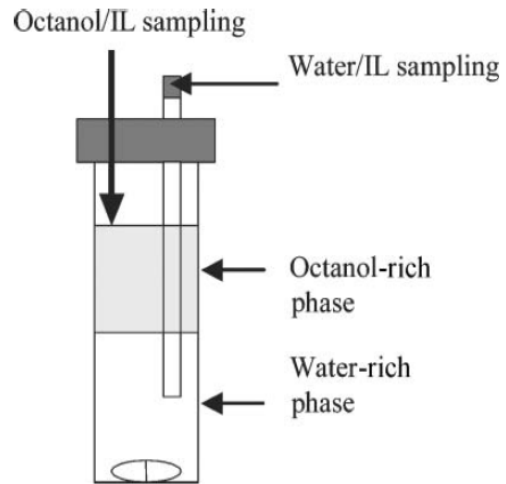
4.2.3 Methods

Slow stir device preparation. Glass vials (~40 mL capacity) with Teflon coated caps were used to prepare sampling devices as described previously by Brennecke *et al.* [4.38] and pictured in Figure 4.1. Water-saturated 1-octanol was used to prepare ~0.1 mM solution of each ionic liquid. Equal volumes (17 mL) of 1-octanol-saturated water and 0.1 mM IL solutions were added to each device. A small magnetic stir bar and Teflon tubing (for sampling of the water-rich phase) was inserted into the vial. To the exposed end of the Teflon tubing was attached a luer attachment for ease of sampling.

The water-rich phase was transferred to the vial first followed by gentle addition of the octanol-rich phase. Each vial was capped and the top wrapped with Parafilm to reduce evaporation. Once all vials were prepared, they were left to equilibrate with gentle stirring (< 200 rpm) for up to 382 days. Samples of the octanol-rich and water-rich phases were drawn and

Table 4.1
LC-MS instrument parameters for IL cation quantification

Column	None
Mobile phase	1% formic acid in acetonitrile
Flow rate	0.500 mL/min
Nebulizing gas flow	1.5 L/min
Interface	Dual ion source (DUIS)
Interface voltage	4.5 kV
Interface current	7.8 μ A
Corona needle voltage	4.5 kV
Corona needle current	0.2 μ A
DL temperature	250 $^{\circ}$ C
Heat block temperature	400 $^{\circ}$ C
Qarray RF voltage	10.1 V
Detector voltage	1.25 kV
PG Vacuum	96 Pa
IG Vacuum	0.00054 Pa
Drying gas flow	15.0 L/min



Apparatus used for the slow-stirring method.

Figure 4.1. Slow stir device used for determination of D_{ow} values [4.38].

analyzed for IL⁺ concentration after 284 days (C₁₂pyr⁺Tf₂N⁻ and N_{14,111}⁺Tf₂N⁻), 293 days (C_{*n*}mim⁺Tf₂N⁻, where *n* = 5, 6, 8, 10, 12, and 14), and 368 days (C_{*n*}pyr⁺Tf₂N⁻, where *n* = 4, 6, 7, 8, 10, 12, 14 and N_{*n*,111}⁺Tf₂N⁻, where *n* = 8, 10 and 12) and again on 298 days (C₁₂pyr⁺Tf₂N⁻ and N_{14,111}⁺Tf₂N⁻), 307 days (C_{*n*}mim⁺Tf₂N⁻, where *n* = 5, 6, 8, 10, 12, and 14), and 382 days (C_{*n*}pyr⁺Tf₂N⁻, where *n* = 4, 6, 7, 8, 10, 12, 14 and N_{*n*,111}⁺Tf₂N⁻, where *n* = 8, 10 and 12) to confirm that equilibrium had been reached. It should be noted that the initial concentration of IL in the octanol-rich phase [4.38-4.40] and the quantification method employed (*i.e.*, slow stir *vs.* shake flask) [4.38] have been shown previously to affect measured D_{ow} values. For the purposes of this work, internal consistency is required if any correlation is to be observed between IL physical properties and extraction behavior, so a fixed set of experimental conditions, selected on the basis of previous work in our laboratory and described above, was used throughout.

4.3 Results and Discussion

4.3.1 Relationship of the IL hydrophilicity index to extraction behavior

The extraction of metal ions from water represents a simpler system than one employing an acidic aqueous phase. Accordingly, such studies are typically the first step in investigations of IL-based systems (see Chapters 2 and 3). The absence of acid from the aqueous phase eliminates extraction of metal ions by IX-2, leaving only NC/IPE and IX-1 as the possible modes of metal ion partitioning. In these simpler systems, the relative contributions of the two paths can be expressed in terms of R, the ratio of the fraction of metal ion extracted (strontium ion in this work) to the fraction of nitrate extracted. As R approaches 1 (*i.e.*, as the amount of metal ion extracted approaches the amount of nitrate extracted), the contribution of IX-1 diminishes and that of NC/IPE increases.

The first parameter considered for the prediction of extraction behavior in IL-based systems is the hydrophilicity index (HI). First proposed by Kohno *et al.* [4.41], HI is a measure of water content, specifically, the number of water molecules per ion pair in the IL phase, and serves as an indicator of IL / water mixture phase behavior. The relationship between R and HI for several $C_n\text{mim}^+$, $C_n\text{pyr}^+$, and $N_{n,111}^+$ ILs is presented in Figure 4.2. As can be seen R decreases sharply as the IL hydrophobicity increases (HI decreases), then levels off as R approaches 1. This is consistent with the previously reported observation that IX processes (here, IX-1) become more difficult as the IL hydrophobicity rises and is in agreement with previous reports of the effect of IL hydrophobicity on extraction behavior [4.15, 4.16, 4.19]. This trend and previous reports of theoretically determined values of water content [4.8-4.11] suggest that HI (*i.e.*, water content) could serve as a useful parameter for the prediction of extraction behavior for IL-based systems.

4.3.2 Relationship of the IL water solubility to extraction behavior

The solubility of an IL in water is an important factor to consider when selecting an IL for use as an extraction solvent. Despite their immiscibility with water, ILs that form biphasic systems with water will dissolve slightly into the aqueous phase. This portion of the IL phase is lost to the aqueous phase even in the absence of a metal ion or extractant. Intuitively, then, it would appear that an IL with a low water solubility would be desired, but, as described in Chapters 2 and 3, it has been reported previously that the use of an IL comprising a very hydrophobic anion will favor IX processes due to mass action considerations [4.42]. It can be seen in Figure 4.3 that a downward trend is observed where R falls as IL water solubility decreases. Similar to HI, this trend and previous reports of the theoretical determination of water solubility suggest [4.8, 4.11] water solubility is a potential parameter for the prediction of extraction behavior in IL-based systems.

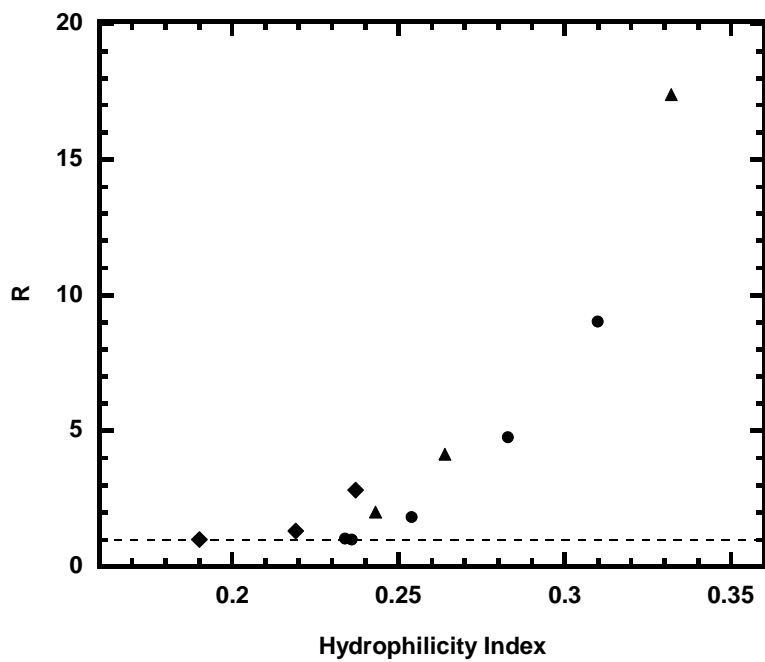


Figure 4.2. Relationship between R and the hydrophilicity index for $C_n \text{mim}^+$ (solid circles), $C_n \text{pyr}^+$ (solid triangles), and $N_{n,111}^+$ (solid diamonds) ILs.

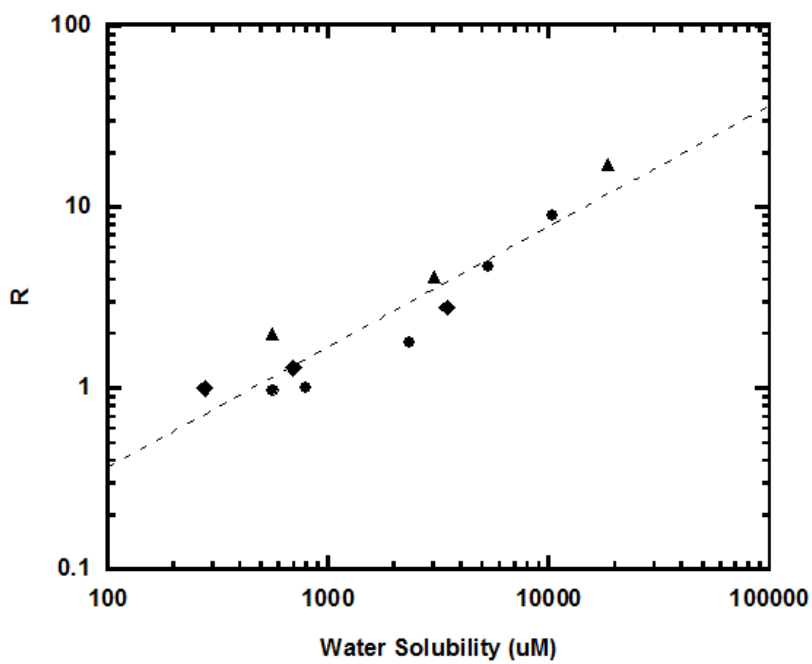


Figure 4.3. Relationship between R and the water solubility of $C_n\text{mim}^+$ (solid circles), $C_n\text{pyr}^+$ (solid triangles), and $N_{n,111}^+$ (solid diamonds) ILs.

4.3.3 Measured octanol-water distribution coefficients

Table 4.2 summarizes the $\log D_{ow}$ values measured for various ILs, as well as the few values found in the published literature [4.38, 4.43-4.46]. Where the conditions employed for D_{ow} determination were the same, the values measured in this work generally agree with those previously reported; any significant differences are probably attributable to differences in the experimental conditions used (*i.e.*, slow stir *vs.* shake flask method) or the initial IL concentration employed, both of which have been shown previously to affect measured D_{ow} values [4.38-4.40]. For all three IL families, an increase in alkyl chain length (*i.e.*, hydrophobicity) results in an increase in D_{ow} , an observation consistent with earlier reports for similar ILs [4.38, 4.46, 4.47]. Plots of $\log D_{ow}$ *vs.* the alkyl chain length are shown in Figure 4.4. The slopes of the best fit lines are 0.39 ($R^2 = 0.9971$), 0.42 ($R^2 = 0.9984$), and 0.56 ($R^2 = 0.9971$) for $C_n\text{mim}^+\text{Tf}_2\text{N}^-$, $C_n\text{pyr}^+\text{Tf}_2\text{N}^-$ and $N_{n,111}^+\text{Tf}_2\text{N}^-$ ILs, respectively. (Note that for the quaternary ammonium ILs, which lack an aromatic head group, the slope falls within the range of 0.53 to 0.66 expected on the basis of thermodynamic principles and the Gibbs free energy associated with the transfer of a methylene group from water to the a water-hydrocarbon interface [4.48].) Due to the extreme concentration differences present for ILs with large D_{ow} values (*i.e.*, 10,000 parts to 1 for $\log D_{ow} = 4.0$), caution must be exercised when considering the validity of D_{ow} values measured for the longest chain ILs (*i.e.*, $C_{14}\text{mim}^+\text{Tf}_2\text{N}^-$, $C_{14}\text{pyr}^+\text{Tf}_2\text{N}^-$ and $N_{14,111}^+\text{Tf}_2\text{N}^-$). The small concentrations in the aqueous phase required as little as a two-fold dilution of the original sample prior to analysis, compared to a ~20,000-fold dilution of the organic phase, making accurate quantification difficult for these ILs.

Table 4.2
Experimentally measured values of log D_{ow} from the present study^a and found in literature.

	logD_{ow}	Literature values of logD_{ow}
<i>C</i> ₅ <i>mimTf</i> ₂ <i>N</i>	-0.274 ± 0.011	-0.11 ^b
<i>C</i> ₆ <i>mimTf</i> ₂ <i>N</i>	0.236 ± 0.018	0.16 ^b , 0.15-0.22 ^c
<i>C</i> ₈ <i>mimTf</i> ₂ <i>N</i>	1.03 ± 0.01	0.79 ^b , 0.80-1.05 ^c , 1.05 ^b , 0.56 ^d
<i>C</i> ₁₀ <i>mimTf</i> ₂ <i>N</i>	1.69 ± 0.03	
<i>C</i> ₁₂ <i>mimTf</i> ₂ <i>N</i>	2.53 ± 0.01	
<i>C</i> ₁₄ <i>mimTf</i> ₂ <i>N</i>	4.03 ± 0.04	
<i>C</i> ₄ <i>pyrTf</i> ₂ <i>N</i>	-0.743 ± 0.025	-0.26 ^e
<i>C</i> ₆ <i>pyrTf</i> ₂ <i>N</i>	0.166 ± 0.024	-0.494- -0.143 ^f
<i>C</i> ₇ <i>pyrTf</i> ₂ <i>N</i>	0.569 ± 0.022	0.301-0.613 ^f
<i>C</i> ₈ <i>pyrTf</i> ₂ <i>N</i>	0.931 ± 0.018	
<i>C</i> ₁₀ <i>pyrTf</i> ₂ <i>N</i>	1.88 ± 0.02	
<i>C</i> ₁₂ <i>pyrTf</i> ₂ <i>N</i>	2.60 ± 0.04	
<i>C</i> ₁₄ <i>pyrTf</i> ₂ <i>N</i>	4.49 ± 0.02	
<i>N</i> _{8,111} <i>Tf</i> ₂ <i>N</i>	0.418 ± 0.024	
<i>N</i> _{10,111} <i>Tf</i> ₂ <i>N</i>	1.35 ± 0.03	
<i>N</i> _{12,111} <i>Tf</i> ₂ <i>N</i>	2.57 ± 0.02	
<i>N</i> _{14,111} <i>Tf</i> ₂ <i>N</i>	3.72 ± 0.02	

^a Uncertainties are reported at the 95% confidence level.

^b Data from [4.43]. Measured using shake flask technique.

^c Data from [4.38]. Measured using slow stir technique.

^d Data from [4.44]. Measured using slow stir technique.

^e Data from [4.45]. Measured using shake flask technique.

^f Data from [4.46]. Measured using shake flask technique.

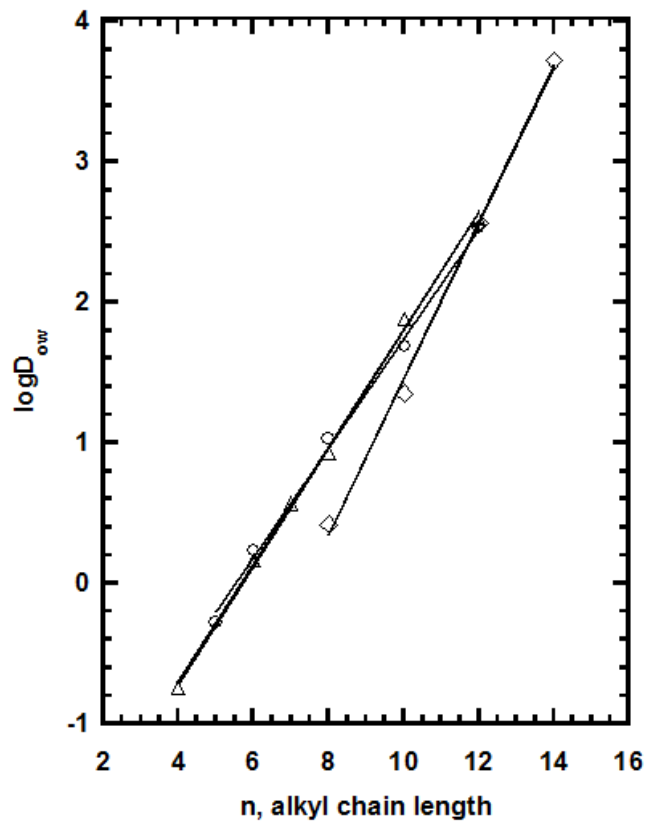


Figure 4.4. Relationship between $\log D_{ow}$ and the alkyl chain length, n , of $C_n\text{mim}^+$ (solid circles), $C_n\text{pyr}^+$ (solid triangles), and $N_{n,111}^+$ (solid diamonds) ILs. Curves are lines of best fit.

4.3.4 Relationship of D_{ow} values to extraction behavior

As shown in Figure 4.5, which includes data for both strontium and barium, an increase in D_{ow} (*i.e.*, an increase in the hydrophobicity of the IL), is accompanied by decreasing values of R , similar to the relationship between R and HI or water solubility. This relationship indicates that extraction of both strontium and barium ions by a crown ether (and by analogy, other divalent metal ions with other neutral extractants) into ILs with D_{ow} values greater than ~ 20 will proceed primarily by NC/IPE, apparently because the IL has been rendered too hydrophobic to participate in ion-exchange. (Note that the extraction of monovalent ions such as sodium is apparently dominated by ion-exchange under essentially all conditions.) It may be, in fact, that a D_{ow} of ~ 20 represents a general cutoff useful in the selection of ILs for application as extraction solvents. (Extraction from an acidic aqueous phase, a situation of greater “real-world” significance, represents a far more complex system, however.) It appears then that all three parameters, HI, water solubility and D_{ow} , could prove useful as predictors of extraction behavior in IL-based systems. Of the three, however, D_{ow} is by far the most commonly measured (or estimated) parameter in developing structure-property relationships. Accordingly, only it was pursued further.

4.3.5 Theoretical prediction of D_{ow}

Although a relationship between R and the octanol-water distribution coefficient of various ILs is of obvious utility, its value would be greatly enhanced if the distribution coefficients could be calculated, rather than experimentally determined. There exist numerous examples of theoretical predictions of D_{ow} values for ILs [4.1-4.7] and other chemicals [4.49-4.52] in the literature. Among the models used in these studies are the conductor-like screening model (COSMO) [4.1, 4.3], linear free energy relationships (LFER) [4.7], Pitzer-Debye-Hückel (PDH) [4.1], density

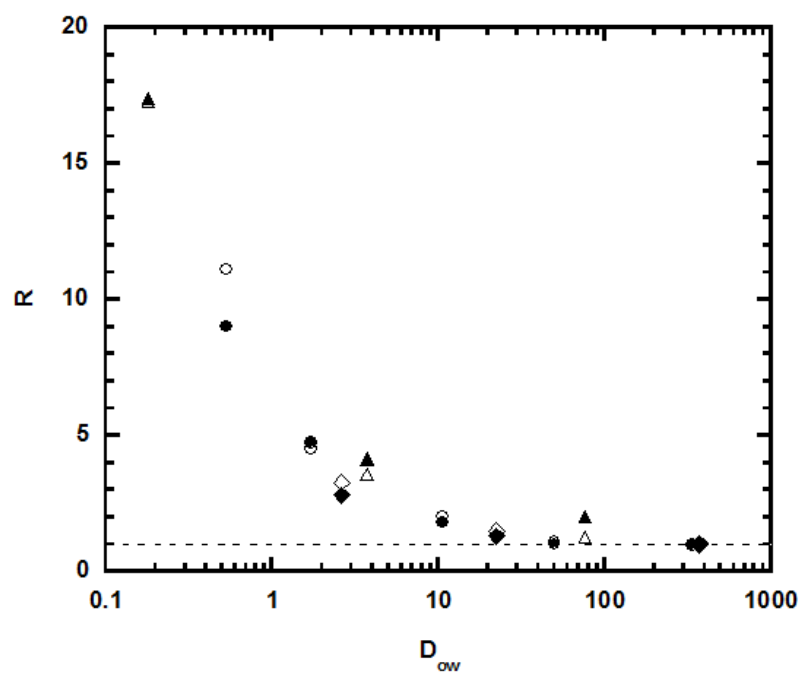


Figure 4.5. Relationship between R and measured D_{ow} values for strontium (solid symbols) and barium (open symbols) into $C_n\text{mim}^+$ (circles), $C_n\text{pyr}^+$ (triangles), and $N_{n,111}^+$ (diamonds) ILs.

functional theory (DFT) [4.7] and quantitative structure property relationships (QSPR) [4.4], along with combinations of these approaches. In developing these models, experimental data are normally measured or extracted from literature and used to develop fit parameters and coefficients. These values are then incorporated into equations used to predict the physical properties of ILs. The predictive efficacy is then evaluated by a comparison of measured and predicted values. Several examples of these relationships are presented in Figure 4.6. It is obvious that differences between measured and predicted values vary greatly depending on the model used, and range from small to as large as two log units (factor of 100, Figure 4.6, left panel).

Thoming *et al.* have developed experimentally- and computationally-derived LFER parameters to predict various IL physical properties [4.7]. They report good agreement between measured and predicted values of D_{ow} (Figure 4.6, right panel), water solubility, and critical micellar concentration using their models. A comparison of D_{ow} values of several ILs measured in this work with those from computationally derived predictions by Thoming *et al.* is presented in Figure 4.7. The remarkable agreement between these two data sets suggests that entirely computational predictions of these physical properties may be possible. Taken together with the ability for extraction behavior to be predicted using D_{ow} , the continued development of more accurate predictive models could provide a means by which to determine extraction behavior computationally, based solely on the structure of the IL.

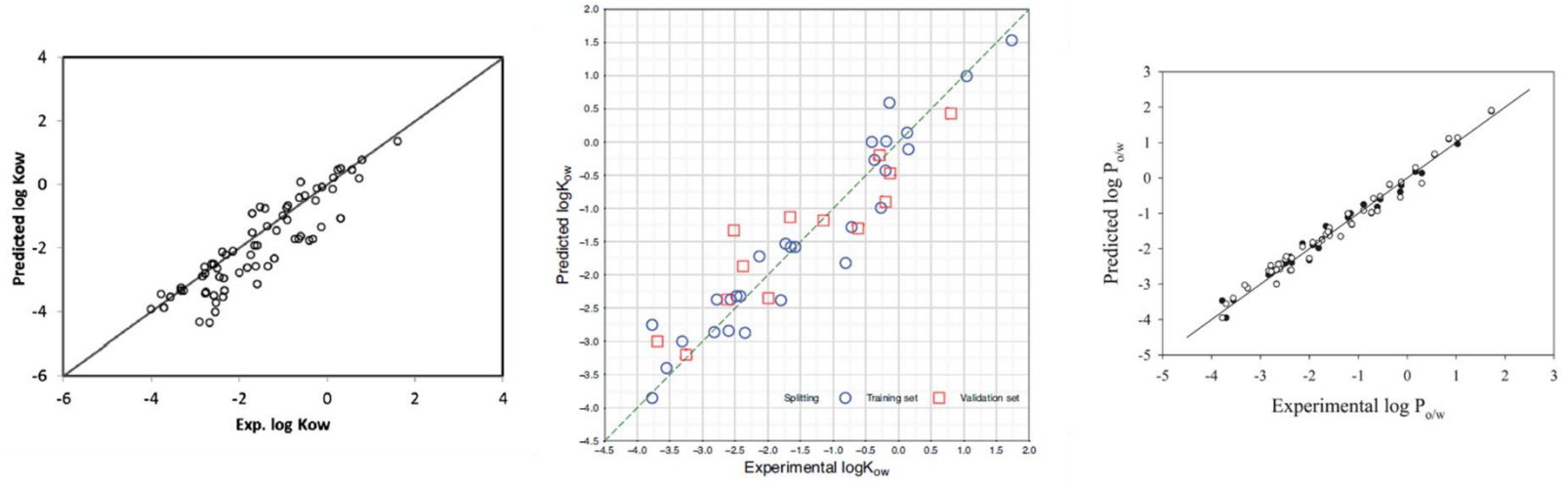


Figure 4.6. Correlation between predicted and measured values using several theoretical models. Left panel: PDH combined with COSMO-SAC (segmented activity coefficients) [4.1]; middle panel: QSPR [4.4]; right panel: LFER [4.7].

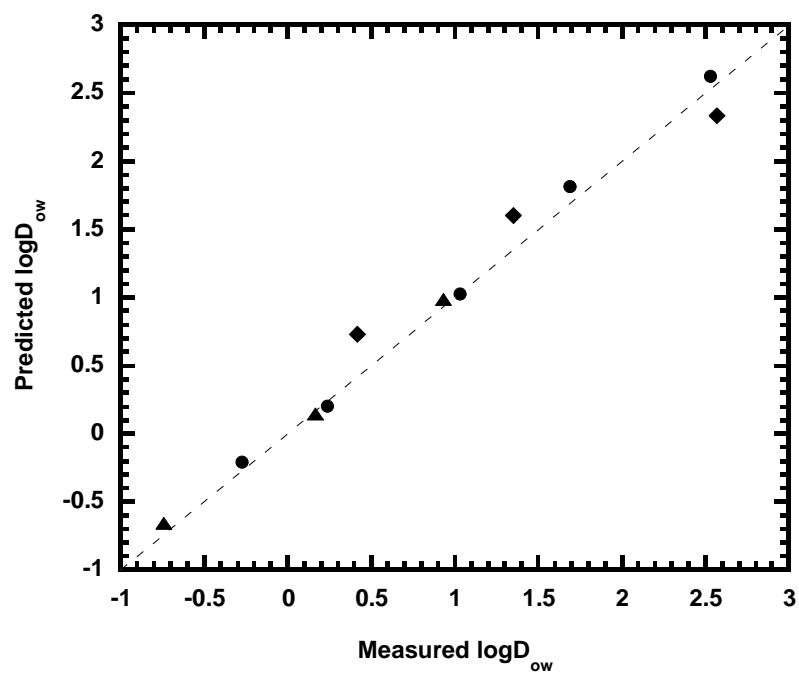


Figure 4.7. Correlation between predicted and measured (this work) values of $\log D_{ow}$ for $C_n\text{mim}^+$ (solid circles), $C_n\text{pyr}^+$ (solid triangles), and $N_{n,111}^+$ (solid diamonds) ILs.

4.4 Conclusions

The results of this study support the use of D_{ow} as a parameter for the prediction of extraction behavior in IL-based solvent extraction systems. Previous reports and work described in the preceding chapters have proven that IL hydrophobicity has a major effect on the mechanism by which metal ions are extracted from acid into ILs by neutral extractants. A clear correlation between IL hydrophobicity (water content, water solubility, and D_{ow}) and metal ion extraction from water was observed. The relationship between D_{ow} and R provides a possible ‘cutoff’ for the rational design of ILs. That is, extraction into ILs whose D_{ow} is greater than 20 is expected to proceed predominately by NC/IPE. This value can be used as a guideline for selection of ILs for future extraction studies. Furthermore, theoretical models developed to predict properties of ILs, specifically D_{ow} , reported in the literature show good agreement with the values measured in this study. This approach may thus provide the basis for an entirely computational prediction of extraction behavior in IL-based systems.

4.5 References

- [4.1] Lee, B.-S.; Lin, S.-T., A Priori Prediction of the Octanol-Water Partition Coefficient (K_{ow}) of Ionic Liquids. *Fluid Phase Equilibria*, **2014**, 363, 233-238.
- [4.2] Kamath, G.; Bhatnagar, N.; Baker, G.A.; Baker, S.N.; Potoff, J.J., Computational Prediction of Ionic Liquid 1-Octanol/Water Partition Coefficients. *Physical Chemistry Chemical Physics*, **2012**, 14, 4339-4342.
- [4.3] Zakari, A.Y.; Waziri, S.M.; Aderemi, B.O.; Mustapha, S.I., Computational Study of Environmental Fate of Ionic Liquids Using Conductor-Like Screening Model for Real Solvents (COSMO-RS) Method. *Journal of Environmental Chemistry and Ecotoxicology*, **2013**, 5, 90-95.
- [4.4] Rybinska, A.; Sosnowska, A.; Grzonkowska, M.; Barycki, M.; Puzyn, T., Filling Environmental Data Gaps with QSPR for Ionic Liquids: Modeling *n*-Octanol/Water Coefficient. *Journal of Hazardous Materials*, **2016**, 303, 137-144.
- [4.5] Chapeaux, A.; Simoni, L.D.; Stadtherr, M.A.; Brennecke, J.F., Liquid Phase Behavior of Ionic Liquids with Water and 1-Octanol and Modeling of 1-Octanol/Water Partition Coefficients. *Journal of Chemical Engineering Data*, **2007**, 52, 2462-2467.
- [4.6] Simoni, L.D.; Lin, Y.; Brennecke, J.F.; Stadtherr, M.A., Modeling Liquid-Liquid Equilibrium of Ionic Liquid Systems with NRTL, Electrolyte-NRTL, and UNIQUAC. *Industrial and Engineering Chemistry Research*, **2008**, 47, 256-272.
- [4.7] Cho, C.-W.; Preiss, U.; Jungnickel, C.; Stolte, S.; Arning, J.; Ranke, J.; Klamt, A.; Krossing, I.; Thöming, J., Ionic Liquids: Predictions of Physicochemical Properties with Experimental and/or DFT-Calculated LFER Parameters to Understand Molecular Interactions in Solution. *Journal of Physical Chemistry B*, **2011**, 115, 6040-6050.
- [4.8] Zhou, T.; Chen, L.; Ye, Y.; Chen, L.; Qi, Z.; Freund, H.; Sundmacher, K., An Overview of Mutual Solubility of Ionic Liquids and Water Predicted by COSMO-RS. *Industrial and Engineering Chemistry Research*, **2012**, 51, 6256-6264.
- [4.9] Torrecilla, J.S.; Tortuero, C.; Cancilla, J.C.; Díaz-Rodríguez, P., Estimation with Neural Networks of the Water Content in Imidazolium-Based Ionic Liquids Using Their Experimental Density and Viscosity Values. *Talanta*, **2013**, 113, 93-98.
- [4.10] Torrecilla, J.S.; Tortuero, C.; Cancilla, J.C.; Díaz-Rodríguez, P., Neural Networks to Estimate the Water Content of Imidazolium-Based Ionic Liquids Using Their Refractive Indices. *Talanta*, **2013**, 116, 122-126.
- [4.11] Kurnia, K.A.; Quental, M.V.; Santos, L.M.N.B.F; Freire, M.G.; Coutinho, J.A.P., Mutual Solubilities Between Water and Non-Aromatic Sulfonium-, Ammonium- and Phosphonium-Hydrophobic Ionic Liquids. *Physical Chemistry Chemical Physics*, **2015**, 17, 4569-4577.

- [4.12] Deetlefs, M.; Seddon, K.R.; Shara, M., Predicting Physical Properties of Ionic Liquids. *Physical Chemistry Chemical Physics*, **2006**, 8, 642-649.
- [4.13] Farahani, N.; Gharagheizi, F.; Mirkhani, S.A.; Tumba, K., Ionic Liquids: Prediction of Melting Point by Molecular-Based Model. *Thermochimica Acta*, **2012**, 549, 17-34.
- [4.14] Garvey, S.L.; Hawkins, C.A.; Dietz, M.L., Effect of Aqueous Phase Anion on the Mode of Facilitated Ion Transfer into Room-Temperature Ionic Liquids. *Talanta*, **2012**, 95, 25-30.
- [4.15] Hawkins, C.A.; Garvey, S.L.; Dietz, M.L., Structural Variations in Room-Temperature Ionic Liquids: Influences on Metal Ion Partitioning Modes and Extraction Selectivity. *Separation and Purification Technology*, **2012**, 89, 31-38.
- [4.16] Garvey, S.L.; Dietz, M.L., Ionic Liquid Anion Effects in the Extraction of Metal Ions by Macrocyclic Polyethers. *Separation and Purification Technology*, **2014**, 123, 145-152.
- [4.17] Dietz, M.L.; Dzielawa, J.A., Ion-Exchange as a Mode of Cation Transfer into Room-Temperature Ionic Liquids Containing Crown Ethers: Implications for the “Greenness” of Ionic Liquids as Diluents in Liquid-Liquid Extraction. *Chemical Communications*, **2001**, 2124-2125.
- [4.18] Jensen, M.P.; Dzielawa, J.A.; Rickert, P.; Dietz, M.L., EXAFS Investigations of the Mechanism of Facilitated Ion Transfer into a Room-Temperature Ionic Liquid. *Journal of the American Chemical Society*, **2002**, 124, 10664-10665.
- [4.19] Dietz, M.L.; Dzielawa, J.A.; Laszak, I.; Young, B.A.; Jensen, M.P., Influence of Solvent Structural Variations on the Mechanism of Facilitated Ion Transfer into Room-Temperature Ionic Liquids. *Green Chemistry*, **2003**, 5, 682-685.
- [4.20] Stepinski, D.C.; Jensen, M.P.; Dzielawa, J.A.; Dietz, M.L., Synergistic Effects in the Facilitated Transfer of Metal Ions into Room-Temperature Ionic Liquids. *Green Chemistry*, **2005**, 7, 151-158.
- [4.21] Dietz, M.L.; Stepinski, D. C., A Ternary Mechanism for the Facilitated Transfer of Metal Ions into Room-Temperature Ionic Liquids (RTILs): Implications for the “Greenness” of RTILs as Extraction Solvents. *Green Chemistry*, **2005**, 7, 747-750.
- [4.22] Song, Z.; Zhou, T.; Qi, Z.; Sundmacher, K., A Systematic Method for Screening Ionic Liquids as Extraction Solvents Exemplified by an Extractive Desulfurization Process. *ACS Sustainable Chemistry and Engineering*, **2017**, DOI: 10.1021/acssuschemeng.7b00024.
- [4.23] Ferreira, A.R.; Freire, M.G.; Ribeiro, J.C.; Lopes, F.M.; Crespo, J.G.; Coutinho, J.A.P., Ionic Liquids for Thiols Desulfurization: Experimental Liquid-Liquid Equilibrium and COSMO-RS Description. *Fuel*, **2014**, 128, 314-329.
- [4.24] Lyon, K.L.; Utgikar, V.P.; Greenhalgh, M.R., Dynamic Modeling for the Separation of Rare Earth Elements Using Solvent Extraction: Predicting Separation Performance Using Laboratory Equilibrium Data. *Industrial and Engineering Chemistry Research*, **2017**, 56, 1048-1056.

- [4.25] Laube, F.S.; Sadowski, G., Predicting the Extraction Behavior of Pharmaceuticals. *Industrial and Engineering Chemistry Research*, **2014**, 53, 865-870.
- [4.26] Sangster, J., Octanol-Water Partition Coefficients of Simple Organic Compounds. *Journal of Physical and Chemical Reference Data*, **1989**, 18, 1111-1229.
- [4.27] Collander, R., Permeability of Plant Cells, *Annual Review of Plant Physiology*, **1957**, 8, 335-348.
- [4.28] Hansch, C.; Quinlan, J.E.; Lawrence, G.L., Linear Free-Energy Relationship between Partition Coefficients and the Aqueous Solubility of Organic Liquids. *Journal of Organic Chemistry*, **1968**, 33, 347-350.
- [4.29] Leo, A.; Hansch, C.; Elkins, D., Partition Coefficients and their Uses. *Chemical Reviews*, **1971**, 71, 525-616.
- [4.30] Van Leeuwen, C.J.; Vermeire, T.G., *Risk Assessment of Chemicals: An Introduction*, Springer, **2007**.
- [4.31] Heuel-Fabianek, B., Partition Coefficients (K_d) for the Modelling of Transport Processes of Radionuclides in Groundwater. *Current Computer-Aided Drug Design*, **2006**, 2, 405-413.
- [4.32] Noble, A., Partition Coefficients (*n*-Octanol—Water) for Pesticides. *Journal of Chromatography A*, **1993**, 642, 3-14.
- [4.33] U.S. Environmental Protection Agency, *Product Properties Test Guidelines: Partition Coefficient (n-Octanol/Water), Shake Flask Method*, OPPTS 830.7550, EPA 712-C-96-038, **1996**.
- [4.34] Brooke, D.N.; Dobbs, A.J.; Williams, N., Octanol:Water Partition Coefficients (P): Measurement, Estimation, and Interpretation, Particularly for Chemicals with $P > 10^5$. *Ecotoxicology and Environmental Safety*, **1986**, 11, 251-260.
- [4.35] U.S. Environmental Protection Agency, *Product Properties Test Guidelines: Partition Coefficient (n-Octanol/Water), Estimation by Liquid Chromatography*, OPPTS 830.7570, EPA 712-C-96-040, **1996**.
- [4.36] U.S. Environmental Protection Agency, *Product Properties Test Guidelines: Partition Coefficient (n-Octanol/Water), Generator Column Method*, OPPTS 830.7560, EPA 712-C-96-039, **1996**.
- [4.37] Hawkins, C.A.; Rud, A.; Guthrie, M.L.; Dietz, M.L., Rapid Quantification of Imidazolium-Based Ionic Liquids by Hydrophilic Interaction Liquid Chromatography: Methodology and an Investigation of the Retention Mechanisms. *Journal of Chromatography A*, **2015**, 1400, 54-64.

- [4.38] Ropel, L.; Belvéze, L.S.; Aki, S.N.V.K.; Stadtherr, M.A.; Brennecke, J.F., Octanol-Water Partition Coefficients of Imidazolium-Based Ionic Liquids. *Green Chemistry*, **2005**, 7, 83-90.
- [4.39] Lee, S.H.; Lee, S.B., Octanol/Water Partition Coefficients of Ionic Liquids. *Journal of Chemical Technology and Biotechnology*, **2009**, 84, 202-207.
- [4.40] Köddernamm, T.; Reith, D., Arnold, A., Why the Partition Coefficient of Ionic Liquids is Concentration-Dependent. *Journal of Physical Chemistry B*, **2013**, 117, 10711-10718.
- [4.41] Kohno, Y.; Ohno, H., Temperature-Responsive Ionic Liquid/Water Interfaces: Relation between Hydrophilicity of Ions and Dynamic Phase Change. *Physical Chemistry Chemical Physics*, **2012**, 14, 5063-5070.
- [4.42] Luo, H.; Dai, S.; Bonnesen, P.V.; Haverlock, T.J.; Moyer, B.A.; Buchanan III, A.C., A Striking Effect of Ionic-Liquid Anions in the Extraction of Sr²⁺ and Cs⁺ by Dicyclohexano-18-Crown-6. *Solvent Extraction and Ion Exchange*, **2006**, 24, 19-31.
- [4.43] Lee, S.H., Biocatalysis in Ionic Liquids: Influence of Physicochemical Properties of Ionic Liquids on Enzyme Activity and Enantioselectivity, Pohang University of Science and Technology, Pohang, Korea, **2005**.
- [4.44] De los Rios, A.P.; Hernández-Fernández, F.J.; Tomás-Alonso, F.; Rubio, M.; Gómez, D.; Vllora, G., On the Importance of the Nature of the Ionic Liquids in the Selective Simultaneous Separation of the Substrates and Products of a Transesterification Reaction Through Supported Ionic Liquid Membranes. *Journal of Membrane Science*, **2008**, 307, 233-238.
- [4.45] Zhao, H.; Baker, G.A.; Song, Z.; Olubajo, O.; Zanders, L.; Campbell, S.M., Effect of Ionic Liquid Properties on Lipase Stabilization Under Microwave Investigation. *Journal of Molecular Catalysis B: Enzymatic*, **2009**, 57, 149-157.
- [4.46] Zheng, T.; Wang, Y., Octanol/Water Partition Coefficients of Pyridinium-Based Ionic Liquids. *Asian Journal of Chemistry*, **2015**, 27, 2819-2822.
- [4.47] Deng, Y.; Besse-Hoggan, P.; Sancelme, M.; Delort, A.-M.; Husson, P.; Gomes, M.F.C., Influence of Oxygen Functionalities on the Environmental Impact of Imidazolium Based Ionic Liquids. *Journal of Hazardous Materials*, **2011**, 198, 165-174.
- [4.48] Hawkins, C., Fundamental and Applied Studies on Metal Ion Extraction by Crown Ethers into Imidazolium-Based Room Temperature Ionic Liquids. Ph.D. Dissertation, University of Wisconsin-Milwaukee, Milwaukee, WI, 2012.
- [4.49] Meylan, W.M.; Howard, P.H., Atom/Fragment Contribution Method for Estimating Octanol—Water Partition Coefficients, *Journal of Pharmaceutical Sciences*, **1995**, 84, 83-92.

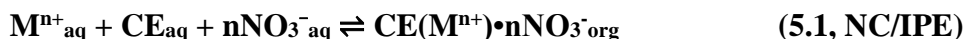
- [4.50] Finizio, A.; Vighi, M.; Sandroni, D., Determination of n-Octanol/Water Partition Coefficient (K_{ow}) of Pesticide – Critical Review and Comparison of Methods. *Chemosphere*, **1997**, 34, 131-161.
- [4.51] Gu, W.; Chen, Y.; Zhang, L.; Li, Y., Prediction of Octanol-Water Partition Coefficient for Polychlorinated Naphthalenes through Three-Dimensional QSAR Models. *Human and Ecological Risk Assessment*, **2017**, 23, 40-55.
- [4.52] Cheng, T.; Zhao, Y.; Li, X.; Lin, F.; Xu, Y.; Zhang, X.; Li, Y.; Wang, R., Computation of Octanol—Water Partition Coefficients by Guiding an Additive Model with Knowledge. *Journal of Chemical Information Modeling*, **2007**, 47, 2140-2148.

Chapter 5:

Quantification of individual modes of Sr²⁺ partitioning into 1-methyl-3-pentylimidazolium *bis*[(trifluoromethyl)sulfonyl]imide (C₅mim⁺Tf₂N⁻)

5.1 Introduction

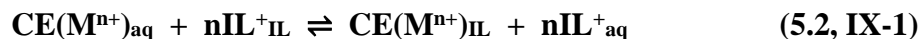
The extraction of metal ions by a neutral extractant (*e.g.*, a crown ether) into conventional (*i.e.*, molecular) organic solvents is known to proceed by a single pathway, one which involves the partitioning of a neutral complex / ion pair (NC/IPE, Equation 5.1) comprising a metal ion bound to the crown ether and an appropriate number of aqueous phase anions to ensure electroneutrality [5.1, 5.2].



This extraction pathway results in low metal ion distribution ratios when the acid concentration, and therefore the concentration of the aqueous phase anion that is required for the formation of the product complex, is low. As the acid concentration is increased, the amount of available anion increases and the formation of the neutral complex / ion pair becomes more favorable, leading to an increase in the metal ion distribution ratio (*i.e.*, the efficiency of extraction). This trend of increasing distribution ratio with acid (*i.e.*, anion) concentration allows extraction to be carried out at high acidity and stripping of the metal ion from the organic phase to be achieved readily with either dilute acid or water.

Studies of analogous IL-based systems have revealed that up to two additional pathways, both ion-exchange processes, arise when ionic liquids are employed in place of a conventional organic solvent [5.3-5.6]. The first form, designated IX-1 and defined by Equation 5.2, was first

noted in studies of the extraction of Sr^{2+} by DCH18C6 into $\text{C}_n\text{mim}^+\text{Tf}_2\text{N}^-$ (with $n = 2-10$) [5.3-5.5].



In these systems, the large metal ion distribution ratios observed for the short-chain (*e.g.*, $\text{C}_2\text{-C}_5$) C_nmim^+ ILs at low acidity cannot be explained simply by the formation of a neutral complex, as the aqueous phase anion concentration is too low to account for the amount of metal ion extracted. Extended X-ray absorption fine structure (EXAFS) measurements of the metal-crown complex in $\text{C}_5\text{mim}^+\text{Tf}_2\text{N}^-$ following extraction from nitric acid revealed little or no nitrate in the metal-crown coordination sphere [5.4], consistent with extraction of a cationic 1:1 Sr-DCH18C6 complex. Also, when the alkyl chain length of the C_nmim^+ cation is increased (*i.e.*, the hydrophobicity of the IL cation is increased, making its exchange into the aqueous phase more difficult), the distribution ratio at the same acid concentration decreases [5.5]. This too is consistent with Equation 5.2. The presence of this pathway is further supported by an increase in the solubility of the IL cation in the aqueous phase as the initial concentration of Sr^{2+} is increased [5.3].

In the extraction of divalent metal ions, an increase of the alkyl chain length from pentyl- to decyl- resulted in a shift from IX-1 to NC/IPE as the predominant mode of metal ion extraction, as evidenced by both the shape / direction of the acid dependencies and measurements of strontium and nitrate extraction from aqueous strontium nitrate solution [5.5]. These two mechanisms alone, however, cannot explain the extraction of sodium ions from nitric acid by DCH18C6 into $\text{C}_{10}\text{mim}^+\text{Tf}_2\text{N}^-$ which, despite its relatively high hydrophobicity, yields decreasing metal ion distribution ratios as the acid concentration is increased [5.6]. Analysis of distribution data at high acid concentration (*i.e.*, ≥ 1 M) indicated that the release of a hydrogen ion from the IL phase occurs, leading to the identification of a second form of ion exchange (IX-2, Equation 5.3).

Because the IL has no ionizable hydrogens and crown ethers are known to extract mineral acids, including nitric acid, protonated crown ether formed during the preconditioning steps has been proposed to be the source of the hydrogen ion that is released from the IL phase.



Further evidence of the plausibility of this pathway was reported by Marin *et al.* [5.7]. NMR studies of the hydrogen bonding interactions between water, acids and $\text{C}_n\text{mim}^+\text{Tf}_2\text{N}^-$ ILs confirms the presence of protonated crown ethers, namely, DCH18C6, in these systems. Both forms of ion exchange are deleterious to the IL phase in that an IL cation is lost to the aqueous phase when it is exchanged for either a metal-crown ether complex (IX-1) or a hydronium ion (or acid proton), which is subsequently exchanged for the metal ion (IX-2) when it is introduced. Although all three modes of extraction are always present, only one, neutral complex / ion pair formation, is desirable, as it allows for extraction of the ion of interest at high acidity and its recovery at low acidity without any loss of the IL phase.

Our studies of LLX systems employing several different IL families (*i.e.*, 1-alkyl-3-methylimidazolium [5.8-5.10], quaternary ammonium [5.11], and *N*-alkylpyridinium) have shown that a number of factors (*i.e.*, IL cation hydrophobicity, anion hydrophobicity, and aqueous phase anion) govern the balance among the three pathways. As both ion exchange processes ultimately involve the exchange of the IL cation into the aqueous phase, an increase in the IL cation hydrophobicity renders this exchange much more difficult [5.9]. A more hydrophilic IL anion reduces the extent of ion exchange due to mass action considerations [5.2] (*i.e.*, an IL with a very hydrophobic IL anion will dissolve less in the aqueous phase, which allows for greater exchange of the IL cation) [5.10]. An aqueous phase anion with lower hydration energy will transfer into the IL phase more easily, favoring neutral complex / ion pair extraction [5.8].

Despite the obvious importance of determining how changes to the extraction system affect the balance of these pathways, the actual contributions of each mode have not yet been quantified. To date, the shape and direction of the acid dependency have been used as the primary indication of the principal extraction mechanism (*i.e.*, decreasing distribution ratios \rightarrow ion exchange processes; increasing distribution ratios \rightarrow neutral complex / ion pair extraction). To fully evaluate ILs as alternative extraction solvents in LLX systems, it is imperative to quantify the exact contributions of each mode of metal ion partitioning to ensure that the desired pathway is actually the most prevalent. To this end, the extraction of Sr^{2+} from nitric acid by DCH18C6 into $\text{C}_5\text{mim}^+\text{Tf}_2\text{N}^-$ was studied in an attempt to quantify each extraction pathway.

5.2 Experimental

5.2.1 Materials

The lithium salt of *bis*[(trifluoromethyl)sulfonyl]imide ($\text{Li}^+\text{Tf}_2\text{N}^-$; TCI America) and 1-methyl-3-pentylimidazolium bromide ($\text{C}_5\text{mim}^+\text{Br}^-$; Iolitec, Tuscaloosa, Al) were purchased and used without purification. The commercially available radiotracer ^{85}Sr (Perkin Elmer, Waltham, MA) was used for extraction studies. The neutral extractant employed was a mixture of the *cis-syn-cis* (A) and *cis-anti-cis* (B) isomers of dicyclohexano-18-crown-6 (DCH18C6, Parish Chemical Company, Orem, UT). Acid solutions were prepared from trace-metal grade concentrated nitric acid (OptimaTM, Fisher, Fair Lawn, NJ) and were standardized by titration with standard sodium hydroxide (Ricca, Arlington, TX) using phenolphthalein indicator (Ricca, Arlington, TX). The mobile phase used for LC-MS analysis was prepared with LC-MS grade ammonium formate (OptimaTM, Fisher), formic acid (Thermo Scientific, Rockford, IL), acetonitrile (Fisher), and water (Fisher). Sodium carbonate (Sigma Aldrich, St. Louis, MO), sodium bicarbonate (Sigma Aldrich, St. Louis, MO) and HPLC grade methanol (Fisher) and

acetonitrile (Honeywell, Muskegon, MI) were used to prepare the mobile phase for ion chromatography. All aqueous solutions were prepared with deionized water with a specific resistance of at least 18 M Ω /cm.

5.2.2 Instruments

A Dionex ICS-1000 ion chromatograph equipped with a conductivity detector, a Dionex IonPac AS12A analytical column (4 \times 200 mm) AG12 guard column (4 \times 50 mm), and a Dionex AERS 500 (4mm) conductivity suppressor ($V = 25$ mA) was employed to measure the nitrate concentration in the ionic liquid phase under various extraction conditions. The mobile phase comprised 3.2 mM Na₂CO₃ and 1.0 mM NaHCO₃ in 20% acetonitrile/20% methanol/60% water (flow rate of 0.800 mL/min). Because organic solvent is a required component of the mobile phase due to the insolubility of the IL phase in water, external water mode (EWM, flow rate \sim 4 mL/min) was used to regenerate the suppressor. An example ion chromatogram is provided in the Appendix.

Radiometric assays were done *via* gamma spectroscopy on a Perkin Elmer Model 2480 Automatic Gamma Counter using standard procedures.

A Shimadzu LC-MS 2020 was employed to measure the IL⁺ and IL⁻ concentration in the aqueous phase under various extraction conditions. The concentration of C₅mim⁺ ($m/z = 153.3$) and the internal standard (C₈mim⁺, $m/z = 195.3$) were measured as two events in single ion monitoring (SIM) positive mode. The concentration of Tf₂N⁻ ($m/z = 280.0$) and the internal standard (PF₆⁻, $m/z = 145.0$) were measured as two events in SIM negative mode. Due to the presence of an overwhelming amount of ions (*e.g.*, nitrate, IL cation, IL anion, etc.) in the aqueous phase, an internal standard (C₈mim⁺ or PF₆⁻) was utilized to account for matrix effects. An

identical amount of internal standard was added to all standards and samples prior to analysis. The Shimadzu LS-MS 2020 was equipped with a dual ion source (DUIS) comprising electrospray (ESI) and atmospheric pressure chemical (APCI) ionization modes. Additional instrument parameters, including the column and mobile phase, are presented in Table 5.1. Example chromatograms and mass spectra are provided in the Appendix.

5.2.3 Methods

Ionic liquid synthesis. The IL used in this study, $C_5mim^+Tf_2N^-$, was prepared by metathesis from $C_5mim^+Br^-$ (Iolitec, Tuscaloosa, Al), as described in Sections 2.2.3 and 3.2.3.

Extraction studies – General description. When studying the extraction of metal ions from water into the quaternary ammonium and *N*-alkylpyridinium ILs (described in Chapters 2 and 3), the percentage of nitrate extracted was determined by measuring the depletion of nitrate in the aqueous phase accompanying extraction (*i.e.*, by measuring the concentration of nitrate in the aqueous phase before and after extraction). If nitric acid is employed as the aqueous phase, there will be a tremendous amount of nitrate present when the aqueous acid concentration is high. Detecting a small change against such a large background is extremely difficult. Therefore, the nitrate concentration in the ionic liquid phase was measured instead using ion chromatography, thereby permitting the direct determination of the amount of nitrate extracted from the aqueous phase. For the same samples, mass spectrometry was employed to measure the concentration of C_5mim^+ in the aqueous phase under various extraction environments in order to monitor the amount of IL cation lost to the aqueous phase due to ion exchange. A more thorough description of the procedures used is provided in the following section where the underlying rationale is described in more detail.

Table 5.1
LC-MS instrument parameters for IL cation and anion quantification

Column	Agilent ZORBAX HILIC Plus 3.0 x 7.5 mm, 3.0 micron
Mobile phase	10% 100 mM ammonium formate buffer in acetonitrile
Mobile phase flow rate	0.800 mL/min
Nebulizing gas flow	1.5 L/min
Interface	Dual ion source (DUIS)
Interface voltage	4.5 kV
Interface current	7.8 μ A
Corona needle voltage	4.5 kV
Corona needle current	0.2 μ A
DL temperature	250 $^{\circ}$ C
Heat block temperature	400 $^{\circ}$ C
Qarray RF voltage	10.1 V
Detector voltage	1.25 kV
PG Vacuum	96 Pa
IG Vacuum	0.00054 Pa
Drying gas flow	15.0 L/min

5.2.4 Extraction studies – Details and Rationale

To accurately assess the contributions of three competing extraction processes occurring in the IL-based extraction systems of interest, it is imperative that the quantification of each individual mode of metal ion partitioning be achieved without ‘interference’ from the other modes present. In other words, when identifying the contributions for one pathway (*e.g.*, IX-1), the means of quantification cannot errantly incorporate any contributions from the other two pathways (*i.e.*, IX-2 or NC/IPE). Fortunately, close examination of the reactions that define each pathway (Equations 5.1-5.3) reveals unique characteristics of each mode of extraction that allow for their individual quantification.

The extraction of metal ions by a neutral complex / ion pair (NC/IPE), as defined by Equation 5.1, involves the partitioning of a neutral metal-nitrato-crown complex / ion pair (when nitric acid or other nitrate salt is present in the aqueous phase). Although all three pathways will obviously yield a higher metal ion concentration in the IL phase, only NC/IPE will result in an increase in the concentration of nitrate as well. The aqueous phase anion does not participate in either form of ion exchange and, therefore, will not affect the nitrate concentration in the IL phase. This provides us then with the means of identifying the contributions of NC/IPE without the possibility of including IX-1 (Equation 5.2) or IX-2 (Equation 5.3) processes.

When considering the two ion exchange processes, it is of concern that the defining aspect of both is the loss of the IL cation to the aqueous phase (Equations 5.2 and 5.3), making their differentiation appear difficult. Fortunately, this loss occurs at two separate steps in the extraction procedure. The first form of ion exchange (IX-1) occurs upon the addition of the metal ion in the aqueous phase. At this point, the crown ether-bound metal ion is exchanged for the IL cation, yielding an increased concentration of IL cation in the aqueous phase. In IX-2, however, the IL

cation is exchanged for a protonated extractant molecule (here, a crown ether-hydronium ion complex) during the preconditioning steps *before* any metal ion is introduced. This acid proton or hydronium ion is subsequently exchanged for the metal ion. Therefore, in terms of the loss of the IL cation, exchange in IX-2 occurs prior to and separately from IX-1, allowing for the quantification of each pathway by monitoring the concentration of IL cation in the aqueous phase during the preconditioning step, where no metal ion is present, and once the metal ion is introduced.

Unfortunately, these modes of metal ion extraction are not the only source of nitrate present in the IL phase and of IL cation present in the aqueous phase, as the IL and aqueous phases exhibit not negligible mutual solubility. A suitable means to correct for the inherent solubility of each phase in the other must therefore be identified. The system under investigation comprises 0.031 M $\text{Sr}(\text{NO}_3)_2$ in various nitric acid concentrations in contact with 0.25 M DCH18C6 in $\text{C}_5\text{mim}^+\text{Tf}_2\text{N}^-$ (System IV, Figure 5.1). Under these conditions, we must account for the solubility of the metal nitrate salt and nitric acid in the IL phase as well as the IL solubility in the aqueous phase. The most obvious system to correct for the IL / aqueous phase mutual solubility would be identical to the system of interest without the metal salt (System III, Figure 5.1), but the complexity of the extraction system under investigation warrants a thorough explanation behind this rationale.

System	I	II	III	IV
Aqueous phase	HNO ₃	0.031 M Sr(NO ₃) ₂ in HNO ₃	HNO ₃	0.031 M Sr(NO ₃) ₂ in HNO ₃
Organic phase	C ₅ mim ⁺ Tf ₂ N ⁻	C ₅ mim ⁺ Tf ₂ N ⁻	0.25 M DCH18C6 in C ₅ mim ⁺ Tf ₂ N ⁻	0.25 M DCH18C6 in C ₅ mim ⁺ Tf ₂ N ⁻
Preconditioning	HNO ₃	HNO ₃	HNO ₃	HNO ₃

Figure 5.1. Various extraction systems considered to correct for the mutual solubility of the IL and aqueous phases. System I represents the simplest system and System IV is currently under investigation.

If we consider the inherent solubility of nitrate in the IL phase, there are two sources of nitrate partitioning into the IL, the metal nitrate salt and the nitric acid. System II (Figure 5.1) represents conditions under which the partitioning of these two species into the IL phase is the only means by which nitrate could transfer into the IL phase. To determine if the partitioning of $\text{Sr}(\text{NO}_3)_2$ contributes in any way to the inherent nitrate content into the IL phase in the absence of a neutral extractant, a sample of $\text{C}_5\text{mim}^+\text{Tf}_2\text{N}^-$ was preconditioned with two aliquots of nitric acid (where the volume of acid is twice the volume of IL). The metal nitrate acid solution was then added to the conditioned IL phase (1:1 phase ratio) and a strontium radiotracer was introduced to the mixture, which was then vortexed and allowed to stand for 15 minutes. This mixture was centrifuged and the phases were separated, sampled and counted using gamma spectroscopy. The results of this study demonstrated that the partitioning of the metal nitrate salt into the IL phase is negligible ($< 0.05\%$ strontium in the IL phase) and therefore does not contribute significantly to the nitrate content of the IL phase.

Because the IL shows no ability to extract strontium without the crown ether, its presence is not necessary in the system used to account for the inherent nitrate solubility. In addition, it has been shown previously that DCH18C6 will extract certain mineral acids, including nitric acid [5.7], suggesting that the system described in System II will underestimate the amount of nitrate in the IL phase because it does not account for acid extracted by DCH18C6. This was confirmed when two samples of $\text{C}_5\text{mim}^+\text{Tf}_2\text{N}^-$ (one without crown ether – System II and one with crown ether – System III) were preconditioned as mentioned above and contacted with either the metal nitrate / acid solution (System II) or nitric acid (System III) (1:1 phase ratio). These mixtures were vortexed and allowed to stand for 15 minutes. Upon centrifugation and separation of the phases, the nitrate concentration of the IL phase was determined by IC, as described in Section 3.2.3. The

amount of nitrate in the IL phase of System III, yielded higher nitrate values than those measured for System II, confirming that System II does not account for acid extracted by DCH18C6.

Similarly, when attempting to quantify the contributions of IX-1 to the overall extraction of strontium from nitric acid, a correction must be made for IL that inherently dissolves / partitions into the aqueous phase not associated with metal extraction. Although the extraction of nitric acid by DCH18C6 will not affect the IL concentration in the aqueous phase, System II will also underestimate the amount of IL in the aqueous phase because it does not account for the increased solubility of the IL due to the presence of the extractant [5.12, 5.13]. It is apparent that only System III can sufficiently account for the inherent mutual solubility of IL in the aqueous phase and nitrate in the IL phase when quantifying the contributions from NC/IPE and IX-1.

The last mode of extraction, IX-2, involves the loss of the IL cation during the preconditioning steps of System IV, before the metal has been introduced. The presence of the crown ether is what results in the exchange of the IL cation for an acid proton or hydronium ion. Unfortunately, as mentioned before, the presence of the crown ether will result in loss of the IL due to two processes, an increase in the IL solubility and the protonation of the crown ether. This complicates our ability to correct for the inherent IL content of the aqueous phase, as we cannot identify a system that accounts for all processes involving the loss of the IL except the crown ether protonation. Furthermore, if the amount of protonated crown ether could be quantified, it does not ensure that all of it will participate in extraction.

Considering that we can measure the fraction of the initial aqueous phase strontium extracted ($\%E_M$) *via* gamma spectroscopy as well as the contributions of neutral complex / ion pair extraction ($\%E_{NC/IPE}$) and IL cation exchange for a metal-crown complex ($\%E_{IX-1}$), any strontium that is not extracted by NC/IPE or IX-1 should be extracted by IX-2 ($\%E_{IX-2}$), *assuming no other*

extraction processes exist. The presence of only two partitioning modes in the extraction of strontium from water by DCH18C6 was confirmed by previous work by Hawkins *et al.* [5.14] who quantified the extraction of strontium nitrate from water into $C_5mim^+Tf_2N^-$. According to Table 5.2, the percentage of nitrate extracted, as measured by depletion of nitrate in the aqueous phase, suggests that 40% of the total strontium extracted proceeds by NC/IPE. Assuming only two modes of extraction, the remaining 60% of strontium is expected to extract by IX-1. To confirm this, the IL concentration in the aqueous phase after extraction, which is proportional to the extraction due to IX-1, was measured. It was found that within experimental error, the two methods (*i.e.*, estimation by nitrate depletion and measurement of $[IL^+]_{aq}$) are in agreement with respect to the contributions of each of the two pathways (Table 5.2). Therefore, only two pathways are present when a metal ion is extracted from water into an IL by DCH18C6.

Knowing that the extraction of strontium from water proceeds by only two pathways, we must next consider if the substitution of an acidic aqueous phase for water in this system will introduce additional modes of extraction. It is already known that the presence of the acidic aqueous phase can result in an increased dissolution of IL in the aqueous phase and of acid into the IL phase [5.12, 5.15]. Although this may affect the balance of the extraction pathways, it does not necessarily introduce a new path for extraction. In contrast, the ability of the crown ether to extract acid [5.7, 5.16-5.22] could provide another route by which metal ions are extracted. That is, protonation of the crown ether (as opposed to extraction of nitric acid as an intact, neutral species, as is observed in 1-octanol [5.16]) results in a new mode of extraction, specifically IX-2. The presence of this path was shown to exist on the basis of observations made in the extraction of sodium from $C_{10}mim^+Tf_2N^-$ by DCH18C6, as described above [5.6].

Table 5.2
Quantification of Sr²⁺ extraction by NC/IPE and IX-1 from water into C₅mim⁺Tf₂N⁻ [5.14].

%E_{Sr}	99.20%
%E_{NC/IPE} (determined by IC)	40 ± 4%
%E_{IX-1} (by difference)	60 ± 5%
%E_{IX-1} (determined by HPLC)	67 ± 5%

Consequently, if only three processes are responsible for the extraction of strontium, then the total amount of metal extracted is the sum of that extracted by the three individual modes, according to Equation 5.4. Thus, the contributions from IX-2 (%E_{IX-2}) can be determined by difference (Equation 5.5).

$$\%E_M = \%E_{NCE} + \%E_{IX-1} + \%E_{IX-2} \quad (5.4)$$

$$\%E_{IX-2} = \%E_M - \%E_{NCE} - \%E_{IX-1} \quad (5.5)$$

It should be noted here that anion exchange has been proposed as a major contributor for metal ion extraction at high acid concentrations in these systems [5.23]. This route obviously requires that a not insignificant amount of hydrophobic IL anion, namely Tf₂N⁻, exchange into the aqueous phase for a metal-nitrato-crown complex comprising one more nitrate than required to form a neutral complex (here, for example, [DCH18C6•Sr(NO₃)₃]⁻). If this is the case, the concentration of Tf₂N⁻ in the aqueous phase following extraction should be measurably higher than that before extraction. To determine if anion exchange is a contributing extraction mechanism in these systems, the aqueous phase Tf₂N⁻ concentration was measured for Systems III and IV at aqueous phase acid concentrations of 4 M and 6 M. The results, which are presented in Table 5.3, show that the amount of strontium that could be extracted by anion exchange is trivial at best. Accordingly, anion exchange is not an important mode of extraction in this system.

Table 5.3
Possible contributions from anion exchange processes at 4 and 6 M HNO₃.

<i>Tf₂N⁻ concentration (mM)</i>	
IV 4 M	IV 6 M
32.2 ± 1.8	45.0 ± 0.37
III 4 M	III 6 M
31.9 ± 0.37	45.7 ± 0.36
<i>Maximum Sr²⁺ extracted by anion exchange</i>	
4 M	6 M
1.14%	< LOD

5.3 Results and Discussion

The results of the meticulous analysis of Sr^{2+} extraction by DCH18C6 from nitric acid into $\text{C}_5\text{mim}^+\text{Tf}_2\text{N}^-$ described above are summarized in Table 5.4, and a plot of this data (as %E versus concentration of nitric acid) is presented in Figure 5.2. When the individual contributions are compared, it becomes readily apparent which extraction pathway predominates at each acid concentration. That is, at the lowest acidities, IX-2 makes only a modest contribution to the overall extraction, while IX-1 dominates. NC/IPE is also modest at low acidities, but becomes more pronounced as the acidity (and thus, the available nitrate concentration) rises. The behavior of the system at low acid concentration can be explained by the reactions that represent each mode (Equations 5.1-5.3). Neutral complex / ion pair extraction requires the presence of aqueous phase anions in order to proceed. At low acid concentration, and therefore, low aqueous phase anion concentration, the contributions from NC/IPE are expected to be low and according to Table 5.4 and Figure 5.2, they are. Similarly, IX-2 requires protonation of the crown ether, which is difficult at low acid concentration; that its contributions are also low. IX-1 does not involve the aqueous phase anion nor does it require extractant protonation. Consequently, it accounts for the majority of strontium extraction at low acid concentrations. As the acidity increases, the contributions of IX-1 diminish and IX-2 and NC/IPE begin to increase in prevalence, with IX-2 becoming the predominant mode in the 0.5-2 M nitric acid ranges. Eventually, as the concentration of acid is increased further, contributions from IX-2 begin to fall and those from NC/IPE predominate at 4 and 6 M nitric acid.

Table 5.4
Contributions from each mode of Sr²⁺ partitioning by DCH18C6 into C₅mim⁺Tf₂N⁻ at various nitric acid concentrations.

[HNO ₃], M	%E _M	%E _{NC/IPE}	%E _{IX-1}	%E _{IX-2}
<i>0.0103</i>	96.2 ± 0.6	11.4 ± 2.5	79.9 ± 0.7	4.9 ± 2.7
<i>0.100</i>	95.0 ± 0.9	20.0 ± 0.3	60.5 ± 1.4	14.6 ± 1.7
<i>0.496</i>	91.6 ± 2.1	32.0 ± 1.2	21.4 ± 0.5	38.2 ± 2.4
<i>1.98</i>	85.4 ± 5.0	30.3 ± 0.7	8.9 ± 0.2	46.2 ± 5.0
<i>3.91</i>	82.7 ± 6.3	46.5 ± 1.2	3.32 ± 0.05	32.9 ± 6.4
<i>5.89</i>	88.5 ± 1.2	72.8 ± 1.3	2.00 ± 0.02	13.6 ± 1.8

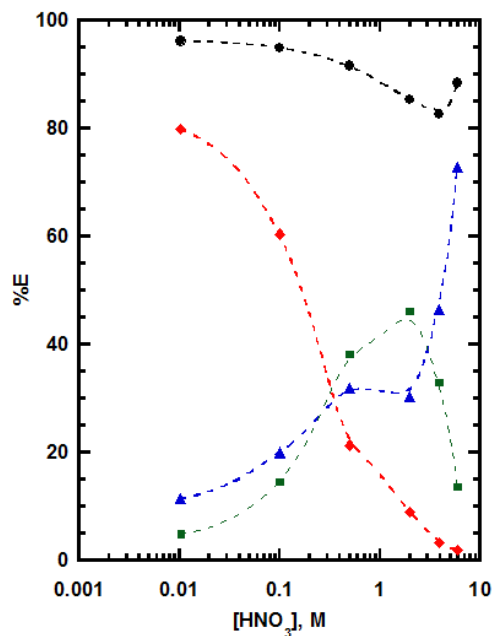


Figure 5.2. The effect of HNO₃ concentration on the extraction percentage of Sr²⁺ (solid, black circles), NC/IPE (solid, blue triangles), IX-1 (solid, red diamonds), and IX-2 (solid, green squares).

It is obvious that an increase in the acid concentration results in conditions that favor both NC/IPE and IX-2 (Equations 5.2 and 5.3) as both depend on the presence of the acid. That is, NC/IPE requires the aqueous phase anion to form a neutral complex / ion pair, while IX-2 requires the protonation of the crown ether, which becomes more likely at higher acid concentrations. Therefore, as the acidity is increased, these two modes of partitioning are in competition with one another, and it appears from the present work that NC/IPE is favored as the nitric acid concentration exceeds 3 M.

The prevalence of NC/IPE as the predominant mode at high acidity is not an intuitive observation due to the short alkyl chain length of the IL cation, but when considering the shape of the acid dependency ($\%E_{Sr}$) this observation becomes more reasonable. As mentioned before, it has been assumed thus far that as acidity increases, decreasing distribution ratios point to ion exchange processes predominating whereas increasing distribution ratios suggests that neutral complex / ion pair extraction is the dominant mode. The upturn present at high acidity then, indicates that there is a shift in extraction mechanism from ion exchange to neutral complex / ion pair extraction, which is supported by and is consistent with the present results.

Of practical importance is the relationship between the contributions from NC/IPE and both IX-1 and IX-2. Reducing the amount of ion exchange processes occurring in these systems has been the recent focus of this laboratory due to the loss of the IL cation to the aqueous phase that occurs during metal ion extraction [5.8-5.11]. It can be seen from Figure 5.3, that ion exchange processes (IX-1 and IX-2 combined) represent the dominant mode of strontium extraction up to ~3 M HNO₃, after which NC/IPE is the predominant mode, which is in agreement with what is expected based on the shape and direction of the acid dependency alone. It is worth noting, however, that no conditions have been identified under which ion-exchange is entirely

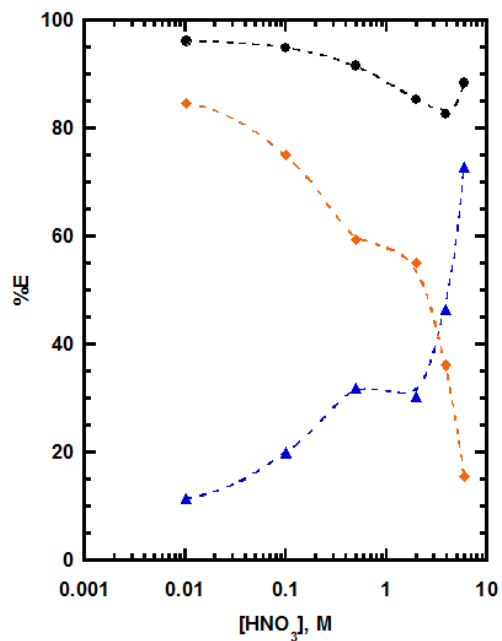


Figure 5.3. The effect of HNO₃ concentration on %E_{Sr} (solid, black circles) and on the contributions from NC/IPE (solid, blue triangles) and IX (IX-1 + IX-2; solid, orange diamonds).

absent. This has important (and negative) implications for the development of practical SX processes based on ILs, for which ion-exchange-induced losses of the solvent could render an otherwise satisfactory process impractical.

This analysis represents the first quantitative description of partitioning in an IL-based solvent extraction system employing an acidic aqueous phase. Although previous work has been able to describe the modes of metal ion extraction from water quantitatively [5.5, 5.8-5.11], it has only provided a qualitative description of metal ion extraction from an acid containing aqueous phase. Applying this analysis to similar systems (*i.e.*, those involving the extraction of alkali and alkaline earth metals by neutral extractants) will provide a means to verify (or disprove) many of the qualitative trends that have been proposed previously (*e.g.*, effect of changing IL anion, IL cation, and aqueous phase anion). In addition and perhaps more importantly, this work provides us with a tool to understand more complex systems, including those involving radiolytic degradation of an extractant or extraction of lanthanides and actinides.

5.4 Conclusions

This study represents the first time since initial work describing ILs as alternative extraction solvents that the individual modes of extraction have been quantified for an IL-based system employing an acidic aqueous phase. The results presented here show that the exact contribution of each of the three modes of metal ion partitioning varies considerably with the experimental conditions. At low aqueous nitric acid concentrations, IX-1 predominates due to the lack of nitrate or protonated extractant required for NC/IPE and IX-2, respectively. Extraction occurs mostly by IX-2 between acid concentrations of 0.5 and 2 M, above which NC/IPE is favored. As noted previously, the predominant mode of partitioning has typically been deduced qualitatively on the basis of the shape and direction of acid dependencies. Although the results of

this work have demonstrated that this is a surprisingly accurate approach, the ability to quantitatively describe metal ion extraction in these systems is expected to provide new and important insights into metal ion extraction processes in ionic liquid-based SX systems, insights that will greatly facilitate the rational design of these systems.

5.5 References

- [5.1] Dietz, M.L., Bond, A.H., Hay, B.P., Chiarizia, R., Huber, V.J., Herlinger, A.W. Ligand Reorganization Energies as a Basis for the Design of Synergistic Metal Ion Extraction Systems. *Chemical Communications*, **1999**, 1177-1178.
- [5.2] Luo, H.; Dai, S.; Bonnesen, P.V.; Haverlock, T.J.; Moyer, B.A.; Buchanan III, A.C., A Striking Effect of Ionic-Liquid Anions in the Extraction of Sr²⁺ and Cs⁺ by Dicyclohexano-18-Crown-6. *Solvent Extraction and Ion Exchange*, **2006**, 24, 19-31.
- [5.3] Dietz, M.L.; Dzielawa, J.A., Ion-Exchange as a Mode of Cation Transfer into Room-Temperature Ionic Liquids Containing Crown Ethers: Implications for the “Greenness” of Ionic Liquids as Diluents in Liquid-Liquid Extraction. *Chemical Communications*, **2001**, 2124-2125.
- [5.4] Jensen, M.P.; Dzielawa, J.A.; Rickert, P.; Dietz, M.L., EXAFS Investigations of the Mechanism of Facilitated Ion Transfer into a Room-Temperature Ionic Liquid. *Journal of the American Chemical Society*, **2002**, 124, 10664-10665.
- [5.5] Dietz, M.L.; Dzielawa, J.A.; Laszak, I.; Young, B.A.; Jensen, M.P., Influence of Solvent Structural Variations on the Mechanism of Facilitated Ion Transfer into Room-Temperature Ionic Liquids. *Green Chemistry*, **2003**, 5, 682-685.
- [5.6] Dietz, M.L.; Stepinski, D. C., A Ternary Mechanism for the Facilitated Transfer of Metal Ions into Room-Temperature Ionic Liquids (RTILs): Implications for the “Greenness” of RTILs as Extraction Solvents. *Green Chemistry*, **2005**, 7, 747-750.
- [5.7] Marin, T.W.; Shkrob, I.A.; Dietz, M.L., Hydrogen-Bonding Interactions and Protic Equilibria in Room-Temperature Ionic Liquids Containing Crown Ethers. *Journal of Physical Chemistry B*, **2011**, 115, 3912-3918.
- [5.8] Garvey, S.L.; Hawkins, C.A.; Dietz, M.L., Effect of Aqueous Phase Anion on the Mode of Facilitated Ion Transfer into Room-Temperature Ionic Liquids. *Talanta* **2012**, 95, 25-30.
- [5.9] Hawkins, C.A.; Garvey, S.L.; Dietz, M.L., Structural Variations in Room-Temperature Ionic Liquids: Influences on Metal Ion Partitioning Modes and Extraction Selectivity. *Separation and Purification Technology*, **2012**, 89, 31-38.
- [5.10] Garvey, S.L.; Dietz, M.L., Ionic Liquid Anion Effects in the Extraction of Metal Ions by Macrocyclic Polyethers. *Separation and Purification Technology*, **2014**, 123, 145-152.
- [5.11] Wankowski, J.L.; Dietz, M.L., Ionic Liquid (IL) Cation and Anion Structural Effects on Metal Ion Extraction into Quaternary Ammonium-based ILs. *Solvent Extraction and Ion Exchange*, **2016**, 34, 48-59.
- [5.12] Ternova, D.; Boltoeva, M.; Cointeaux, L.; Gaillard, C.; Kalchenko, V.; Mazan, V.; Miroshnichenko, S.; Mohapatra, P.K.; Ouadi, A.; Papaiconomou, N.; Petrova, M.; Billiard, I., Dramatic Changes in the Solubilities of Ions Induced by Ligand Addition in Biphasic

- System D₂O/DNO₃//[C₁C₄im][Tf₂N]: A Phenomenological Study, *Journal of Physical Chemistry B*, **2016**, 120, 7502-7510.
- [5.13] Rickert, P.G.; Stepinski, D.C.; Rausch, D.J.; Bergeron, R.M.; Jakab, S.; Dietz, M.L., Solute-Induced Dissolution of Hydrophobic Ionic Liquids in Water. *Talanta*, **2007**, 72, 315-320.
- [5.14] Hawkins, C. Fundamental and Applied Studies of Metal Ion Extraction by Crown Ethers into Imidazolium-Based Room Temperature Ionic Liquids. Ph.D. Thesis, University of Wisconsin-Milwaukee, Milwaukee, WI, **2012**.
- [5.15] Mazan, V.; Billard, I.; Papaiconomou, N., Experimental Connections between Aqueous-Aqueous and Aqueous-Ionic Liquid Biphasic Systems. *RSC Advances*, **2014**, 4, 13371-13384.
- [5.16] Dietz, M.L.; Bond, A.H.; Clapper, M.; Finch, J.W., Isomer Effects in the Extraction of Metal Ions from Acidic Nitrate Media by Dicyclohexano-18-crown-6. *Radiochimica Acta*, **1999**, 85, 119-129.
- [5.17] Yakshin, V.V.; Abashkin, V.M.; Zhukova, N.G.; Tsarenko, N.A.; Laskorin, B.N., Extraction of Nitric Acid by Polyethers.. *Doklady Akademii Nauk SSSR*, **1979**, 247, 1398-1401.
- [5.18] Rozen, A.M.; Nidolotova, Z.I.; Kartasheva, N.A.; Bol'shakova, A.S.; Fokin, A.V., Complexing in Extraction of Nitric, Hydrochloric, and Sulfuric Acids by Trioctylamine Oxide. *Doklady Akademii Nauk SSSR*, **1982**, 265, 1193-1198.
- [5.19] Yakshin, V.V.; Korshunov, M.B.; Fedorova, A.T.; Laskorin, B.N., Reactivity of Diastereomers of Dicyclohexyl-18-crown-6 in the Extraction of Inorganic Acids and Metal Salts. *Doklady Akademii Nauk SSSR*, **1994**, 279, 407-410.
- [5.20] Filippov, E.A.; Yakshin, V.V.; Abashkin, V.M.; Fomenkov, V.G.; Serebryakov, I.S., Extraction of Alkaline Earth Metals from Nitric Acid Solutions by the Crown Ether Dicyclohexyl-18-crown-6. *Radiokhimiya*, **1982**, 24, 214-216.
- [5.21] Abashkin, B.M.; Yakshin, V.V.; Laskorin, B.N., Extraction of Alkali Metal Salts from Acid Solutions by Crown Ethers. *Doklady Akademii Nauk SSSR*, **1981**, 257, 1374-1377.
- [5.22] Abashkin, V.M.; Yakshin, V.V.; Komolova, I.A.; Zarubin, A.I.; Laskorin, B.N., Thermodynamics of the Extraction Interaction between Dicyclohexyl-18-crown-6 and Strong Mineral Acids, *Doklady Akademii Nauk SSSR*, **1987**, 296, 622-625.
- [5.23] Billard, I.; Ouadi, A.; Gaillard, C., Is a Universal Model to Describe Liquid-Liquid Extraction of Cations by Use of Ionic Liquids in Reach? *Dalton Transactions*, **2013**, 42, 6203-6212.

Chapter 6:

Conclusions and Recommendations

6.1 Conclusions

The work reported here comprises an investigation of the fundamental aspects of metal ion extraction from acidic media into ionic liquids by DCH18C6, motivated by the need for guiding principles for the rational design of ILs for use as alternative extraction solvents. Trends observed for metal ion extraction into quaternary ammonium- and *N*-alkylpyridinium-based ILs have been found to be consistent with previous reports for 1, 3-dialkylimidazolium-based IL systems. Specifically, increases in the IL cation hydrophobicity are accompanied by greater contributions from NC/IPE, while a similar increase in IL anion hydrophobicity results in greater contributions from IX processes. Also, aqueous phase anions with larger hydration enthalpies are less likely to partition into the organic phase as part of a neutral complex / ion pair and therefore, more likely to facilitate IX processes. These trends and the ‘three-path model’ [6.1] have thus been proven to represent a general description of metal ion extraction into ILs by a neutral extractant. Additionally, it has been found that systems employing trimethylalkylammonium-based ILs show marked improvements in Sr²⁺ extraction efficiency and selectivity compared to other IL families.

Extraction studies employing *N*-alkylpyridinium-based ILs with long alkyl chains (*i.e.*, C₁₂pyr⁺ or C₁₄pyr⁺) have revealed a previously unappreciated aspect of extraction in IL-based systems, namely the resemblance of certain IL cations to cationic surfactants and their ability to aggregate. Micellization of the IL cation in the aqueous phase has been found to promote undesirable ion exchange processes by providing a means by which transfer of the IL cation into the aqueous phase was facilitated. The result is a reduced ability to exploit highly hydrophobic IL

cations to promote NC/IPE and reduced Sr^{2+} selectivity. This was observed for all systems studied that employed micelle-forming ILs and represents yet another aspect of IL-based extraction systems that must be taken into account when selecting an IL as an alternative to traditional organic solvents in these applications. Micelle formation does not introduce a new mechanism by which metal ions are extracted into ILs; it merely increases contributions from IX processes. Therefore, the ‘three-path model’ appears to provide a general description of metal ion extraction in these systems as well. The ability for an IL cation to form micelles can be eliminated by the incorporation of a dimethylamino- group into the *N*-alkylpyridinium ring opposite the alkyl chain. Furthermore the presence of this substituent has been shown to enhance contributions from NC/IPE when compared to analogous unsubstituted and non-micelle forming versions of *N*-alkylpyridinium ILs.

IL cation and anion hydrophobicity have proven to have a major effect on the mode by which metal ions partition into the IL. Increased hydrophobicity is desired for the IL cation as it favors NC/IPE, whereas a more hydrophobic IL anion enhances contributions from IX processes. The octanol-water distribution coefficient, D_{ow} , represents a parameter capable of capturing the overall hydrophobicity of an IL. This work has shown that a relationship exists between D_{ow} values for various ILs and extraction behavior. Specifically, it appears that extraction of metal ions from nitric acid by a neutral extractant into (non-micelle forming) ILs with a D_{ow} greater than 20 will proceed by NC/IPE. This represents a potential ‘cutoff’ that could be employed for the rational design of ILs for use as alternatives to conventional organic solvents in these types of extraction systems. Furthermore, models previously proposed to predict D_{ow} values for various ILs [6.2-6.4] have proven to be quite accurate, especially when compared to values measured here

suggesting that D_{ow} values (and therefore extraction behavior) could be determined entirely theoretically.

It is obvious then, that the selection of IL cation and anion is crucial in determining the feasibility of a given extraction process. This work confirms that these observations (*i.e.*, extraction trends) are generic and applicable to all IL systems. The establishment of a general description of metal ion extraction into ILs by a neutral extractant (*i.e.*, the ‘three-path model’) allows for a shift from extensive investigations of IL-based extraction systems to more specific studies aimed at explaining these qualitative trends in a quantitative manner. To this end, an analysis method was developed to quantify the individual contributions of each mode of partitioning. This method was successfully applied to the extraction of strontium from nitric acid into $C_5mim^+Tf_2N^-$ by DCH18C6. The exact contribution of each extraction mechanism has been determined, and the results show that all modes of partitioning are present in varying proportions under all conditions. Ion exchange processes predominate up to ~3 M nitric acid concentration, above which NC/IPE becomes the primary mode of partitioning. This is in agreement with expectations based on previously reported qualitative studies.

6.2 Recommendations

Several critical aspects of IL-based extraction systems have been investigated in this work. Despite providing a certain level of clarity to these complex systems, the results presented here point to the need for additional studies to further understand extraction into ionic liquids. The true potential of ILs as alternative extraction solvents will not be reached until they are applicable for all types of metal ions. The systems studied here comprising alkali and alkaline earth metal ions, nitric and hydrochloric acid, and one neutral extractant (*i.e.*, DCH18C6) represent relatively simple systems to investigate when compared to those proposed for lanthanide and actinide extraction.

For example, alkali and alkaline earth metal ions tend to have only one oxidation state, whereas lanthanides and actinides can occupy several oxidation states and form positive, negative and neutral complexes. Extractants for the separation of lanthanides and actinides can be neutral (*e.g.*, TBP or TODGA), acidic (*e.g.*, HDEHP) or basic (*e.g.*, Aliquat 336). Acidic and basic extractants are often considered to be liquid ion exchangers, as ion exchange is the process by which they extract metals. This could pose a problem because ionic liquids have been found to be ion exchangers themselves. Therefore, the general description of metal extraction into ionic liquids developed from studies of alkali and alkaline earth metal ion extraction could represent a simple description with which to begin understanding IL-based lanthanide and actinide extraction.

Micelle formation by the IL cation in the aqueous phase has added another complication to what have already proven to be complex systems and has facilitated undesirable ion exchange processes. It was found that the incorporation of a dimethylamino- group into the *N*-alkylpyridinium ring structure effectively blocks micellization and enhances metal ion extraction by NC/IPE. Further work must explore additional functional or substituent groups to block micelle formation, lest it arise for other ILs utilized in solvent extraction systems.

Both forms of ion exchange have been treated as undesired mechanisms in the extraction of metal ions into ILs. The loss of the IL cation to the aqueous phase is considered detrimental as it results in the deterioration of the extraction solvent and contamination of the aqueous phase. Despite the fact that many studies have focused on *reducing* the contributions of ion exchange in IL-based extraction systems, the exceptional selectivity observed in these systems stems from the ability for ion exchange processes to occur. The acid dependencies for the extraction of sodium and strontium by DCH18C6 into $C_{10}mim^+Tf_2N^-$ are shown in Figure 6.1. Decreasing sodium distribution ratios as the acidity is increased indicates ion exchange processes are the primary

mechanism by which sodium is extracted, whereas rising strontium distribution ratios indicates NC/IPE predominates when strontium is extracted from up to ~1 M HNO₃. These diverging trends yield marked improvements in strontium selectivity over sodium compared to traditional organic solvents (*e.g.*, 1-octanol) which do not allow for extraction *via* ion exchange. Clearly then, additional work should be devoted to exploiting the differing properties of the possible extraction mechanisms to improve extraction selectivity.

Many reports have noted the marked effect that IL hydrophobicity has on extraction behavior [6.5-6.7]. Contributions from NC/IPE are favored when IL cation hydrophobicity is increased, while an increase in IL anion hydrophobicity enhances IX processes. D_{ow} represents a parameter that embodies the overall hydrophobicity of the IL. Correlations between D_{ow} and extraction efficiency have provided a potential guide for future IL design. It appears that metal ion extraction into ILs with a D_{ow} value greater than 20 will proceed by NC/IPE. This guideline must be confirmed through similar studies of ILs with different IL anions, as Tf₂N⁻ represented the only IL anion studied here. Furthermore, predictive models were shown to be in good agreement with measured D_{ow} values and the continued development of more accurate models could provide an entirely computational prediction of extraction behavior into ILs.

Up to this point, a broad and qualitative description of metal ion extraction into ILs has been reported [6.5-6.8]. Trends have been identified largely on the basis of the shape and direction of the acid dependencies for these systems. The method of analysis developed to determine the exact contributions from each individual mode of strontium partitioning described here can be used to quantitatively confirm all of the qualitative trends reported in literature regarding extraction of metal ions into ILs. Of particular importance are the effects of IL cation hydrophobicity, IL

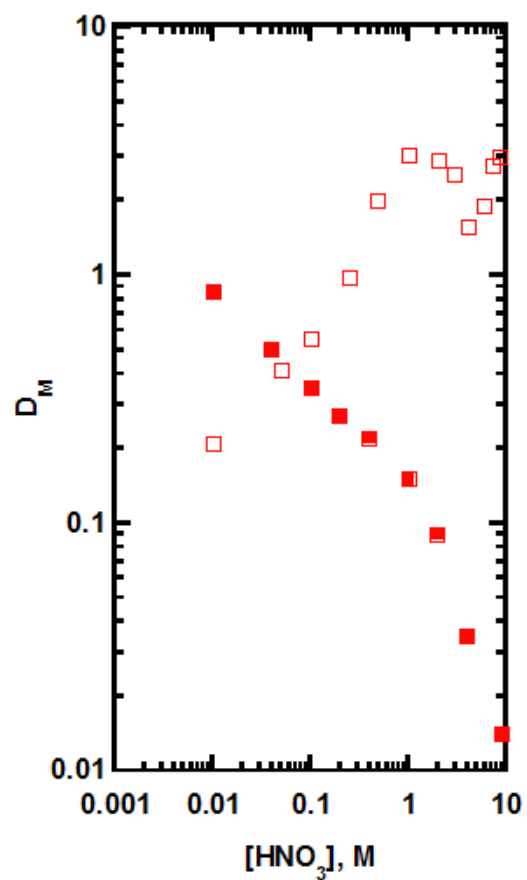


Figure 6.1. Effect of HNO_3 concentration on the extraction of Na^+ (solid, red squares) and Sr^{2+} (open, red squares) by 0.1 M DCH18C6 into $\text{C}_{10}\text{mim}^+\text{Tf}_2\text{N}^-$.

anion hydrophobicity, and hydration enthalpy of the aqueous phase anion on extraction behavior. Along with the three-path model, this approach to quantitative analysis provides a framework by which to study more complicated IL-based extraction systems.

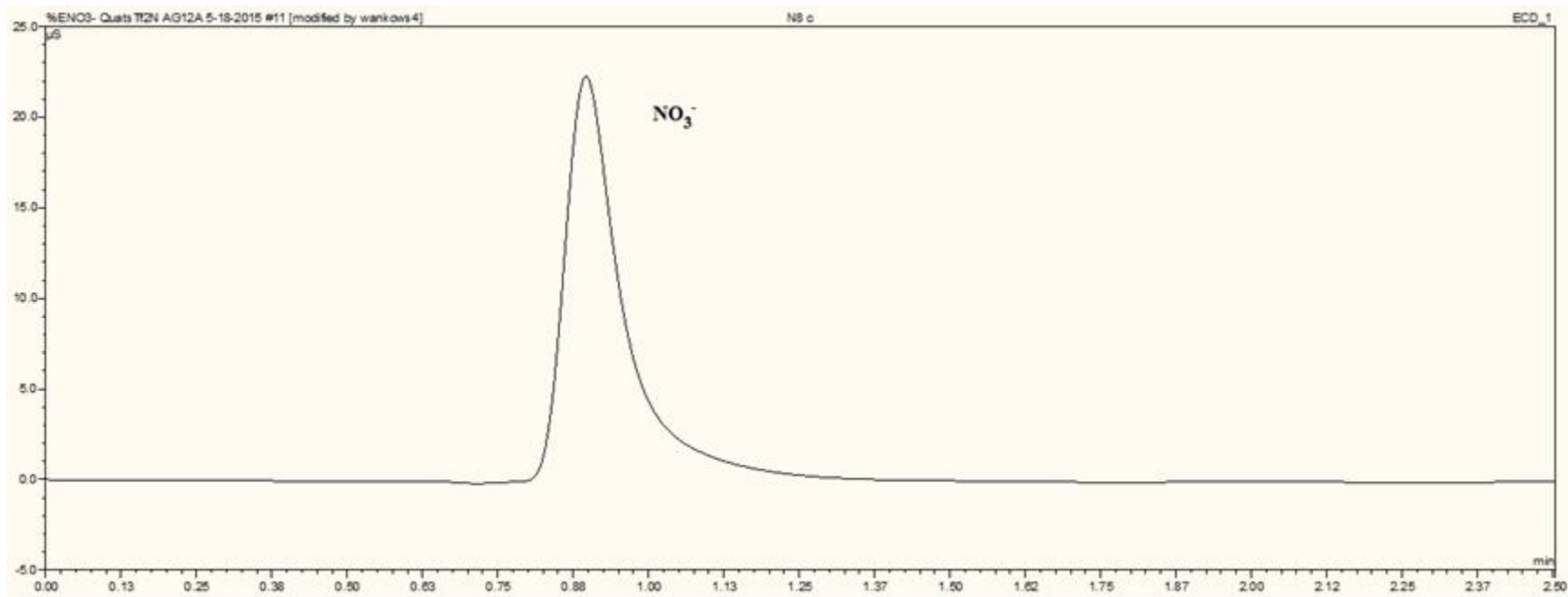
6.3 References

- [6.1] Dietz, M.L.; Stepinski, D. C., A Ternary Mechanism for the Facilitated Transfer of Metal Ions into Room-Temperature Ionic Liquids (RTILs): Implications for the “Greenness” of RTILs as Extraction Solvents. *Green Chemistry*, **2005**, 7, 747-750.
- [6.2] Cho, C.-W.; Preiss, U.; Jungnickel, C.; Stolte, S.; Arning, J.; Ranke, J.; Klamt, A.; Krossing, I.; Thöming, J., Ionic Liquids: Predictions of Physicochemical Properties with Experimental and/or DFT-Calculated LFER Parameters to Understand Molecular Interactions in Solution. *Journal of Physical Chemistry B*, **2011**, 115, 6040-6050.
- [6.3] Lee, B.-S.; Lin, S.-T., A Priori Prediction of the Octanol-Water Partition Coefficient (K_{ow}) of Ionic Liquids. *Fluid Phase Equilibria*, **2014**, 363, 233-238.
- [6.4] Rybinska, A.; Sosnowska, A.; Grzonkowska, M.; Barycki, M.; Pusyn, T., Filling Environmental Data Gaps with QSPR for Ionic Liquids: Modeling *n*-octanol/Water Coefficient. *Journal of Hazardous Materials*, **2016**, 303, 137-144.
- [6.5] Dietz, M.L.; Dzielawa, J.A.; Laszak, I.; Young, B.A.; Jensen, M.P., Influence of Solvent Structural Variations on the Mechanism of Facilitated Ion Transfer into Room-Temperature Ionic Liquids. *Green Chemistry*, **2003**, 5, 682-685.
- [6.6] Hawkins, C.A.; Garvey, S.L.; Dietz, M.L., Structural Variations in Room-Temperature Ionic Liquids: Influences on Metal Ion Partitioning Modes and Extraction Selectivity. *Separation and Purification Technology*, **2012**, 89, 31-38.
- [6.7] Garvey, S.L.; Dietz, M.L., Ionic Liquid Anion Effects in the Extraction of Metal Ions by Macrocyclic Polyethers. *Separation and Purification Technology*, **2014**, 123, 145-152.
- [6.8] Dietz, M.L, Ionic Liquids as Extraction Solvents: Where do We Stand? *Separation Science and Technology*, **2006**, 41, 2047-2063.

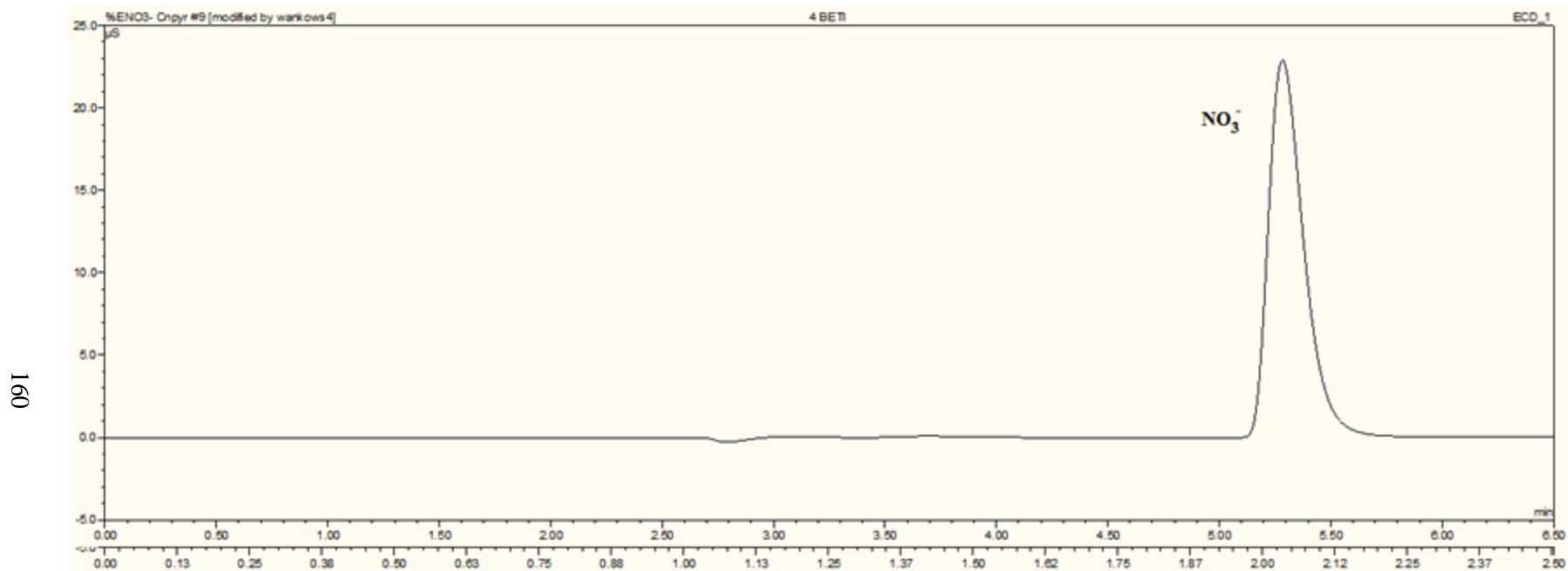
Appendix:
Example Liquid Chromatograms and Mass Spectra

Nitrate determination – Section 2.2.2

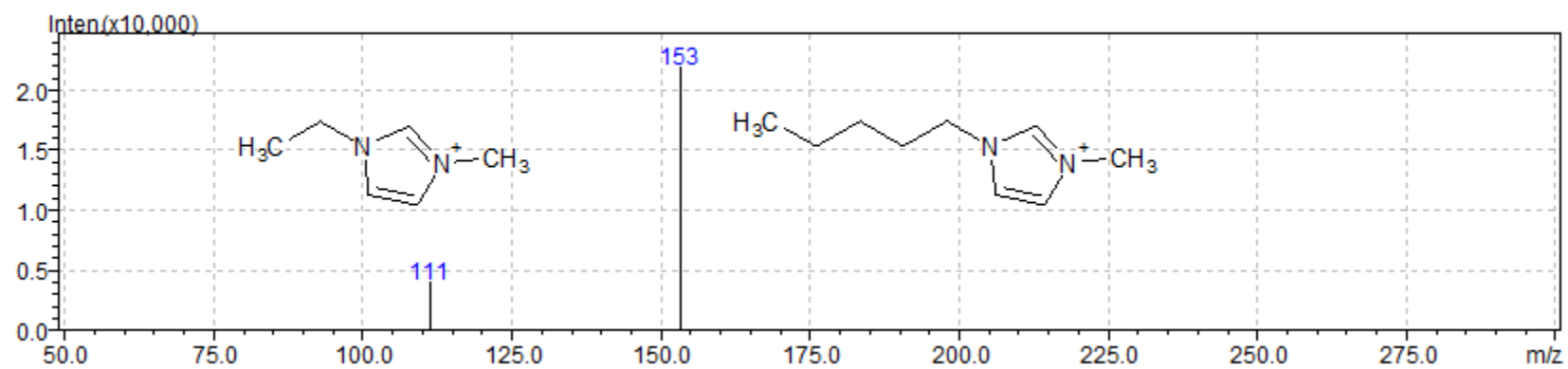
159



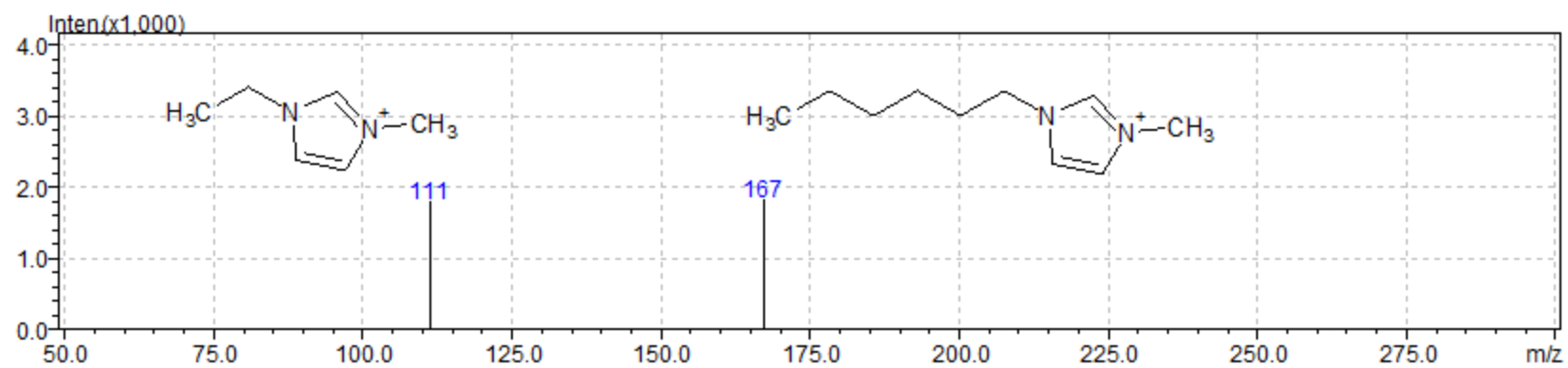
Nitrate determination – Section 3.2.2



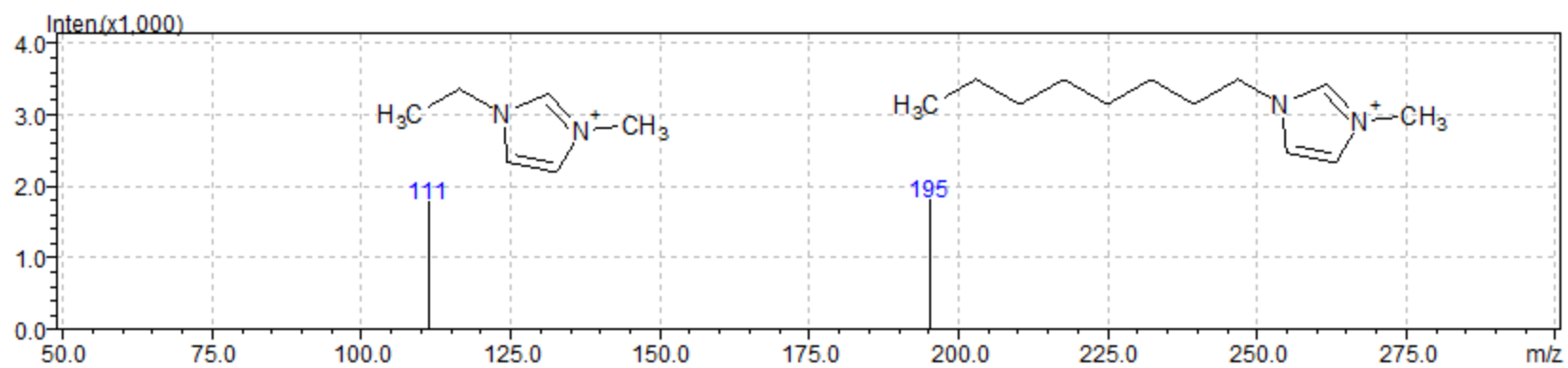
Mass spectrum of C₅mim⁺ and C₂mim⁺ (IS)



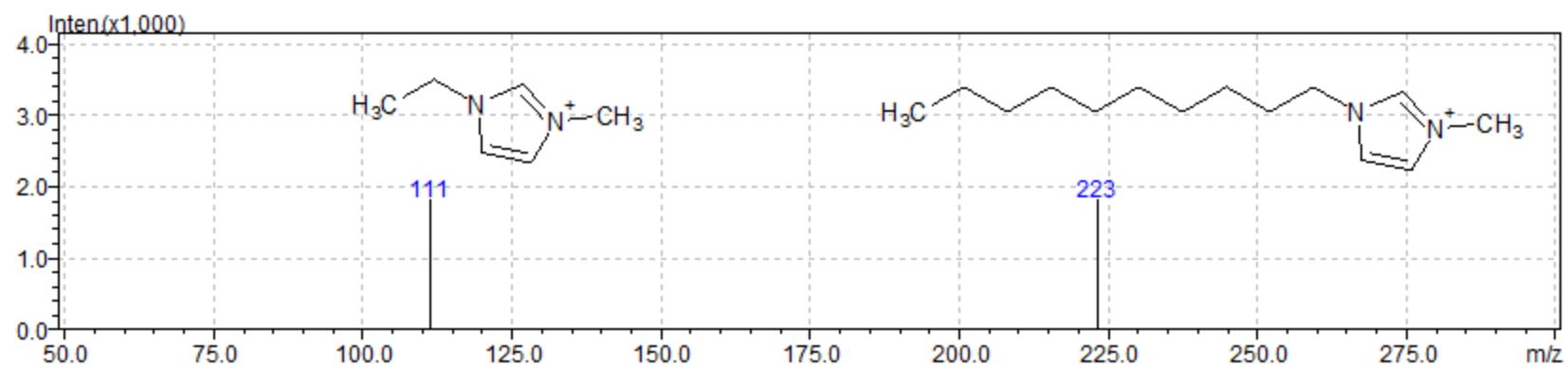
Mass spectrum of C₆mim⁺ and C₂mim⁺ (IS)



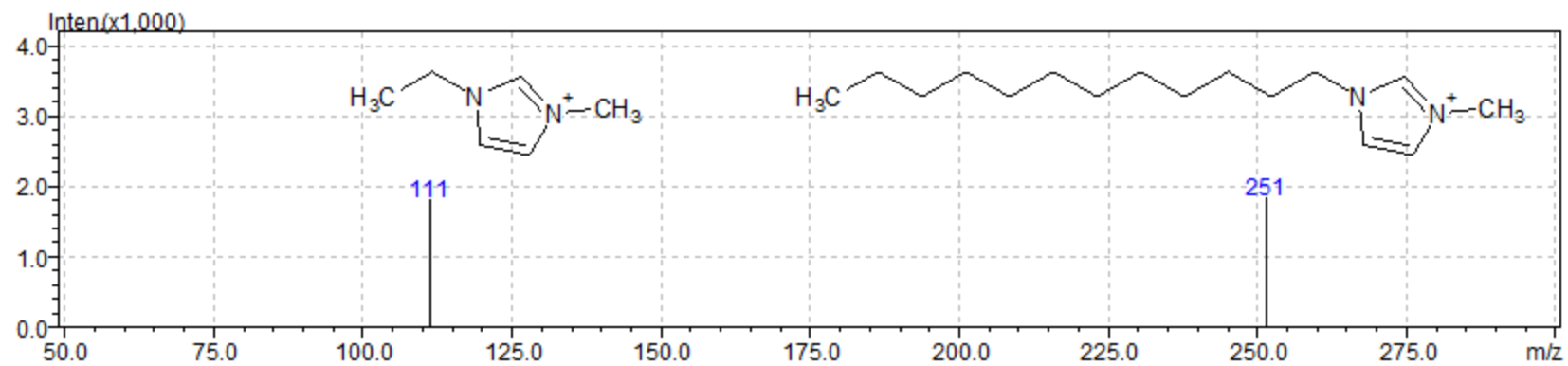
Mass spectrum of C₈mim⁺ and C₂mim⁺ (IS)



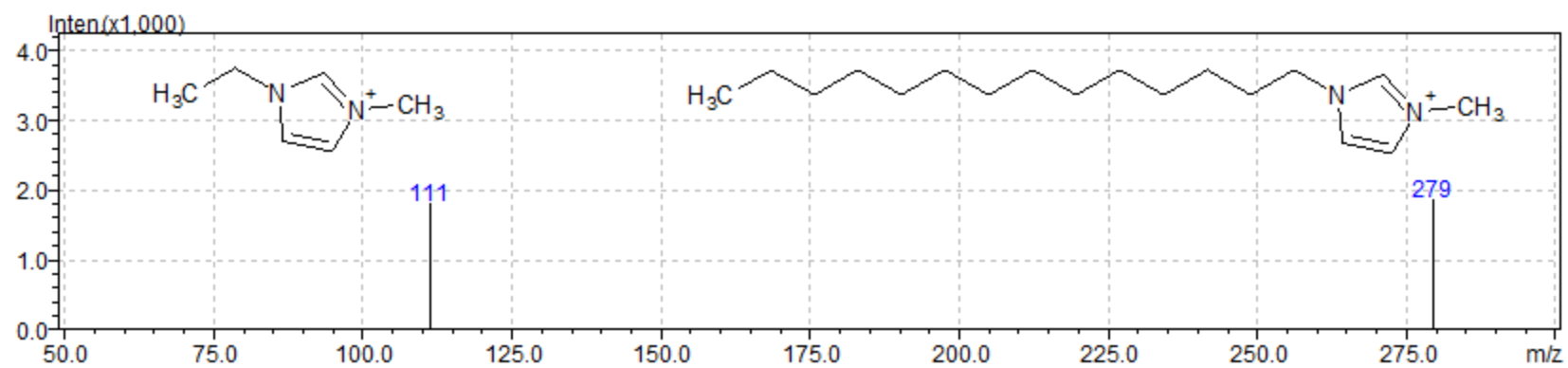
Mass spectrum of C₁₀mim⁺ and C₂mim⁺ (IS)



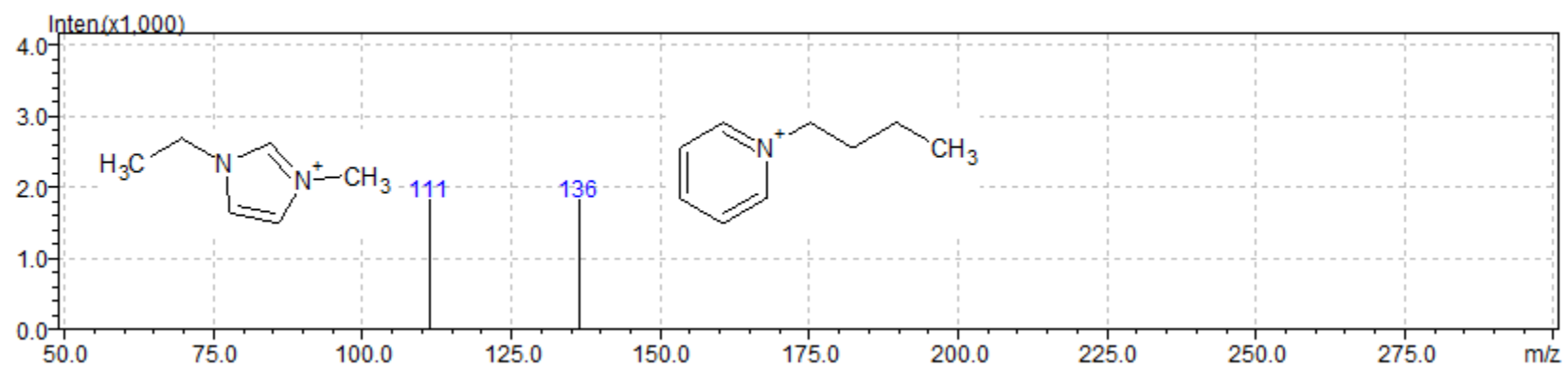
Mass spectrum of C₁₂mim⁺ and C₂mim⁺ (IS)



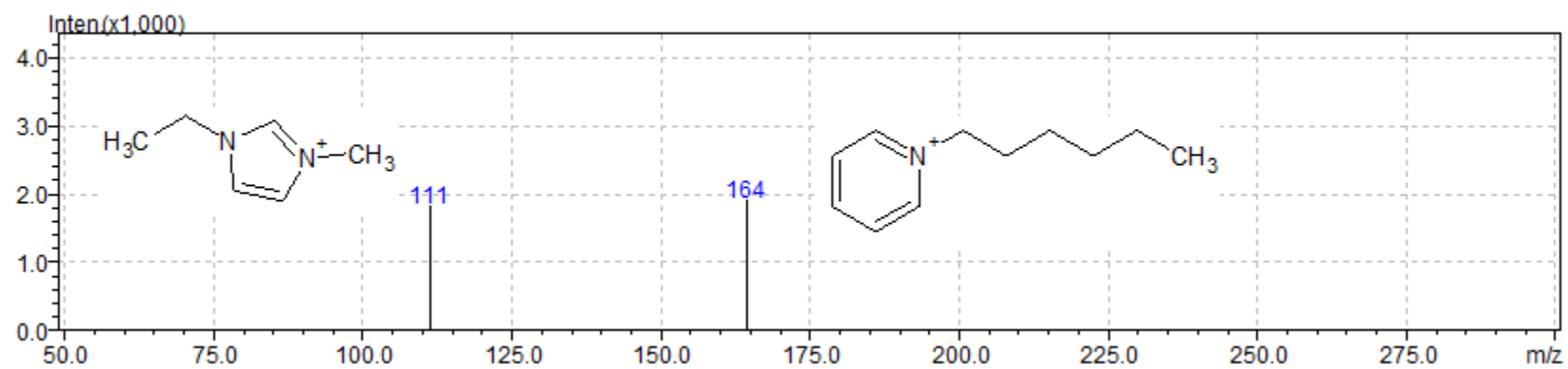
Mass spectrum of C₁₄mim⁺ and C₂mim⁺ (IS)



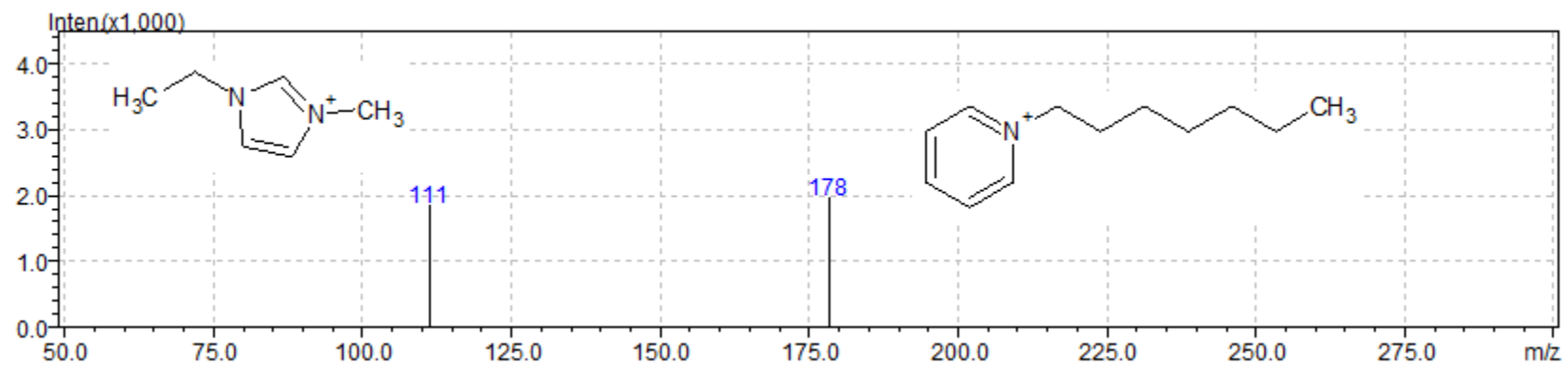
Mass spectrum of C₄pyr⁺ and C₂mim⁺ (IS)



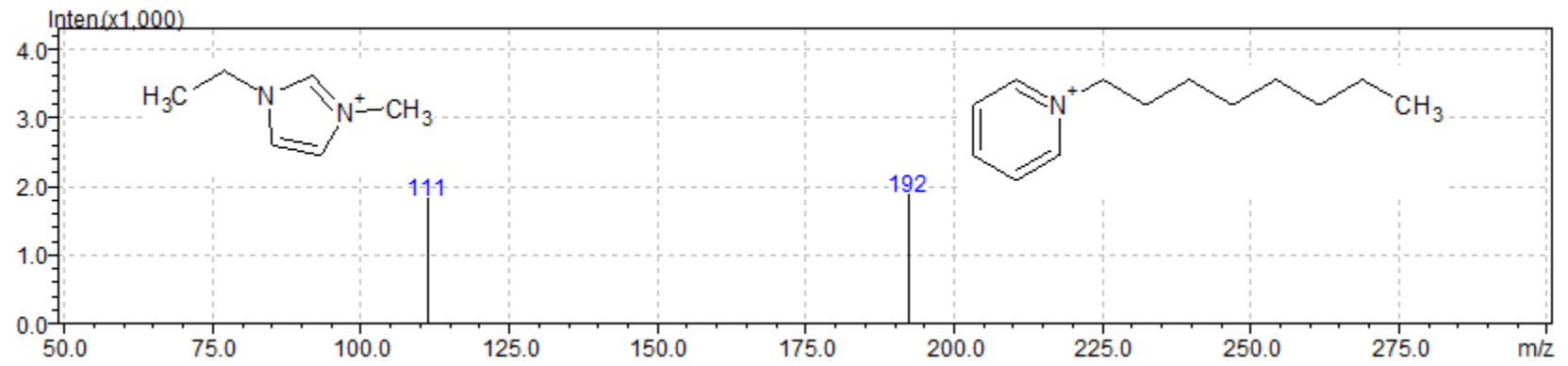
Mass spectrum of C₆pyr⁺ and C₂mim⁺ (IS)



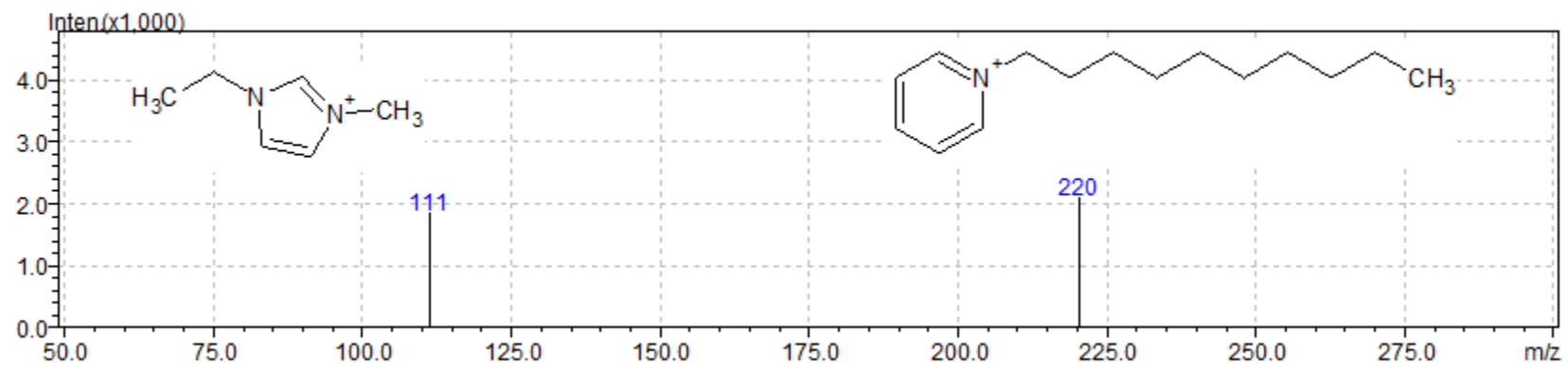
Mass spectrum of C₇pyr⁺ and C₂mim⁺ (IS)



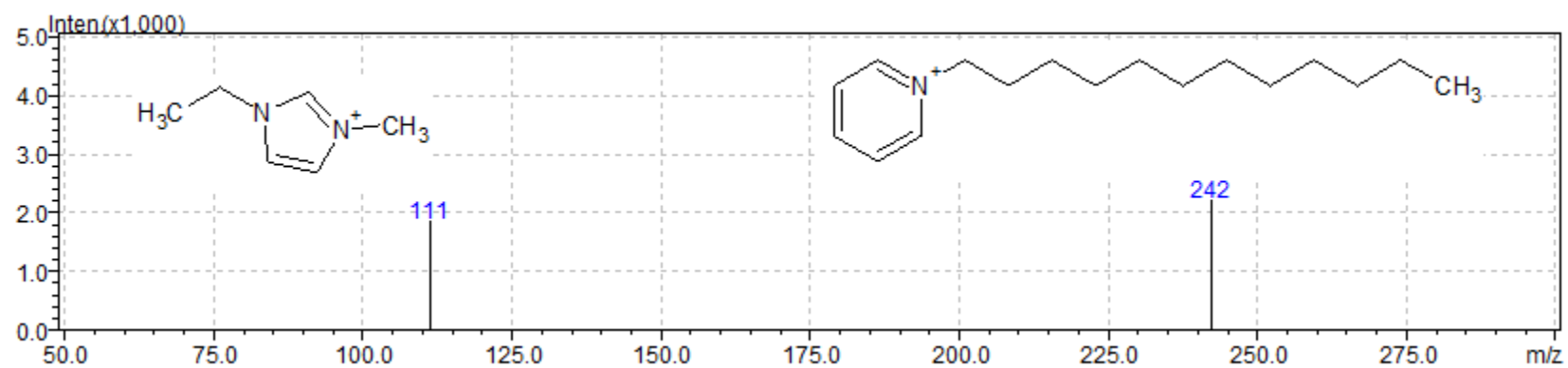
Mass spectrum of C₈pyr⁺ and C₂mim⁺ (IS)



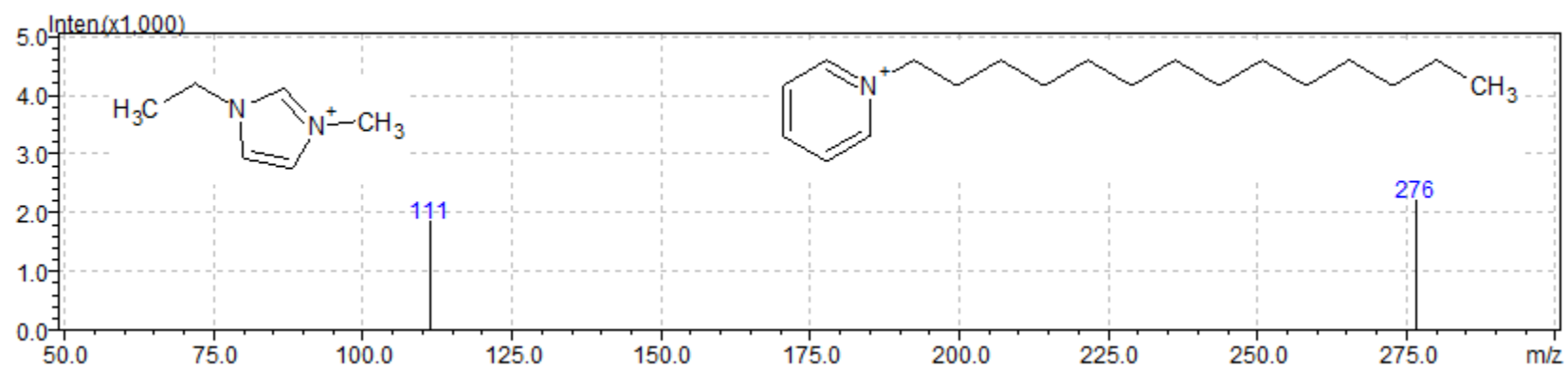
Mass spectrum of C₁₀pyr⁺ and C₂mim⁺ (IS)



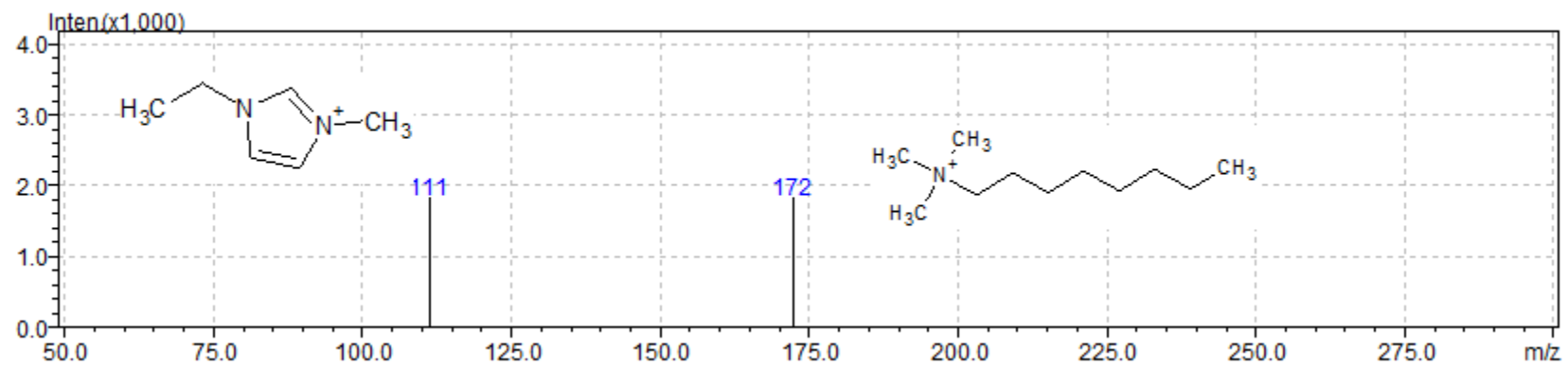
Mass spectrum of C₁₂pyr⁺ and C₂mim⁺ (IS)



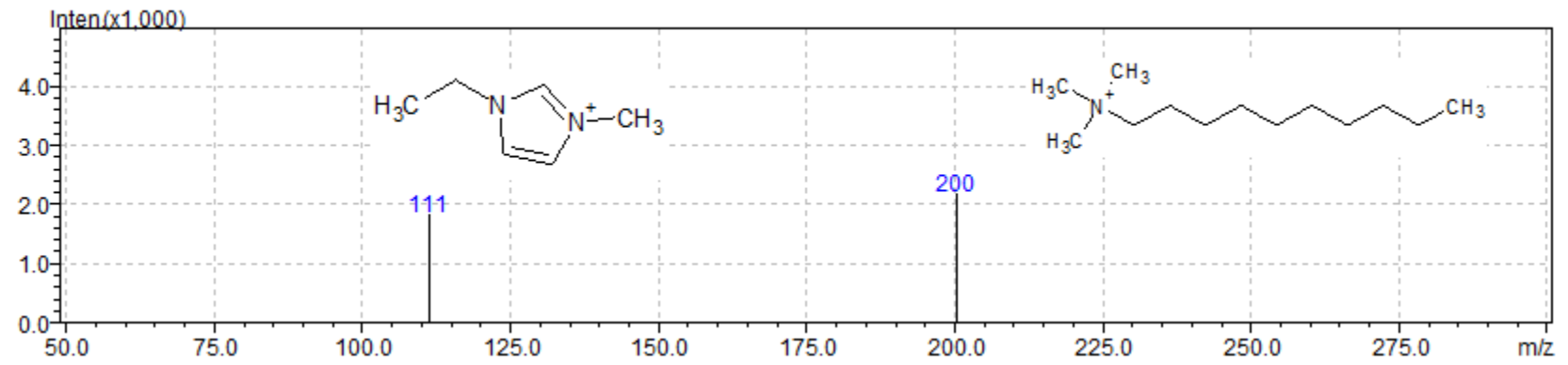
Mass spectrum of C₁₄pyr⁺ and C₂mim⁺ (IS)



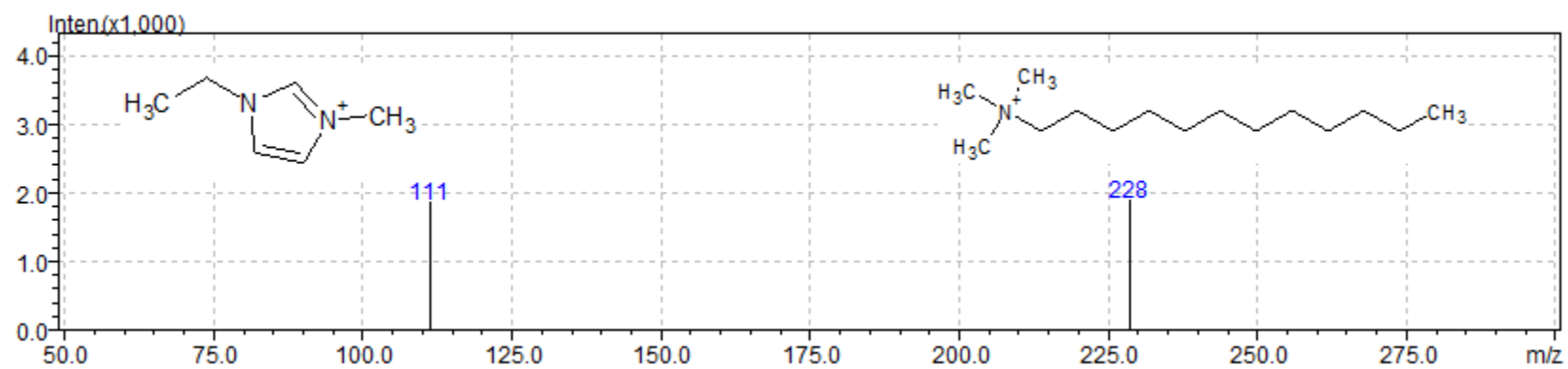
Mass spectrum of N_{8,111}⁺ and C₂mim⁺ (IS)



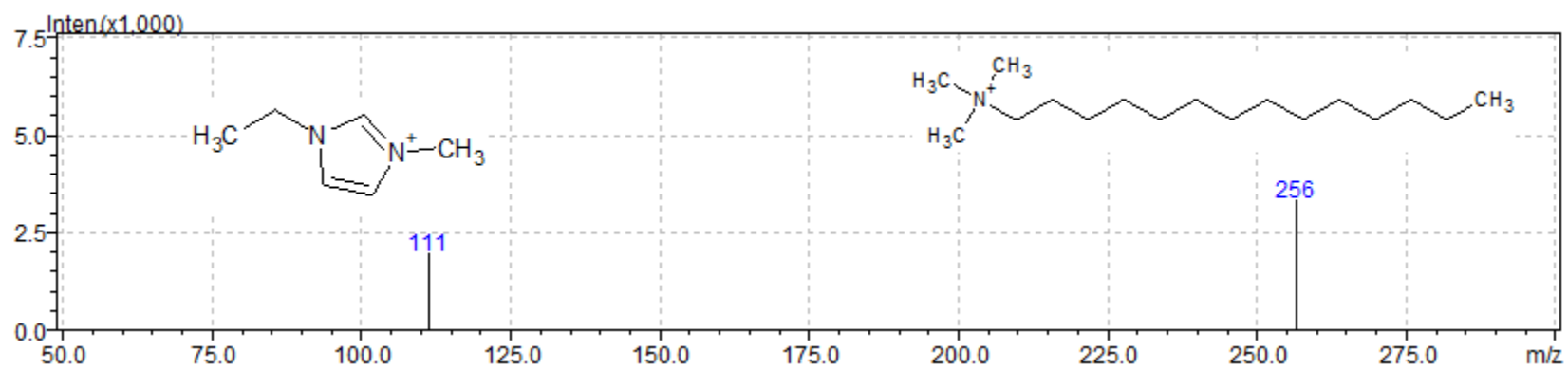
Mass spectrum of N_{10,111}⁺ and C₂mim⁺ (IS)



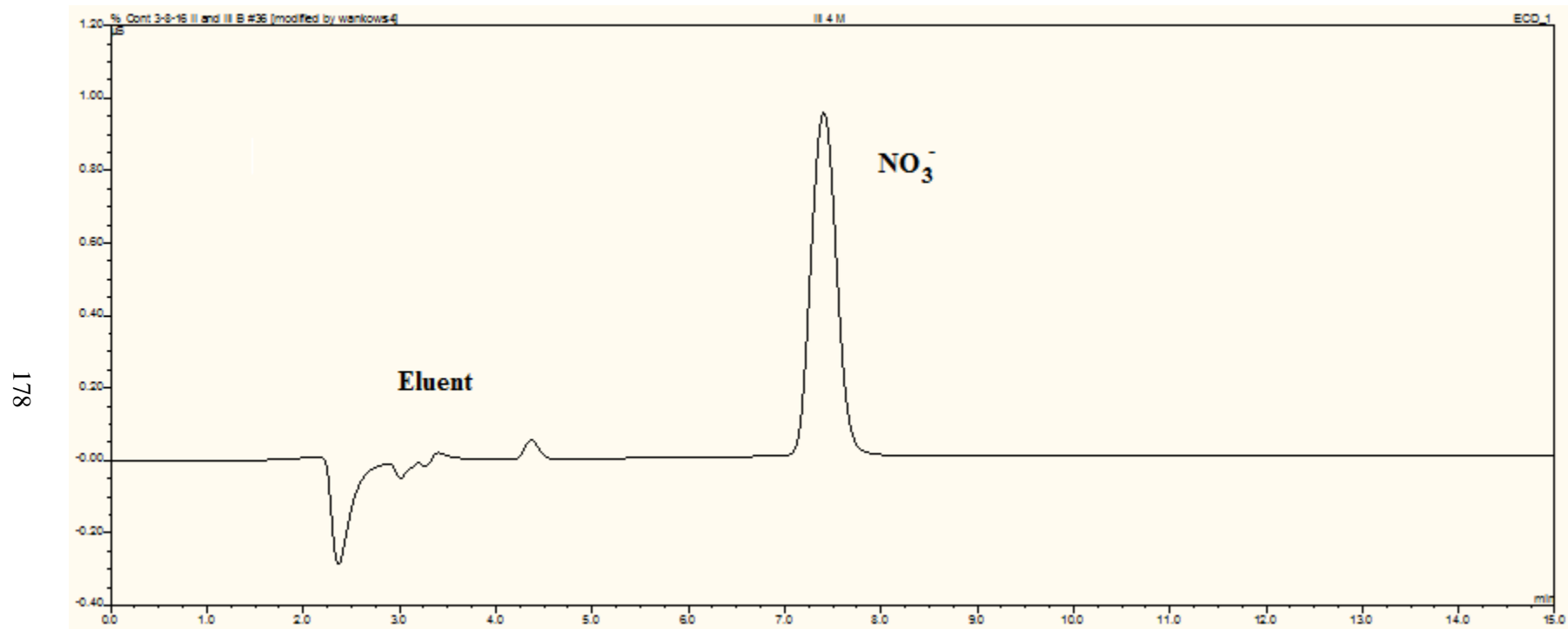
Mass spectrum of $N_{12,111}^+$ and C_2mim^+ (IS)



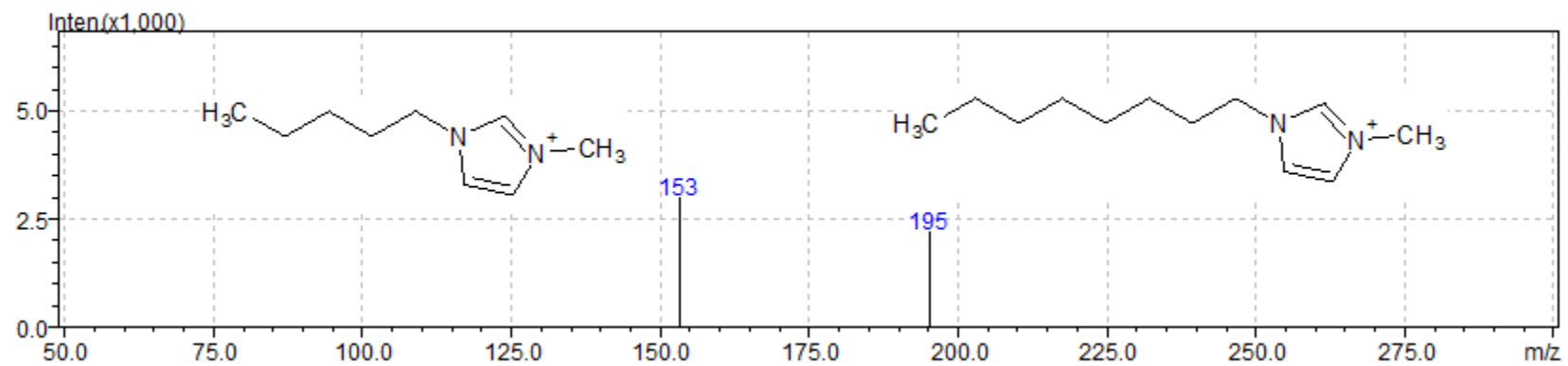
Mass spectrum of $N_{14,111}^+$ and $C_{2}mim^+$ (IS)



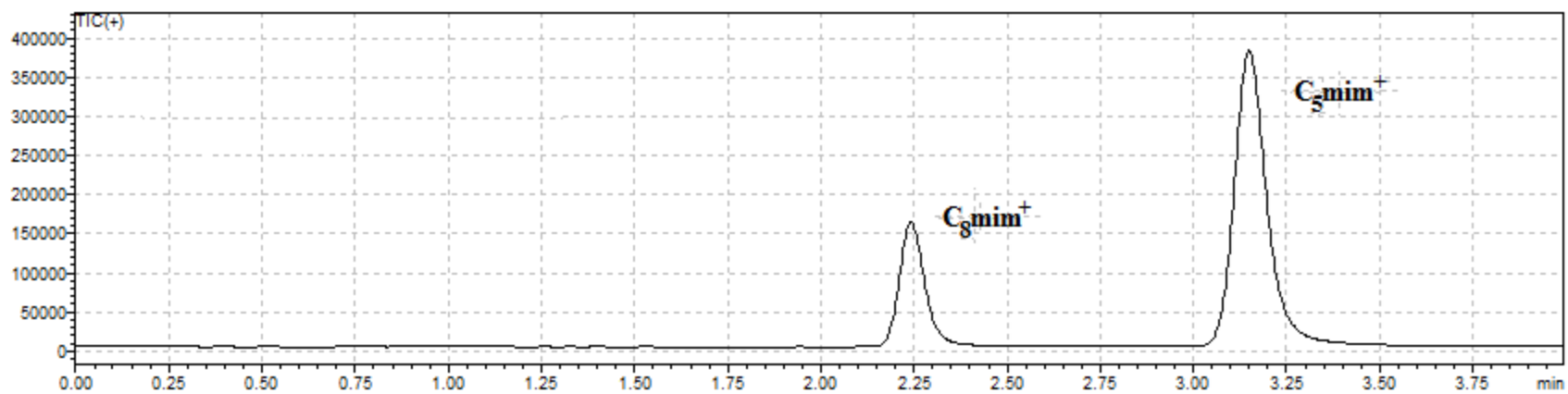
Nitrate determination – Section 5.2.2



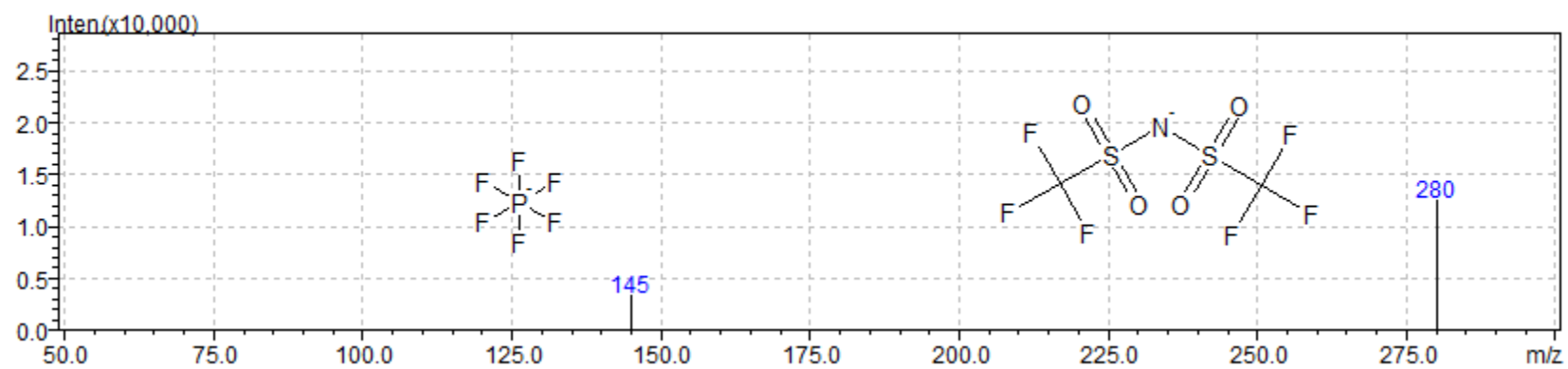
Mass spectrum of C₅mim⁺ and C₈mim⁺ (IS)



Chromatogram of C₅mim⁺ and C₈mim⁺ (IS)



Mass spectrum of Tf₂N⁻ and PF₆⁻ (IS)



Curriculum Vitae

James L. Wankowski

Graduate Research / Teaching Assistant
Department of Chemistry & Biochemistry
University of Wisconsin-Milwaukee
3210 N Cramer St.
Milwaukee, WI 53211

Education

Ph.D. in Chemistry, University of Wisconsin-Milwaukee, Milwaukee, WI, May 2016

Dissertation: “Fundamental studies of metal ion extraction into ionic liquids by macrocyclic polyethers”, Advisor: Mark L. Dietz

B.S. in Chemistry, Carroll University, Waukesha, WI May 2011

Experience

Research Assistant, University of Wisconsin-Milwaukee, Milwaukee, WI 2011-present

- Conducted research elucidating the fundamental aspects of the extraction of alkali and alkaline earth metal ions by crown ethers in ionic liquid-based liquid-liquid extraction systems.
- Trained and supervised junior graduate and undergraduate researchers.

Teaching Assistant, University of Wisconsin-Milwaukee, Milwaukee, WI 2011-present

- Taught discussions and laboratories for General and Analytical Chemistry

Participant, 16th National School on Neutron and X-Ray Scattering, Oak Ridge National Laboratory – Oak Ridge, TN and Argonne National Laboratory – Argonne, IL Summer 2014

- Hands on training with neutron and X-Ray scattering techniques utilizing the High Flux Isotope Reactor (HFIR, ORNL), Spallation Neutron Source (SRS, ORNL) and Advanced Photon Source (APS, ANL).

Honors and Awards

Moczynski Outstanding Teaching Assistant, University of Wisconsin-Milwaukee Spring 2016
Moczynski Outstanding Teaching Assistant, University of Wisconsin-Milwaukee Spring 2012
Finalist, Thronson International Program, Carroll University Summer 2011

Publications

J. L. Wankowski, M. L. Dietz, “Ionic liquid (IL) cation and anion structural effects on metal ion extraction into quaternary ammonium-based ILs”, *Solvent Extraction & Ion Exchange* 2016, 34, 48-59.

J. L. Wankowski, M. J. Kaul, M. L. Dietz, “Micelle formation as a factor influencing the mode(s) of metal ion partitioning into *N*-alkylpyridinium ionic liquids (ILs): Implications for the design of IL-based extraction systems”, *Green Chem.*, submitted (2017).

Presentations

J. L. Wankowski, M. J. Kaul, and M. L. Dietz, “Factors influencing the mode(s) of facilitated ion transfer into room-temperature ionic liquids containing crown ethers”, 252nd ACS National Meeting & Exposition, Philadelphia, PA, August 21-25, 2016.

J. L. Wankowski, “General trends for metal ion extraction into ionic liquids (ILs)”, UW-Milwaukee Graduate Student Breakfast, August 26, 2015.

J. L. Wankowski and M. L. Dietz, “Factors influencing the mode(s) of metal ion partitioning into *N*-alkylpyridinium-based ionic liquids (ILs)”, UW-Milwaukee Chemistry and Biochemistry Research Symposium, April 3, 2015

J. L. Wankowski and M. L. Dietz, “Factors influencing the mode(s) of metal ion partitioning into *N*-alkylpyridinium-based ionic liquids (ILs)”, 249th ACS National Meeting & Exposition, Denver, CO, March 22-26, 2015

J. L. Wankowski and M. L. Dietz, “Ionic liquid (IL) cation and anion structural effects on the mode(s) of metal ion partitioning into quaternary ammonium-based ILs”, 18th Symposium on Separation Science and Technology for Energy Applications, Oak Ridge, TN, October 27-30, 2014

J. L. Wankowski and M. L. Dietz, “Ionic liquid (IL) cation structural effects on the mode(s) of metal ion partitioning into pyridinium- and quaternary ammonium-based ILs”, UW-Milwaukee Chemistry and Biochemistry Research Symposium, April, 2014

J. L. Wankowski and A. R. Kennedy, “Nickel carbonate cage synthesis through degradation of [Ni₃(Trensal)₂]", 241st ACS National Meeting & Exposition, Anaheim, CA, March 27-31, 2011

Professional Affiliations

American Chemical Society

2010-present